NTNU
Norwegian University of
Science and Technology

Numerical study of Soil Nailing Technique

Empirical, classical limit equilibrium and 2D-3D FEM applications

Kidist Getu Biria

Trondheim, October 2016

MASTER THESIS

Main supervisor: Professor Gustav Grimistad (NTNU)
Co-supervisor: Dr. Anteneh Biru Tsegaye (Multiconsult)

Department of Civil and Transport Engineering
Norwegian University of Science and Technology (NTNU)

To the memory of my mother...the kind and the loving.

NORWEGIAN UNIVERSITY OF SCIENCE AND TECHNOLOGY
DEPARTMENT OF CIVIL AND TRANSPORT ENGINEERING

Report Title: **Numerical Study of Soil Nailing Technique** **Empirical, classical and 2D-3D FEM applications**	Date: **October 27, 2016** Number of pages (incl. appendices): **136**			
	Master Thesis	×	Project Work	
Name: **Kidist Getu Biria**				
Professor in charge/supervisor: **Professor Gustav Grimstad (NTNU)**				
Other external professional contacts/supervisors: **Dr Anteneh Biru (Multiconsult)**				

Abstract:
The stability of steep cuts is one of the challenging problems. There are several ways of tackling this problem. One of these methods is the soil nailing technique. The technique, although relatively young, is becoming popular for stabilizing steep cuts.
The focus of this thesis is numerical investigation of:

- the effect of various configuration (geometric) parameters such as nail inclination, wall batter, back slope nail length and nail pattern, and
- the effect of various soil parameters such as cohesion, friction angle and dilatancy angle on the stability and deformation of nailed soil slopes and various structural forces.

Prior to the numerical investigations, literatures review will be conducted on the state-of-the practice and the state-of-the art of the soil nailing technique and design and analysis of soil-nail systems.
Following the literature review, the numerical investigations will be carried out using:

- 2D limit equilibrium applications using own implemented wedge method and the Geosuite software.
- 2D and 3D finite element applications using the commercial finite element packages, Plaxis 2D and Plaxis 3D.

Comparison will then be made between

- global stability analyses results obtained from the limit equilibrium methods and the finite element applications.
- results obtained from Plaxis 2D and the 3D finite element analyses.

Conclusions will be made about the various findings of the numerical investigation and areas that need further investigation will be recommended.

Keywords:

1. Soil nailing
2. Parameter study
3. Soil nail configuration parameters
4. Factor of safety

Problem Description

The stability of steep cuts is one of the challenging problems. There are several ways of tackling this problem. One of these methods is the soil nailing technique. The technique, although relatively young, is becoming popular for stabilizing steep cuts. There are various methods that can be used for designing and analyzing of soil systems. Amongst are empirical methods, limit equilibrium methods, finite element (FEM) methods. The first two are frequently applied. Various limit equilibrium methods are extended to accommodate the soil nailing practice. Such extended limit equilibrium methods are implemented in different software products. One such software that shall be considered in this study is Geosuite. In the outset two limitations are identified with limit equilibrium methods. One is unrealistic stress distribution and the other is lack of stress-strain relation. FEM methods can be employed for enhancing the results. One such FEM software widely used among the practicing engineers and considered in this study is the Plaxis FEM package. In this study

- literature review will be conducted on existing practices.
- analysis results from Plaxis 2D and from Geosuite will be compared.
- for the selected constitutive model in Plaxis 2D sensitivity of parameters analysis will be done.
- furthermore, 3D effects, for example due to different nail patterns, will be studied employing the Plaxis 3D FEM environment.
- the various structural forces obtained from the Plaxis analyses will be compared amongst each other and with suggested values and patterns in the state-of-the art.

Preface

This master thesis was conducted at the geotechnical department at the Norwegian university of Science and Technology (NTNU), as part of MSc in geotechnical engineering. This thesis has 30 ECTS and taught in the spring semester of 2016. The thesis focuses on numerical methods of soil nailing technique with empirical, classical limit equilibrium and 2D-3D FEM applications.

Trondheim, October 2016

Kidist Getu

Acknowledgement

This thesis becomes a reality with the kind support and help of many individuals. I would like to extend my sincere thanks to all of them.

Thanks to merciful lord for all the countless gifts you have offered me.

I would like to express my gratitude to my supervisor professor Gustav Grimstad for allowing me to do this thesis with freedom.

Special thanks to my considerate and supportive husband and co-supervisor Anteneh Biru Tsegaye. I am the luckiest to have my supervisor at home. The completion of this thesis could not have been possible without your continuous guidance and encouragement. My son Edor, you fill my heart with joy and give me every positive bit of energy. Grow in wisdom.

I would also like to express my gratitude to my father and to my brothers for their advice and encouragement. Special thanks to my mother Yenenesh, I am grateful for your love, encouragement and concern. Your kindness, your love, your spirit will always be with me.

Summary

Literature review was conducted on the state-of-the art and the state-of-the practice of the soil nailing technique. The literature review focused on design analysis and constructional aspects of the soil nailing technique and effects of the most important soil-nail system configuration (geometric) parameters such as nail spacing, nail inclination, wall-batter, back terrain slope and nail length. Some classical methods of analysis of internal and external stability of a soil-nail system were also presented and discussed.

After conducting the literature review, numerical investigations were conducted on the effect soil-nail system configuration parameters and some soil parameters on the degree of stability and deformation of a soil-nail system. The numerical investigations were carried out using an own implemented simple wedge method followed by analysis using the Geosuite software product and the Plaxis 2D and 3D finite element packages. The different analysis results were then compared. In addition, in the finite element analyses, the effects of the different configuration parameters on the structural forces in the soil-nail system were investigated. Finally, a preliminary design and analysis of a soil-nail system was carried for a steep cut adjacent to a road construction.

List of Symbols and Abbreviations

S_V	Vertical soil-nail spacing
S_H	Horizontal soil-nail spacing
H	Soil-nail wall height
L	Soil-nail length
D_{DH}	Drill hole diameter
d	soil-nail diameter
i	Soil-nail inclination
η	Face batter
β	Back slope
φ	Friction angle
c	Cohesion
a	Attraction
ψ	Dilatancy angle
$T_{\max}$	Maximum tensile nail force
z	Vertical distance from the bottom of the excavation
FS_G	Global factor of safety
K_a	Active earth pressure
γ	Unit weight
γ_{Sat}	Saturated unit weight
γ_{unsat}	Unsaturated unit weight
T_o	Tensile force at the face wall (soil-nail head force)
δ_h	Horizontal wall deformation
λ	Distance of influence caused by the wall deformation

L_r	Length ratio
f_r	Friction ratio
S_r	Strength ratio
d_r	Deformation ratio
q	Permanent surcharge load
K_o	At rest earth pressure coefficient
σ_n	Normal stress
j	Nail number
$\sigma_{nj,\max}$	Maximum normal force for the j^{th} nail
$\sigma_{nj,\min}$	Minimum normal force for the j^{th} nail
τ	Shear force
T_n	Mobilized soil-nail tension
q_u	Bond strength
FOS_T	Factor of safety against nail tension
l_e	Length of the nail behind the slip surface
μ	Mobilized soil-nail interface friction angle
F_H^a	Horizontal seismic load
F_V^a	Vertical seismic load
T_{EQ}	Equivalent nail tensile force
SF	Mobilized shear forces
C_m	Mobilized cohesion
B	Foundation width
N_c	Undrained bearing capacity factor
c_u	Undrained strength

ϕ_{LS}	Resistance factor for lateral sliding
γ_{EH}	Maximum load factor for horizontal earth loads
γ_{ES}	Maximum load factor for horizontal effect of permanent surcharge
P_a	Lateral earth thrust
R_S	Nominal soil resistance
H_1	Effective height over which the earth pressure acts
θ_c	Critical angle of the wedge mechanism
$\sigma_{\max}$	Major principal stresses
$\sigma_{\min}$	Minor principal stresses
E	Young's modulus
E_{oed}	Oedometer modulus
v	Poisson's ratio
r	Roughness coefficient
E_n	Young's modulus of the soil-nail
E_g	Young's modulus of the cement mix grout
E_{eq}	Equivalent Young's modulus
A_n	Area of the soil-nail
A_g	Area of the cement mix grout
t_s	Traction force along the embedded pile skin
K_s	Stiffness along the skin
G_{soil}	Shear modulus of the soil
F_{foot}	Mobilized force at the embedded pile foot
$F_{\max}$	Maximum force allowed at the foot of the embedded pile

K_{foot}	Stiffness at the embedded pile foot
δ_{foot}^{ps}	Displacement of the foot of the pile relative to the surrounding soil
$N_{comp,tens}$	Tensile force and the compressive stress
EA	Axial stiffness
EI	Flexural stiffness
M_p	Structural moment capacity
N_p	Structural axial load capacity
ΣMsf	Total multiplier
ISF_{RS}	Axial skin stiffness factor
ISF_{RN}	Lateral skin stiffness factor
ISF_{KF}	Pile base stiffness factor
$FHWA$	Federal Highway Administration (U.S. Department of Transportation)
FEM	Finite Element Method

Table of Contents

List of Figures

List of Tables

CHAPTER 1: Introduction

1.1 Background

Soil nailing has long been used for reinforcing ground during tunneling. Its application for stabilizing slopes and steep excavations is relatively new. Application of soil nailing for stabilization of slopes started in France in the 1970's-with 18m high cut for rail way [1]. In the following years, full scale research projects have been conducted. Design and analysis methods were (and are being) developed. Its use in practice has also become significant. The method is used both for new constructions and for remediation and stabilization of older stonewalls. In France and Germany alone over 125000-150000 sq. meter slopes are constructed with soil-nail stabilization yearly. Initially used for temporary walls, nowadays it is increasingly used for permanent constructions as well. The highest soil-nail wall constructed in France is 21 m high. They are particularly suited for vertical or near vertical walls. They are suitable for [2]

- road way cut excavations
- road widening under existing bridge end
- repair and reconstruction of existing retaining structures
- temporary and permanent excavations in urban environment'

1.2 Advantages and disadvantages

Soil nailing has both pros and cons. The pros of a soil nailing approach are that[1, 3]

- the method is economical, flexible and environmentally friendly.
- active design is possible. That is the design approach can be combined with an onsite measurement and various specifications can be changed accordingly.
- it is less disruptive to traffic
- construction is relatively rapid

- it uses less construction materials than ground anchors
- it is advantageous at sites with remote access-as smaller equipment is needed
- is found to perform well during seismic events

The cons are that [1]:

- When (as it is mostly used) in masses such as sands, gravel and moraine, the mass must have some cohesion – 3 to 5 kPa – for the open-cut excavation must stand unsupported on its own for a while.
- When (sometimes) used in stiff and overconsolidated clay, undrained shear strength higher than 50 kPa is required. In addition, the clay must not have plasticity index higher than 20. Creep and little friction between the soil and the nails can also be problematic.
- The method is not used when ground table is higher than the excavation bottom. Surface water and other water in the ground must be drained away [2].
- It may be costly when very strict deformation control is required for structures and utilities behind the proposed wall [3].

1.3 Elements of a soil-nail system

The basic components of a soil-nail system are steel reinforcing bars, grout, facing, drainage system, nail head and corrosion protection. Different parts of a soil-nailed system formed by the drill-and-grout method are the following. See [2].

1. *Steel reinforcing bars* - The steel reinforcing bars are the main component of the soil-nail wall system and it can be hollow or solid. Its primary function is to provide tensile resistance. These elements are placed in pre-drilled drill holes and grouted in place.

2. *Spacers or centralizers* – Which are PVC material used for centering the steel bar in the borehole and placed with center to center distance of 1.5m to 2m.

3. *Grout* - cement and water grout mix, is injected in a pre-drilled hole after the soil-nail reinforcement installation. It helps transferring stress from the ground to the nail and used as a corrosion protection to the soil-nail.

4. *Corrosion Protection Elements* - Protective sheathings made of corrugated synthetic material [HDPE (High Density Polyethylene) or PVC tube) surrounding the nail bar re usually used to provide additional corrosion protection.

5. *Nail Head* - A nail head typically contains a steel bearing plate, hex nuts and washer. It is transfer the bearing load from the soil to the soil-nail and promotes local stability of the ground near the slope surface and between soil-nails.

6. *Wall Facing* - A slope facing generally serves to provide the slope with surface protection, and to minimize erosion and other adverse effects of surface water on the slope. It may be soft, flexible, hard, or a combination of the three (CIRIA, 2005) [4].

7. *Drainage System* - vertical geocomposite strip drains are usually installed between the temporary facing and the excavation to prevent water pressure from developing behind the wall facing.

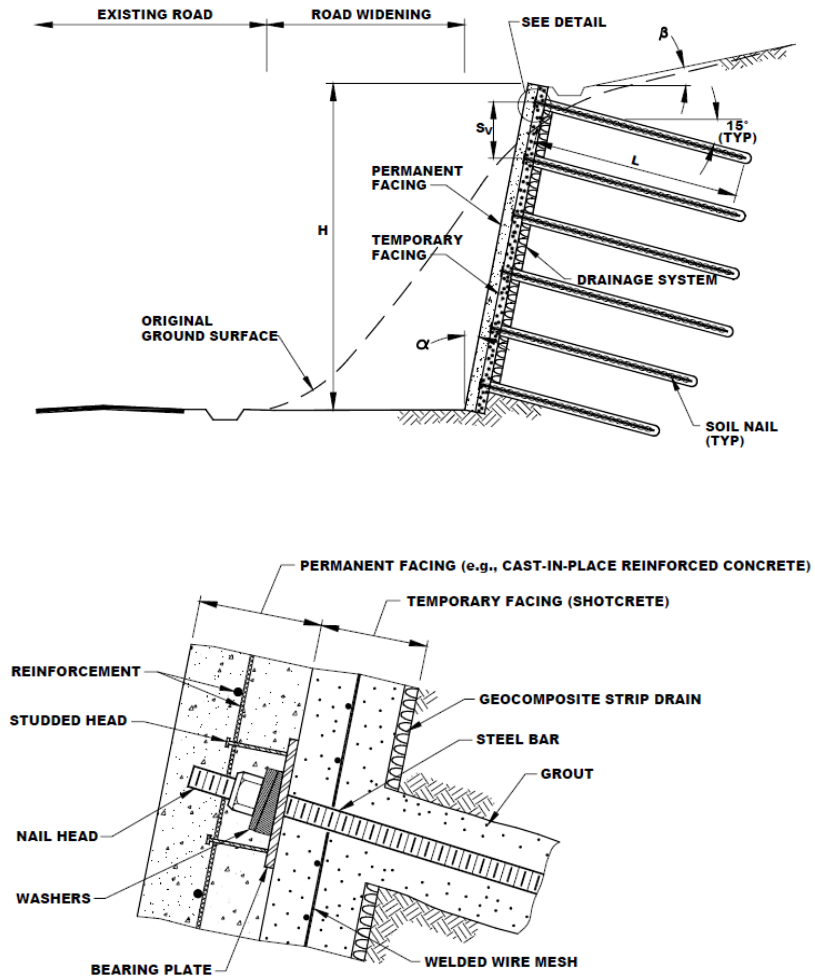

Figure 1. 1: Typical cross section of soil-nail system [2]

1.4 Design parameters of a soil-nail system

The design parameters of a soil nail system may be distinguished into *configuration parameters* and *material parameters*. Configuration parameters include geometric parameters such as *nail inclination*, *nail spacing*, *wall-batter*, *back slope*, *nail pattern* and *height*. Whereas material parameters include *soil properties*, *nail properties*, *facing wall material parameters* and *interaction parameters*.

1.5 Objectives of the thesis

The main objective of this thesis is conducting numerical studies on

1) The effect of various *configuration parameters* such as

- nail inclination,
- Nail spacing,
- wall-batter,
- back slope, and

2) The effect of *soil parameters* such as
   - cohesion,
   - friction angle, and
   - dilatancy angle, on the stability of a soil nail system.

Related objectives are

- conducting literature review on the state-of-the art and the state-of-the practice of soil nailing as an inclined ground stabilization technique.
- comparison of results from Geosuite analysis based on limit equilibrium methods and Finite element analysis results using the Plaxis-2D commercial finite element package.
- comparison of results between Plaxis-2D and Plaxis-3D analyses results such as safety, structural forces and deformations
- investigation of '3D effects' and effect of nail pattern on the stability of nailed slopes.

1.6 Methodology

The methodology employed in this thesis are mainly literature review, theoretical analysis and numerical investigation.

1.7 Limitations

Due to the limited study period, certain components of a soil-nail configuration-particularly the effect of the back-slope is not investigated in both Geosuite and Plaxis

analyses. The study is mainly numerical and experimental investigations have not been carried out as part of this study.

1.8 Organization of the thesis

The thesis is organized as follows. In Chapter 2, literature review is conducted. In chapter 3, Classical methods of analysis of internal and external stability of a soil nail system are presented. A base case is selected and the simple wedge method is applied for investigation of effect of the various configuration and soil parameters on the safety factor of a given soil-nail slope. Chapter 4 employs the Geosuite software for numerical investigation of effect of the soil nail configuration parameters on the safety factor. In chapter 5, Plaxis-2D, a finite element method is employed. Effects of the different parameters on safety and failure mechanism are numerically studied and compared to the previous results. Furthermore, the effect of the various parameters on deformation and nail and facing structural forces are investigated. Chapter 6 employs the Plaxis-3D so as to investigate '3D effects'. In Chapter 7, a case study, that concerns the design and analysis of a soil nail system is presented. Finally, Chapter 8 presents summary, conclusions and recommendations for further work.

CHAPTER 2: Literature review

In this chapter, a literature review is conducted with the objective of presenting structural components that make up the soil-nail system, construction procedures, design considerations, stability and effect of nail configuration parameters and deformation characteristics.

2.1 Construction phases

The typical sequence of a soil nailing system is described as follows:

1. *Excavation.* Excavation is done in multiple stages. The depth of each excavation is determined by the ability of the excavated face to remain stable without support for a short period-often a day or two. For this reason, the soil must have some cohesion for soil nailing to be applicable. The excavation must be carried out with due care such that ground disturbance is minimized [2].

2. *Drilling nail holes.* After each unsupported excavation, holes are drilled according to the specified inclination-often 10-20^0 [1], diameter (100-200 mm), length and spacing-often 1-1.5 m [1].

3. *Installation of nails and grouting.* Nails can be solid or hollow. The details of the soil-nails depend on whether the construction is temporary or permanent. For permanent construction, placeholders (also called centralizers, spacers) will be placed on the nail bars-usually c/c 1.5 – 2 m. If corrosion is expected corrugated, plastic cover is used. Then, the bars will be placed in the pre-drilled hole. They can also be self-drilling-but rarely used [1]. The drill hole is grouted using cement grout delivered into the drill hole through grout pipes.

4. *Construction of temporary shotcrete facing.* Before the next excavation phase, the open-cut soil section is supported with a temporary facing-often a shotcrete with reinforcement net or fiber reinforcement. For temporary construction, the thickness of the shotcrete slab is 8-10cm [1]. The reinforcement –typically a welded wire mesh-is placed at the middle of the facing thickness. Following the curing of the shotcrete construction, the nail head is secured against a bearing plate placed on the facing. Before proceeding to the next excavation sequence, the shotcrete must cure until it achieves a specified strength-often for about 3 days.

5. Steps 1 to 4 are repeated for the next excavation stages. After the last excavation stage a final facing-which can be cast in place reinforced concrete, reinforced shotcrete or prefabricated panels-may be installed.

2.2 Design considerations of a soil-nail system

The design of a soil-nail system follows the following considerations, which are iterated at different stages of the design.

1. *Wall lay out.* Wall lay out includes wall height, length and the face batter of the wall. The determination of the wall height depends on the height of the soil mass that needs to be supported during excavation. The face batter typically ranges between 0 -10^0. For a face batter greater than 10^0, stability is greatly improved the required nail length may also reduce [1]. On the other hand, increasing the face batter-for a given excavation depth-increases the wall length and may increase the construction cost.

2. *Soil-nail pattern, vertical and horizontal spacing.* The soil-nail pattern can be rectangular/square, staggered, etc. Square pattern is the most commonly adopted. This is mainly because, a square soil-nail pattern facilitates easier installation of precast concrete and enables continuous installation of geocomposite drain strips. Staggered patterns result in a uniform distribution of earth pressure. They can be selected in the case of soils that have less margins to redistribute loads. The design forces and global stability are affected by the choice of nail spacing. The choice of the vertical spacing is governed mainly by the excavation depth that can be carried out without support. According to [2], Each nail has an influence area of $S_V \times S_H \leq 4m^2$ and the vertical (S_V) and horizontal (S_H) nail spacing range from 1.25 – 2m. Statensvegvesens [1] manual recommends 1 – 1.5 m. A soil-nail spacing of 1.5 m is routinely used and is preferred for conventional drilled and grouted soils. The use of uniform distribution of nail spacing is beneficial for it simplifies construction and quality control.

3. *Soil-nail inclination.* The choice of soil inclination depends on the presence of utilities, other ground structures and the location of the stronger soil zone. According to FHWA [2], typical inclination of soil-nails is 10-20^0 and soil-nail inclination less than 10^0 is not recommended as the chance of creating voids in the grout is high. However, the Statensvegvesens manual [1] gives a range of 5-20^0 to be the usual.

4. *Nail length and distribution.* Nail length can be variable or uniform. FHWA recommends that a uniform length should be selected whenever possible. Non-uniform nail length if variable soil conditions are encountered. For a pre-bored

and grouted nails, using nail length 0.5H-0.8H is common [1]. For a sloping back terrain the nail length must increase up to 1.2H [1].

5. *Soil-nail material type*. The steel reinforcing bars are commonly threaded and may be either hollow or solid. For ductility reason, bars with low grade are preferred. They are also less susceptible to corrosion and readily available in market.

Other considerations. The site condition-such as the soil type, the geotechnical characterization, the ground water level and the corrosion potential need to be investigated and the various components should be adjusted accordingly.

2.3 Possible failure modes of a soil-nail system

Sol-nail systems can fail for several reasons and in various ways. In literature, the different failure modes are grouped into-*internal*, *external* and *facing failures*. The internal failures are due to *nail-soil pullout failure*, *bar-grout pullout failure*, *nail tensile failure*, *nail bending and shear failure* whereas external failures are failures due to *global instability*, *sliding* and *bearing failure*. Geotechnical design focuses on designing safety soil-nail system for the external and the internal failure modes. The third types of failure-facing failures are more of structural failures. They include failures due to buckling and punching of the facing and shearing and breakage of facing nail connections.

Table 1. 1: Internal failures [5]

Internal failures	**Description**	**Illustrations**
1.1 Slippage of bar grout interface	It is the mechanical interlocking of grout between the protrusions and "valleys" of the nail bar surface that provides resistance against slippage along the grout and steel bar interface. It is recommended that threaded bars be used such that higher interlocking is developed.	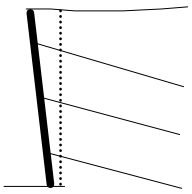 Bar-grout pullout failure
1.2 Nail Pullout Failure	The soil-nail-system can fail along the soil-grout interface due to insufficient intrinsic bond strength and/or insufficient nail length.	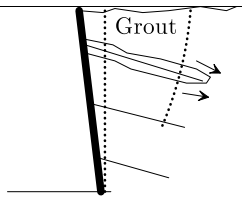 Soil nail pullout failure
1.3 Tensile Failure of the Nail	The nail can fail in tension if there is inadequate tensile strength.	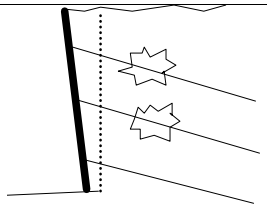 Nail tensile failure
1.4 Bending and Shear of the Nails	Soil-nails work predominantly in tension, but they also mobilize stresses due to shear and bending at the intersection of the slip surface with the soil-nail (Schlosser, 1983; Elias and Juran, 1991) [6, 7]. The shear and bending resistances of the soil-nails are mobilized only after relatively large displacements have taken place along the slip surface. Some researchers have found that shear and bending nail strengths contribute no more than approximately 10 percent of the overall stability of the wall. Due to this relatively modest contribution,	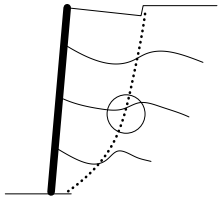 Nail bending and/or shear failure

	the shear and bending strengths of the soil-nails are conservatively disregarded in the guidelines contained in this document. A discussion of a methodology to account for shear and bending contributions is included in Elias and Juran (1991) [6].	

Table 1. 2: External failures [5]

External failures	**Description**	**Illustrations**
2.1 Global stability failure	Refers to the overall stability of the soil nail wall. Instability occurs deriving forces on the mass within the lip surface exceed the resisting forces. The soil nail increases the resisting forces.	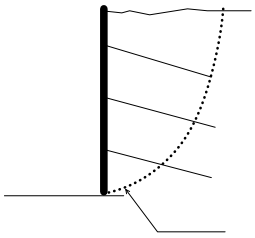 Global stability failure
2.2 Sliding stability failure	Sliding stability failure occurs when due to earth pressure behind the soil nails exceeds the sliding resistance along the base of the retained system.	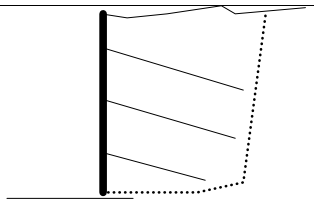 Sliding stability failure
2.3 Bearing failure	This is due to bearing failure of the foundation and may be problematic in the case of fine-grained soils.	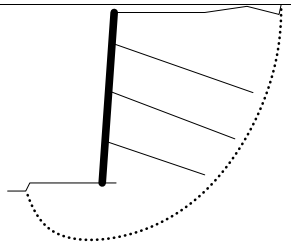 Bearing failure

Table 1. 3: Facing failures [5]

Facing failures	**Description**	**Illustrations**
3.1 Flexural failure	-Due to excessive bending beyond the capacity of the facing.	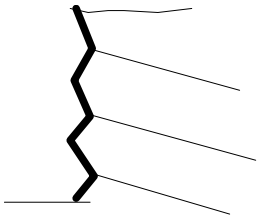 Facing flexure failure
3.2 Punching shear failure	Failure mode around nails.	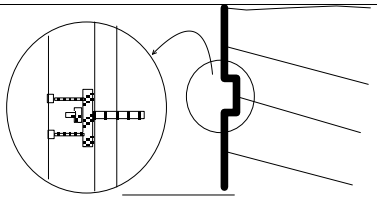 Facing punching shear failure
3.3 Head stud failure	Failure of connection bolts at nail heads	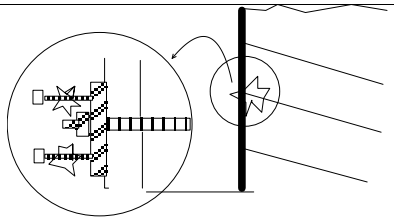 Headed-stud failure

2.4 Soil-nail system interaction

The principal idea behind soil nailing is that the soil-nails lend resistance to limit front wall deformation and reduce the risk of global slope stability failure-mainly through mobilization of shear stresses along the grout- soil interface. The interaction between soil-nails, the soil and the facing is quite complex and the mobilized shear stress at soil-nail grout-soil interface is not uniform in general. It also depends where the slip surface cuts the soil-nail. The mobilized shear stress at the grout-soil interface that contributes to the stability of the system is the one that occurs behind the slip surface. The length of the nail behind its intersection with the slip surface is the length that

develops pull out resistance. See Figure 2. 1. According to the FHWA [2] report, the maximum tensile forces, as obtained from full scale instrumented tests, in the upper portion of the walls occurs approximately between 0.3H and 0.4H, where H is the vertical height of the wall and in the lower portion of the walls approximately between 0.15H to 0.2H behind the wall facing. In the same report, based on data collected from 11 instrumented sites, the estimates of the maximum tensile nail force were given, on average as

$$T_{\max} = \begin{cases} 0.75K_a\gamma_s HS_V S_H, & z \geq \dfrac{1}{3}H \\ 0.37K_a\gamma_s HS_V S_H, & z < \dfrac{1}{3}H \end{cases}$$

in which, H is the wall height, z is vertical distance from the bottom of the excavation, K_a is the active earth pressure, γ_s is the saturated unit weight of the soil mass behind the proposed wall, S_V is the vertical nail spacing and S_H is the horizontal wall spacing.

The empirical equation given above implies that $T_{\max}/S_V S_H$ is smaller than that which could have been estimated from active lateral earth pressure.

The tensile force at the face wall is referred to as nail head force and often denoted T_0 . Excluding frost action and other factors, it may be roughly estimated, according to FHWA [2], from the following empirical equation.

$$T_0 = (0.4 - 0.7)K_a\gamma_s HS_V S_H, \; z \geq \frac{1}{3}H$$

Other suggestions are also available in literature. For instance, Clouterre (2002) [8] suggested

$$T_0 = T_{\max}\left[0.6 + 0.057(\max\{S_V, S_H\} - 3)\right]$$

where S_V and S_H are measured in feet. In FHWA, for normal conditions of loading, a typical value of the nail head force 70% of the maximum tensile nail force is suggested.

The Statensvegvesen manual [1] adopts an earlier publication of [9] which probably needs updating.

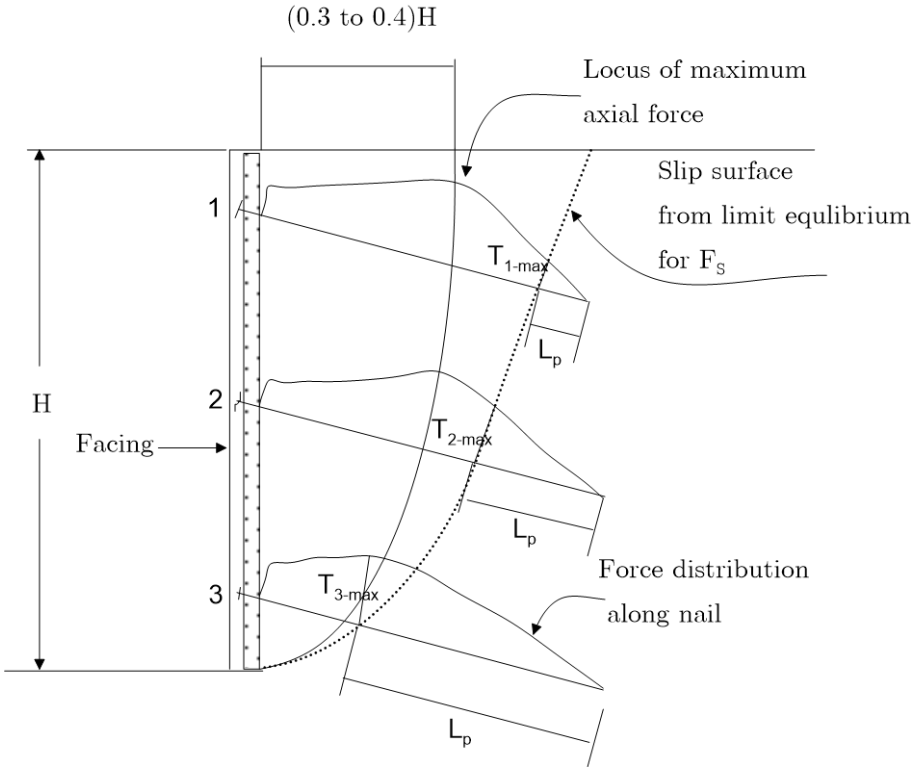

Figure 2. 1: Illustration of location of maximum tensile forces in soil-nails [2]

The application of a soil-nail system is to limit deformation of the slope and make sure adequate safety factor against sliding, bearing and global instability. Bearing capacity is often checked for short-term stability conditions-if undrained conditions are expected. Such may be required when the soil mass in consideration is clay or when it contains significant amounts of clay and the rate of construction is fast. The most important geometric parameters that affect the stability of soil nailing constructions are [1]

- nail length
- nail inclination
- wall-batter- front wall (facing) inclination
- the inclination of the terrain at the back of the wall

2.3 Effect of soil-nail configuration on the global stability

The important soil-nail system geometric parameters are nail length, nail inclination, back terrain inclination and wall-batter.

2.3.1 Effect of soil-nail inclination

For a given configuration, observations confirm that with a variation of nail inclination the factor of safety varies. The variation is not random. For lower nail inclination, safety factor increases with an increase in nail inclination until it reaches a critical value. Beyond the critical nail inclination, factor of safety is seen to decrease consistently with an increase in nail inclination, Figure 2. 2. Research results also show that, for a given safety factor, the required nail length per unit meter wall decreases with increasing nail inclination, Figure 2. 3.

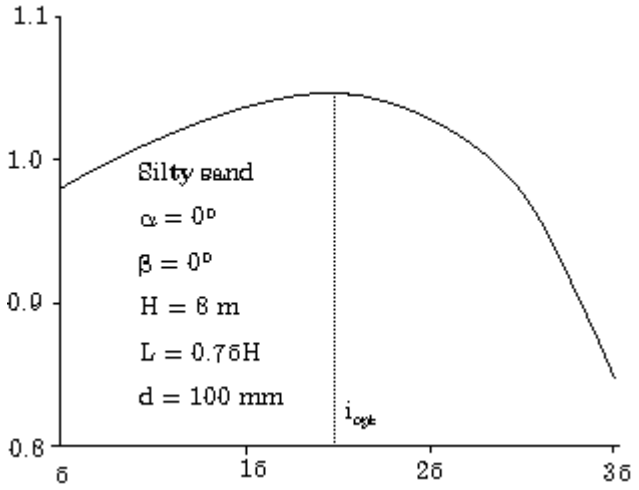

Figure 2. 2: Optimal inclination of the soil nail from the horizontal direction [10]

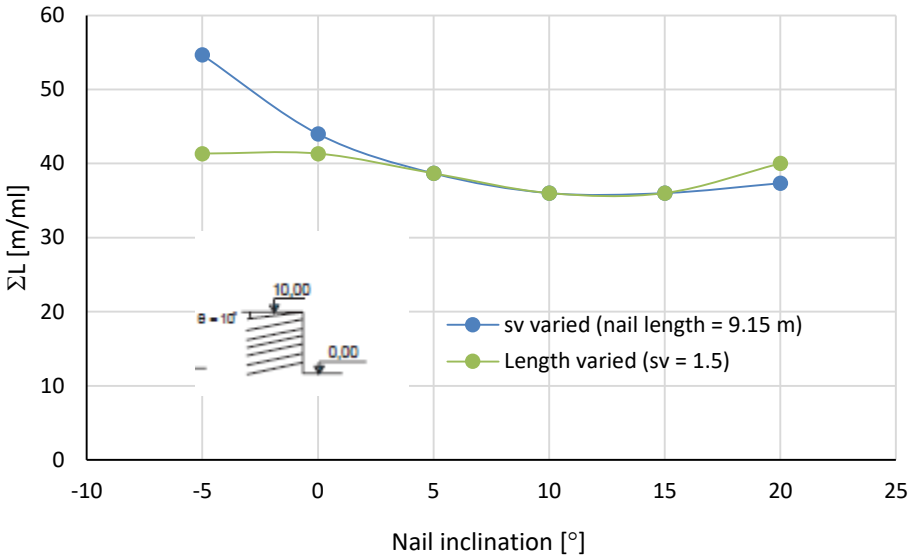

Figure 2. 3: Influence of nail inclination on nail length (for γ'= 20 kN/m^3, c' = 0, ϕ = 30^o, T_L/L = 40 kN/ml, F =1.5). Cloutere [9]

2.3.2 Effect of wall-batter

For a given configuration, both common sense and observation confirm that with an increase in inclination of the wall-batter the factor of safety increases. For a given soil-nail configuration and factor of safety, with an increase in wall-batter the required nail length per meter wall decreases. Figure 2. 4 is taken from Cloutere [9] and shows plot of nail length per meter wall length against wall-batter angle for a given factor of safety. One of the curves is obtained by directly varying the length and the other one is obtained by changing nail spacing.

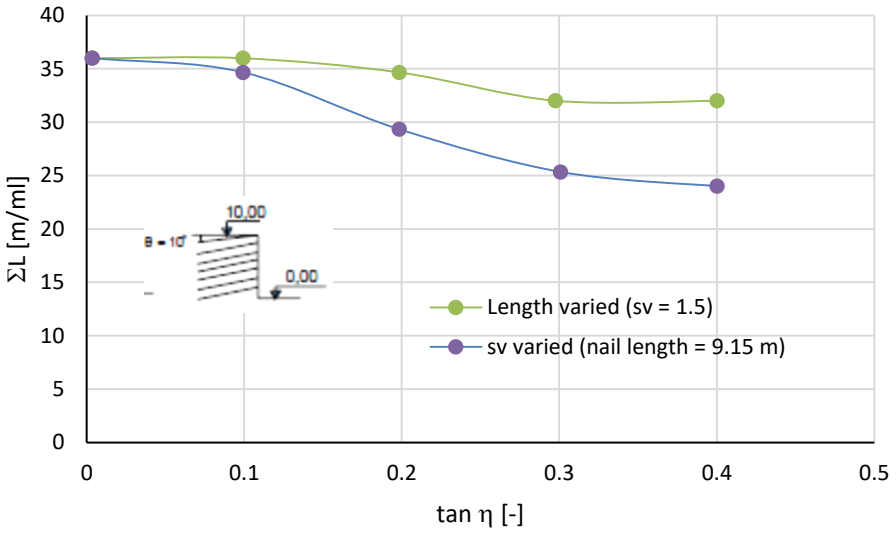

Figure 2. 4: Influence of wall-batter on nail length (for γ'= 20 kN/m^3, c' = 0, ϕ = 30^o, T_L/L = 40 kN/ml, F 1.5). Reproduced from Cloutere [9]

2.3.3 Effect of back-slope

For a given configuration, both common sense and observation confirm that with an increase in inclination of the back-slope the factor of safety decreases. For a given soil-nail configuration and factor of safety, the required nail length per meter wall increases with an increase in back-slope. Figure 2. 5 is taken from [9] and shows nail length per meter wall length for obtaining the same factor of safety. One of the curves is obtained by directly varying the length and the other by changing nail spacing.

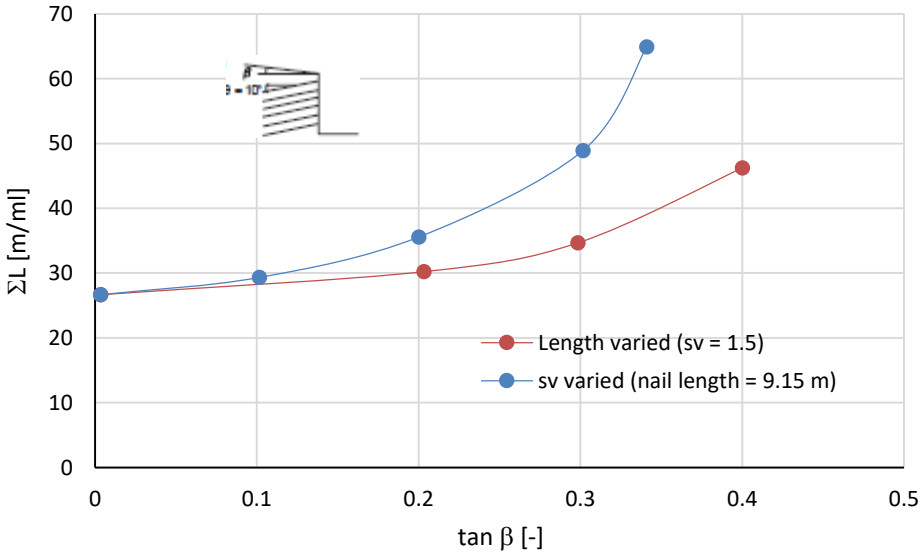

Figure 2. 5: Influence of back slope on nail length (for γ'= 20 kN/m^3, c' = 0, ϕ = 30^o, T_L/L = 40 kN/ml, F =1.5). Reproduced from Cloutere [9]

2.4 Deformation considerations

Serviceability of the soil-nail wall depends on the amount of deformation the wall undergoes. A soil-nail wall and the soil behind it have a tendency to deform outwards at any phase (during construction or after its completion). Vertical displacements (i.e., settlements) of the wall at the facing are generally small, and are on the same order of magnitude as the horizontal movements at the top of the wall. Maximum horizontal displacements occur at the top of the wall and decrease progressively toward the toe of the wall. In general, horizontal and vertical displacements of the facing depend on the following factors (FWHA) [11].

- wall height, H, (deformation increases approximately linearly with height);
- wall geometry (a vertical wall produces more deformation than a battered wall);
- the soil type surrounding the nails (softer soil will allow more deformation);
- nail spacing and excavation lift heights (larger nail spacing and thicker incremental excavation lifts generate more deformation);
- global factor of safety (smaller FSG's are associated with larger deformation);
- nail-length-to wall-height ratio (shorter nail lengths in relation to the wall height generates larger horizontal deformation);
- nail inclination (steeper soil-nails tend to produce larger horizontal deformation because of less efficient mobilization of tensile loads in the nails); and
- magnitude of surcharge (permanent surcharge loading on the wall increases deformation).

Typical deformations are given in Table 2. 1

Table 2. 1: Values of (δh/H) and C as functions of soil conditions [11].

Variable	Weathered rock and stiff soil	Sandy soil	Fine-grained soil
h/H and v/H	1/1000	1/500	1/333
C	1.25	0.8	0.7

For sloping terrain with inclination angle β the following relation is proposed for the horizontal deformation;

$$\delta_{h,slope} = \delta_h(1+\sin\beta)$$

where δ_h is the deformation of a vertical wall top and β is the back slope.

The size of the zone of influence which is caused by the wall deformation is defined by the horizontal distance behind the soil-nail wall, λ (see Figure 2. 6). This distance of influence is estimated according to [11]:

$$\lambda = CH(1-\tan\eta)$$

where C is constant given in Table 2. 1 and η is the face batter. The Statensvegvesen design manual adopts slightly different values for both the deformation ratio and the value of C.

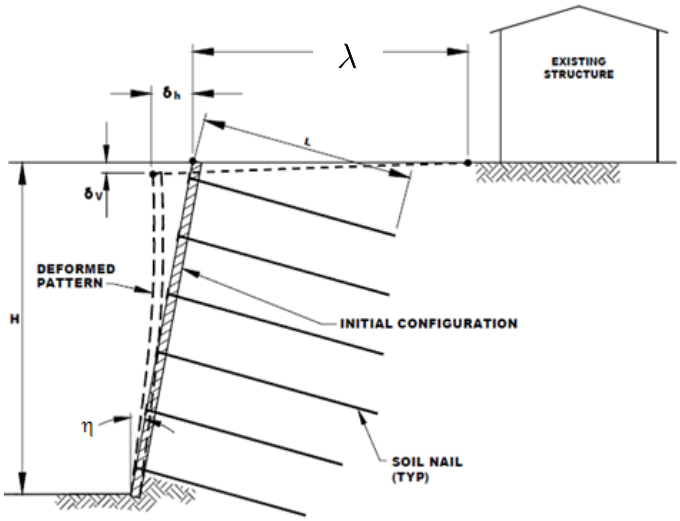

Modified after Byrne et al. (1998).

Figure 2. 6: Deformation of soil-nail wall [11]

2.5 Experience based design parameters

The four ratios that are considered for an initial design of a soil nail system based on previous experiences are defined as follows.

1) Length ratio,

$$L_r = \frac{Nail\,length}{Excavation\,height} = \frac{L}{H}$$

2) Friction ratio,

$$f_r = \frac{drillhole\,diamater \cdot nail\,length}{nail\,spacing} = \frac{D \cdot L}{S_v \cdot S_h}$$

3) Strength ratio,

$$s_r = \frac{nail\,diamater^2}{nail\,spacing} = \frac{D^2}{S_v \cdot S_h}$$

4) Deformation ratio,

$$d_r = \frac{Horizontal\,deformation}{Excavation\,depth} = \frac{\delta_h}{H}$$

Table 2. 2: Experience for soil nails, after Bruce and Jewell [12]

Parameter	**Bored and grouted (Gravel and sand)**	**Bored and grouted (moraine and hard clay)**	**Driven**
Length ratio	0.5-0.8*	0.5-1*	0.5-0.6*
Friction ratio	0.3-0.6	0.15-0.2	0.6-1.1
Strength ratio	$0.4x10^{-3}$-$0.8x10^{-3}$	$0.1x10^{-3}$-$0.25x10^{-3}$	$1.3x10^{-3}$-$1.9x10^{-3}$
Deformation ratio	0.001-0.003	0.001-0.003	No data

*The given table is for horizontal terrain at the back. For inclined back terrain, the nail length can increase up to 1.2H.

CHAPTE 3: Classical methods for analysis of internal and external stabilities

In this chapter, some classical methods of evaluation of internal and external stabilities of a soil-nail system are presented. In the end, one of the simple methods-called the wedge method is applied for numerical investigation of effect of various soil-nail configuration parameters on stability of a soil-nail system.

3.1 Nail pullout capacities

In general, nail capacities are distinguished into pullout capacity, tensile capacity, facing capacity. Among these capacities we shall here describe and estimate the pullout capacity.

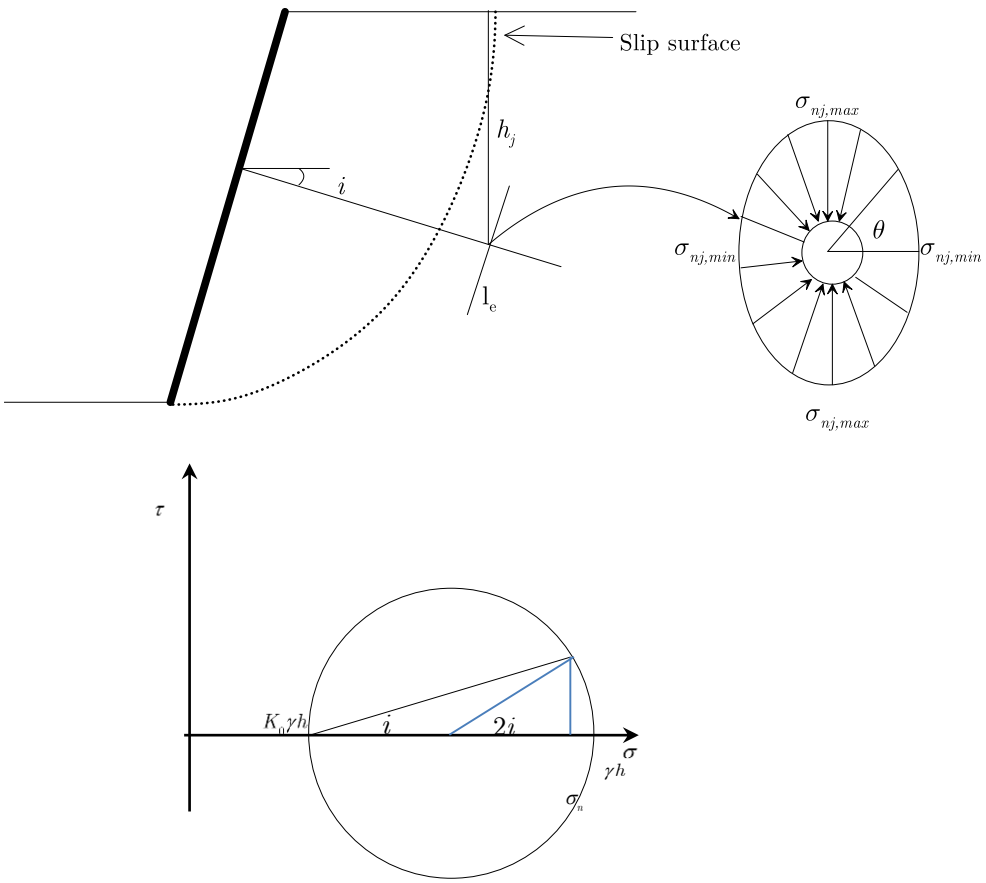

Figure 3. 1: Schematization of normal forces on nails and stress state in Mohr's stress circle.

For j^{th} nail the confining pressure onto the nails at any depth h_j may be estimated from

$$\sigma_{nj,\max} = \left\{K_0 + (1-K_0)\cos^2 i\right\}(\gamma h_j + q)$$

$$\sigma_{nj,\min} = \left\{K_0 + (1-K_0)(1-\cos^2 i)\right\}(\gamma h_j + q)$$

where i is the soil inclination, q is the permanent surcharge load on the slope, K_0 is the at rest earth pressure coefficient. Note that, here, the major and the minor principal stresses are considered to be vertical and horizontal respectively. If such is not the case, the inclination can be taken an angle between the direction of the minor principal stress and that of the nail.

Let us assume an elliptic pressure distribution around the nail. Tsegaye suggested the following equation for the normal stress (Tsegaye, AB. 2016, personal communication)

$$\sigma_{nj}\left(\theta, h_j\right) = \frac{\left(K_0 + (1-K_0)\sin^2 i\right)^2}{K_0 + (1-K_0)\cos^2 i + \sqrt{(1-K_0^2)\cos 2i}\cos\theta}(\gamma h_j + q)$$

Let the back terrain has a slope, β. Let the facing slope be η and the nail inclination be i. Let x be measured from the bottom of the facing towards the back. Let the vertical spacing between the nails be S_v. Then for $x \geq x_{ss}$, where x_{ss} is the horizontal distance to the point where the particular nail crosses the slip surface, h_j may be calculated as

$$h_j = (\tan\beta + \tan\eta\tan i)x - (\tan\beta + \tan i)\tan\eta H + \frac{1}{2}(1 + \tan\eta\tan i)jS_v, \quad j = 1,2,3,\ldots.$$

$$T_n = \frac{1}{FOS_T}\int_{x_{ss}}^{l} \pi d c \mathrm{d}x + \frac{1}{FOS_T}\int_{x_{ss}}^{l}\int_{0}^{2\pi} \frac{d}{2}\mu\sigma_n \theta \mathrm{d}\theta \mathrm{d}x$$

$$T_n = \frac{1}{FOS_T}\int_{x_{ss}}^{l} \pi d c \mathrm{d}x + \frac{1}{FOS_T}\frac{d}{2}\mu\int_{h_{j,ss}}^{h_{j,l}}\int_{0}^{2\pi} \frac{K_0 + (1-K_0)\sin^2 i^{\,2}(\gamma h_j + q)}{K_0 + (1-K_0)\cos^2 i + \sqrt{(1-K_0^2)\cos 2i}\cos\theta}\frac{1}{\sin i}\theta \mathrm{d}\theta \mathrm{d}h_j$$

It is assumed that only part of the nail behind the slip surface contributes to stabilize the slope. The mobilized nail tension is thus calculated using

$$T_n = \frac{\pi d q_u l_e}{FOS_T} = \frac{\pi d(c + \mu\bar{\sigma}_n) l_e}{FOS_T}$$

where

FOS_T is the factor of safety against nail tension. In literature a value of 1,5 is recommended.

$q_u = c + \mu\bar{\sigma}_n$ is the bond strength value

l_e is the length of the nail behind the slip surface

d is the diameter of the nail.

$\mu = k\tan\phi$ is mobilized soil-nail interface friction angle. $k \leq 1$ is a constant. $k \leq 2/3$ is suggested in literature. For driven nails, the skin friction may increase by a factor.

It is thus evident that the nail forces depend on the kind of slip surface is chosen.

The soil-nail interaction that occurs behind the wall facing is complex. Part of the soil-nail behind the failure surface is pulled out of the soil. Conceptual models in literature suggest that the tensile forces in the nail varies from the anchoring zone to the facing starting from zero at the end of the nail, increases to a maximum value in the intermediate length and decreases to a certain value at the facing. This typical diagram is shown in Figure 3. 3 [2]

For preliminary design purposes, a simplified distribution of nail tensile forces, shown in Figure 3. 4 is considered.

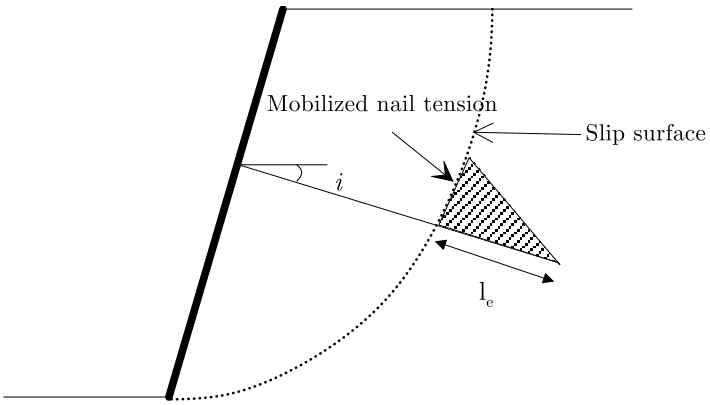

Figure 3. 2: Schematization of effective nail length and slip surface

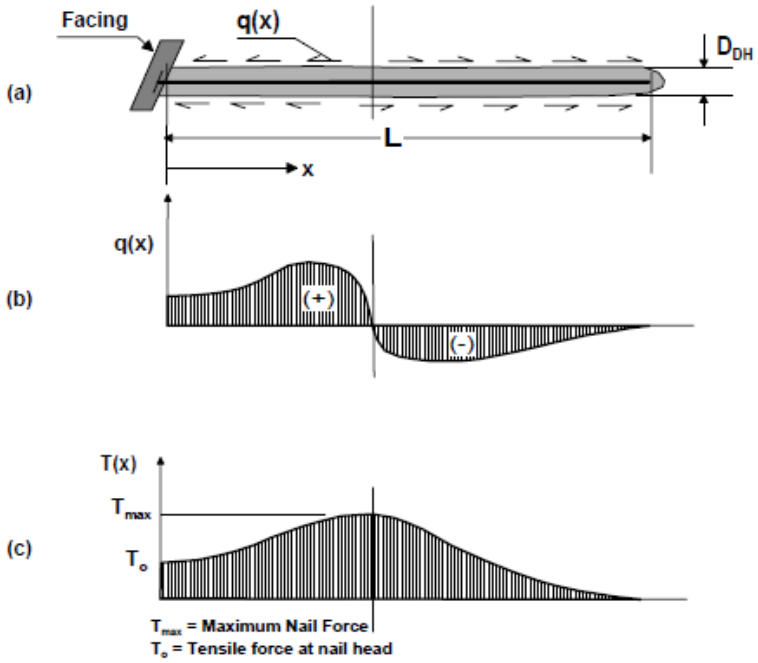

Figure 3. 3: Soil nail stress-transfer mechanism [2]

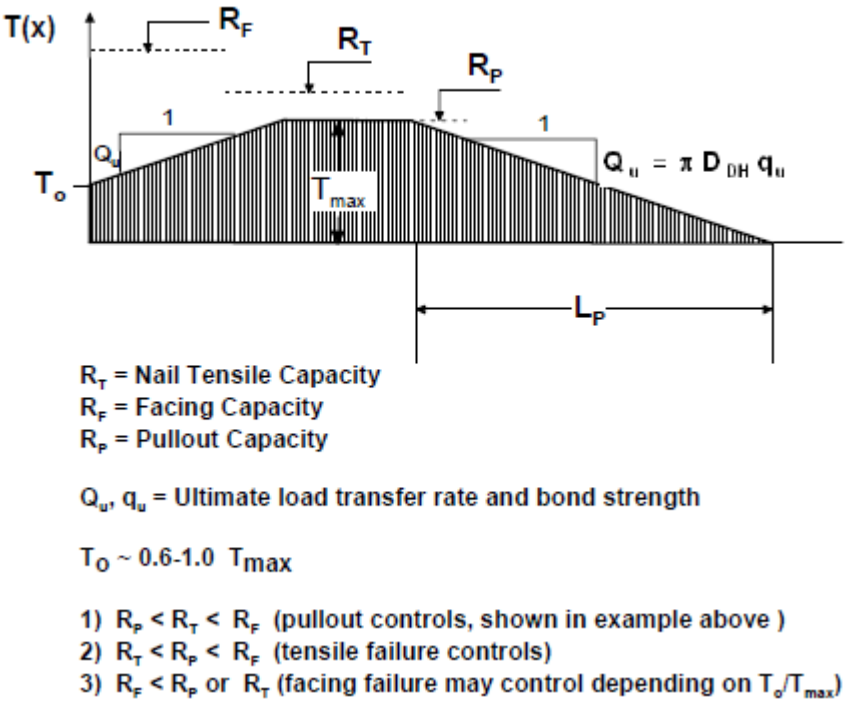

Figure 3. 4: Simplified distribution of nail tensile forces [2]

3.2 Global stability analysis

The stability of soil-nail system can be investigated using empirical methods, limit equilibrium methods, finite element methods (FEM) methods. The first two are frequently applied. Various limit equilibrium methods were extended to accommodate the soil nailing practice.

In the analysis of global stability of slopes, two dimensional limit equilibrium principles are quite popular. The same techniques could be used for soil-nailed slopes as well – with appropriate modification. In these approaches, the potentially sliding mass is modelled as a rigid block or a series of slices. Safety factors for various potential surfaces are calculated until the critical one with the least factor of safety is obtained.

1) Block Methods
2) Method of slices

Different shapes of failure surfaces have been proposed. Some of the proposed surfaces are planar, bi-linear, circular, parabolic and log spiral. However, comparisons among the different methods show that the differences in the factor of safety due to the use of different geometries of failure surfaces are insignificant. There have also been obtained comparable nail lengths for the same target safety factor.

3.2.1 Block methods

Block methods assume the sliding soil as a single block. The methods vary mainly in the assumption of the slip surface. One can find several of these methods in literature. Some of them are presented here.

1. Wedge method

In this method, a rigid block-failure mechanism is considered. The forces are then grouped into *stabilizing* and *destabilizing*. The destabilizing forces are the deriving component of the weight of the wedge (a component parallel to the slip surface), the surcharge load and inertial forces (specially the horizontal component). The stabilizing forces are the part the mobilized shear forces and the mobilized equivalent nail tensile forces. From this information, it is easy to calculate the factor of safety. In this method, only equilibrium of forces is considered and moment equilibrium is not guaranteed.

Let us look more closely at the formulation of this method. We begin by defining the different properties necessary to carry out analysis using this method.

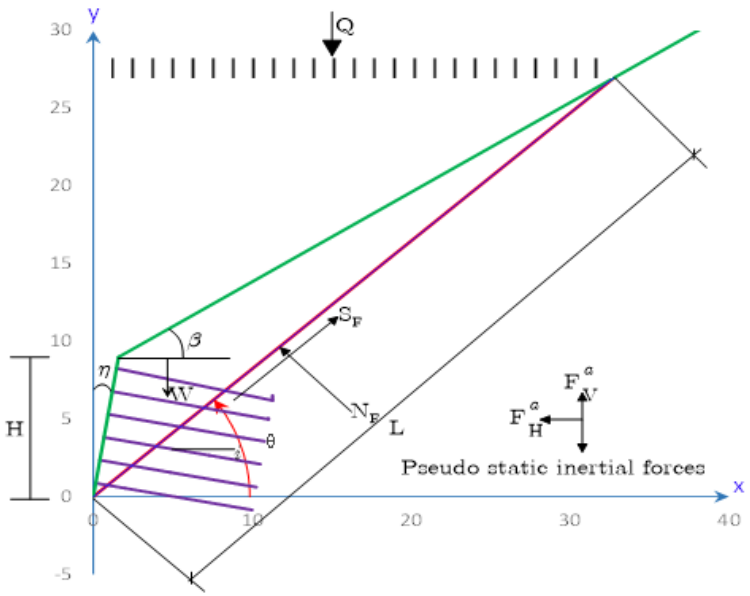

Figure 3. 5: Schematization of wedge method for global stability analysis of nailed slopes

Table 3. 1: Denotation of geometric properties and material parameters for the wedge method

Geometric properties		Nail		Soil properties		External loads	
H	Wall height	i	inclination of nails	γ	soil unit weight	Q	surcharge load
η	wall-batter			φ	friction angle	F_H^a	horizontal seismic load
β	back slope			c	cohesion	F_V^a	vertical seismic load
θ	inclination angle of the failure surface						

Next, we proceed to establish the equilibrium condition of the wedge using the variables presented in Table 3. 1.

- *Wedge properties*

  The length of the slip surface

$$L = \frac{H}{\cos\eta}\frac{\cos(\eta+\beta)}{\sin(\theta-\beta)}$$

The weight of the wedge

$$W = \frac{1}{2}\gamma H^2\left[\frac{\cos(\eta+\theta)}{\cos^2\eta}.\frac{\cos(\eta+\beta)}{\sin(\theta-\beta)}\right]$$

SF = mobilized shear forces

- *The normal and tangential forces on the failure surface*

$$\sum Normal\ forces = (W+Q\pm F_V^a)\cos\theta + T_{EQ}\cos(\theta-i) - F_H^a\sin\theta - N_F = 0$$

$$\sum \text{Tan}\ gential\ forces = (W+Q\pm F_V^a)\sin\theta - T_{EQ}\sin(\theta-i) - F_H^a\cos\theta - S_F = 0$$

The equivalent nail tensile force T_{EQ} can be determined by plotting a force polygon. Since we are considering the same inclination angle for all nails,

$$S_F = c_m L + N_F\tan\varphi_m$$

$$c_m = \frac{c}{F_{SG}},\ \varphi_m = \frac{\varphi}{F_{SG}}$$

c_m is the mobilized cohesion and φ_m is the mobilized friction angle

- *Factor of safety*

$$F_{SG} = \frac{\sum resisting\ forces}{\sum deriving\ forces}$$

$$F_{SG} = \frac{cL + (W+Q\pm F_V^a - F_H^a\sin\theta)\cos\theta\tan\varphi_m + T_{EQ}\cos(\theta-i)}{(W+Q\pm F_V^a)\sin\theta - T_{EQ}\sin(\theta-i) - F_H^a\cos\theta}$$

2. Circular arc method

This too is one of the block methods. Instead of the planar mechanism, a circular block is considered. It is often used for clayey mass (or in the so-called undrained or short-term stability-s_u approach as it is often referred in the Norwegian practice). A circular slip surface chosen and a factor of safety is calculated.

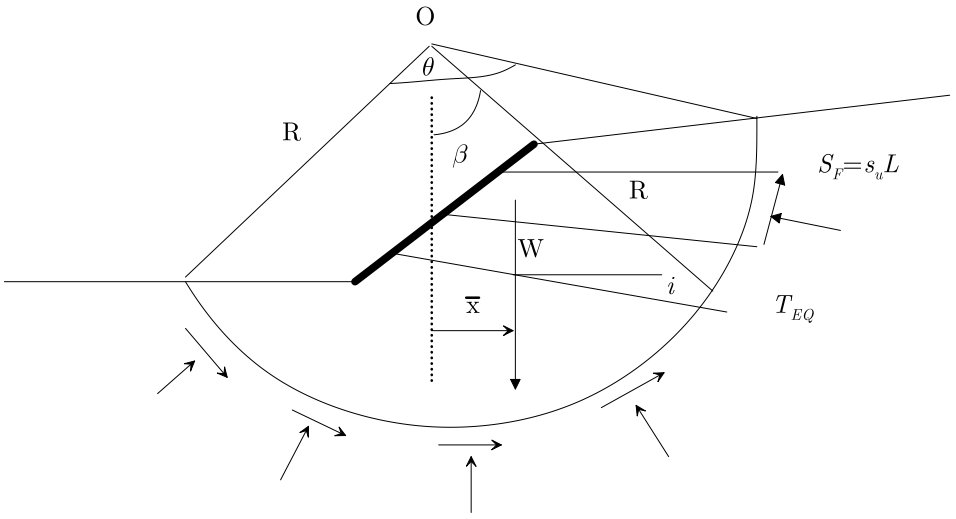

Figure 3. 6: Schematization of nailed-slope stability analysis with a circular arc method

The task is repeated until a configuration with a minimum factor of safety is obtained. The factor of safety is derived from moment equilibrium about the center of the slip circle. Equilibrium of forces is not guaranteed. A typical configuration of a circular arc failure for nailed slope is shown in Figure 3. 6.

Considering equilibrium of moment about O, the factor of safety for such a block stability analysis is given by

$$FS_G = \frac{S_u R^2\theta + (T_{EQ}\cos i)(R\cos\beta)}{W\overline{x} + T_{EQ}\sin iR\sin\beta}$$

in which:

θ = angle subtended by the slip circle at the center, O.

β = angle between horizontal plane and the tangent at the point of intersection of nail equivalent force with the failure surface.

i = Nail inclination of equivalent nail tensile force.

R = Radius of circular arc

$L = R\theta$ = Length of the slip surface

S_F = Shear force on failure surface

3. Friction circle method-

Friction circle method is again one of the block methods. It is similar to the circular arc method. Indeed, as far as the geometric set up is considered there is no much difference between the two. Here, a toe circle is used. However, instead of the undrained strength, the friction-attraction strength couple is used along the slip circle. This method is suitable for a rough calculation of long-term stability, or when the mass in consideration is a frictional mass. The method satisfies both force and moment equilibrium. It is a graphic method. With a careful setup, a spreadsheet program may be developed to facilitate the analysis.

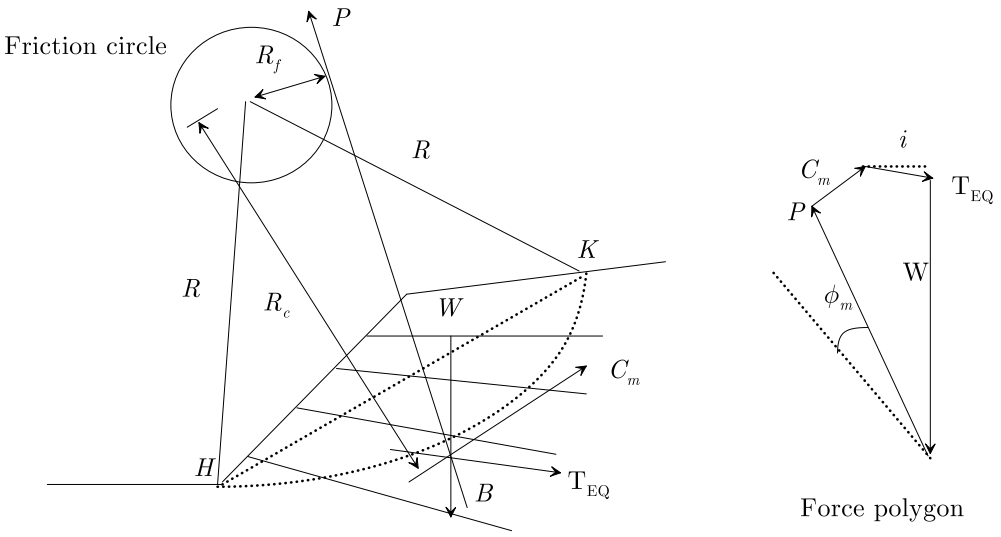

Figure 3. 7: Schematization of the friction circle method

Steps:

- The resultant force of the block weight and the equivalent nail force passes through B.
- The direction of C_m is parallel to chord HK.

- The value of mobilized cohesion, C_m, is calculated from the closed force polygon.
- The factor of safety is calculated assuming that the factor of safety against cohesion and friction is the same.

4. The German method: -

The method is summarized in Gassler (1987) [13]. It is based on bilinear failure mechanism, Figure 3. 8.

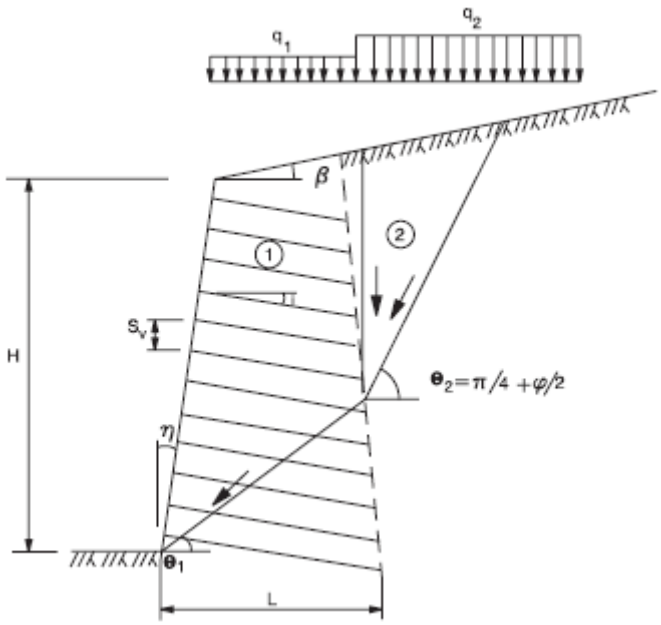

Figure 3. 8: Bi linear failure mechanism in the German method, after Gasssler (1987) [13]

5. The French method

This method is summarized in Clouterre (1991) [9]. The method takes into account both tension, shear and bending in the nails (hence is called a multi criteria method).

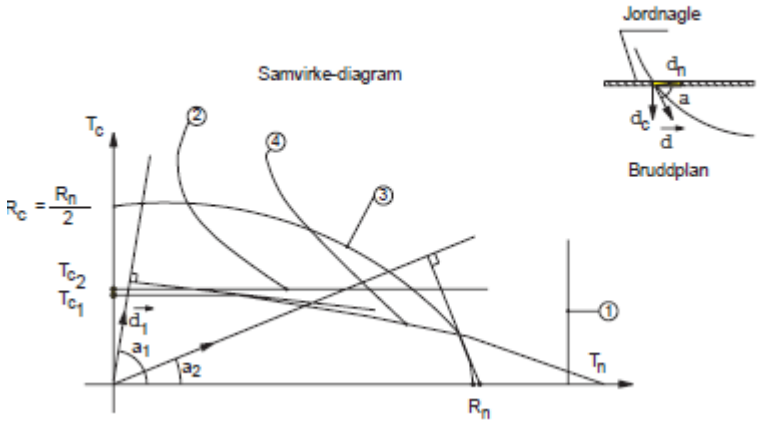

Figure 3. 9: Combination of failure mechanisms in the French method. Cloutere (1991) **[9]**

6. Juran's method

The method is developed by Juran (1991) [6] and assumes a log spiral failure mechanism. The method is summarized in [9] .

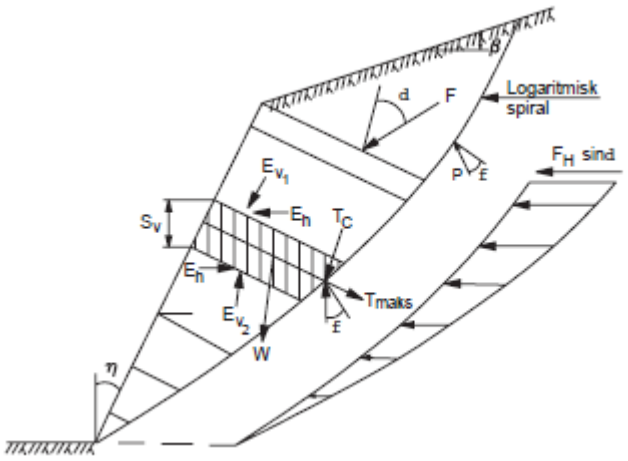

Figure 3. 10: Jurans method with logarithmic failure mechanism, after Cloutere (1991) **[9]**

3.2.2 Methods of slices

In this category of slope-stability analysis methods, the domain of soil within the assumed failure surface is discretized into a number of slices for which force and/or moment equilibrium is to be satisfied. Accordingly, the global factor of safety is calculated.

1. Bishop's simplified method

Bishop's simplified method is one of the earliest among the methods of slices. A circular failure surface discretized into a number of vertical slices is used. Each slice is then treated as a unique sliding block. Simplified Bishop Method satisfies vertical force equilibrium for each slice and the overall moment equilibrium of the system. The normal stress is considered at the midpoint of the base of the slice. Nail tensile forces are considered in the slices in which nails emerge at their base. The method does not assume inter slice forces and fails to satisfy horizontal force equilibrium.

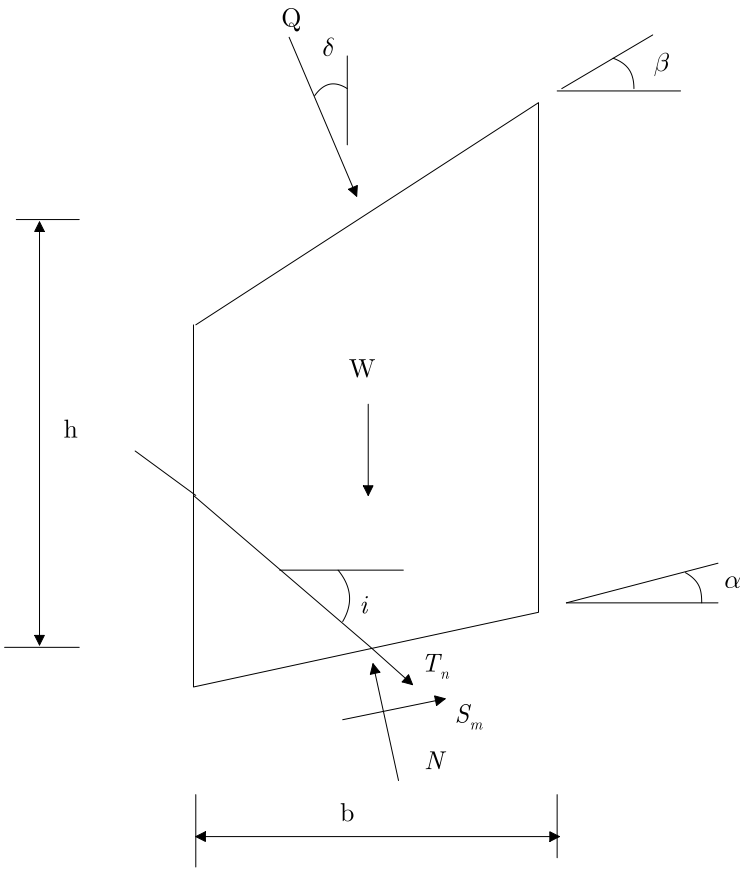

Figure 3. 11: Forces acting on a typical slice including nail tension

Table 3. 2: Slice parameters

Slice properties		**Nail**		**Soil properties**		**External loads**	
R	radius of failure surface	i	inclination of nails	γ	soil unit weight	Q	surcharge load
β	inclination of slice base			φ	friction angle	$F_H^a = k_h W$	horizontal seismic load
θ	Inclination of slice base			c	cohesion	$F_V^a = k_v W$	vertical seismic load
δ	angle of line of action of surcharge with vertical					N	Effective normal force
b	width of slice						
h	height of slice						
W	weight of the slice						

Satisfying the moment equilibrium, the factor of safety is obtained as

$$FS_G = \frac{\sum_{i=1}^{n} C + N\tan\phi}{\sum_{i=1}^{n} A_1 - \sum_{i=1}^{n} A_2 + \sum_{i=1}^{n} A_3 - \sum_{i=1}^{n} A_4}$$

in which

$$A_1 = W(1-k_v) + Q\cos\delta \ \sin\alpha$$
$$A_2 = Q\sin\delta(R\cos\alpha - \frac{h}{R})$$
$$A_3 = k_h W(\cos\alpha - \frac{h_c}{R})$$
$$A_4 = T_n\cos(\alpha + i)$$

From vertical force equilibrium of each slice one finds

$$N = \frac{1}{m_\alpha}\left[W(1-k_v) - \frac{C\sin\alpha}{FS_G} + Q\cos\delta + T_n\sin i\right]$$

where

$$m_{\alpha} = \cos\alpha\left[1 + \frac{\tan\alpha\tan\phi}{FS_{G}}\right]$$

These equations are simple and can be easily implemented in a spreadsheet.

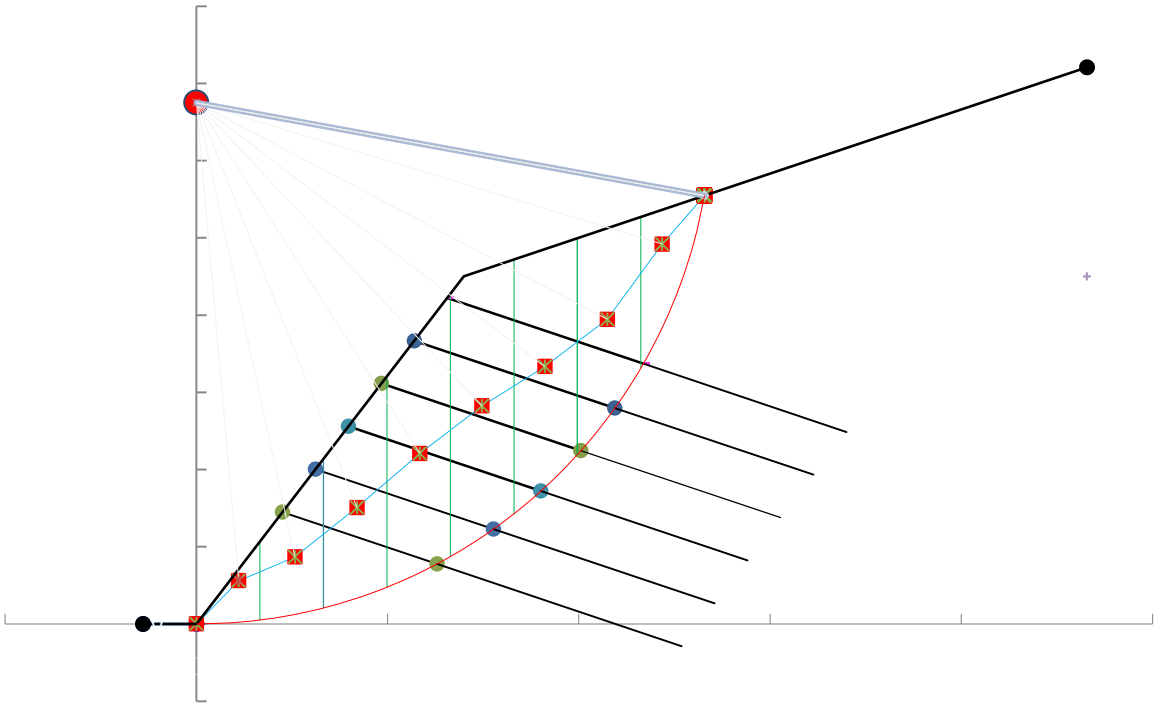

Figure 3. 12: Illustration of slicing a slope with a soil-nail application

2. Janbu's simplified method

Janbu's simplified method uses the method of slices to determine the stability of the sliding mass. As far as forces on a typical slice is considered, it is similar to the simplified Bishop method. As is the case of the simplified Bishop method, nail tensile forces can be considered in the slices in which nails emerge at their base. The method assumes no inter slice shear forces. In an attempt to compensate for this limiting assumption, Janbu introduced a slide geometry dependent modification factor on the factor of safety. It satisfies both horizontal and vertical force equilibrium for each slice but fails to satisfy moment equilibrium.

The factor of safety of nailed slopes according to Janbu's simplified method is given by

$$FS_G = \frac{\sum_{i=1}^{n}(C + N\tan\phi)\cos\alpha}{\sum_{i=1}^{n} A_6 + \sum_{i=1}^{n} N\sin\alpha}$$

in which

$$A_5 = Wk_h - Q\sin\delta - T_n\cos i$$

$$N = \frac{1}{m_\alpha}\left[W(1-k_v) - \frac{C\sin\alpha}{FS_G} + Q\cos\delta + T_n\sin i\right]$$

where

$$m_\alpha = \cos\alpha\left[1 + \frac{\tan\alpha\tan\phi}{FS_G}\right]$$

3.3 Bearing capacity of nailed slopes

As the wall facing does not extend bellow the bottom of the excavation, the unbalanced load caused by the excavation may cause the bottom of the excavation to heave and trigger bearing capacity failure in the foundation soil. Should a soil nailing technique be used for ensuring stability of fine-grained materials, bearing capacity of the foundation soil should be checked.

Suppose we have a nailed slope of height H with unit weight γ . For purely cohesive soils or saturated soils under undrained conditions, bearing capacity is calculated with $c_u N_c$ where c_u is the undrained shear strength of the foundation soil and N_c is the undrained bearing capacity factor. The minimum undrained bearing factor is $N_c = 5.14$

.

The factor of safety is thus calculated by dividing the resistance by the driving force, $H\gamma + q$, where q is the surcharge load, i.e.,

$$FS_S = \frac{c_u N_c}{H\gamma + q}$$

For long-term stability or for frictional materials, the so-called c-ϕ bearing capacity $cN_c + 0.5BN_\gamma$ is used, where B is the foundation width and N_γ is the depth factor. Hence, the factor of safety against sliding is given by

$$FS_S = \frac{cN_c + 0.5\gamma B_e N_\gamma}{H\gamma + q}$$

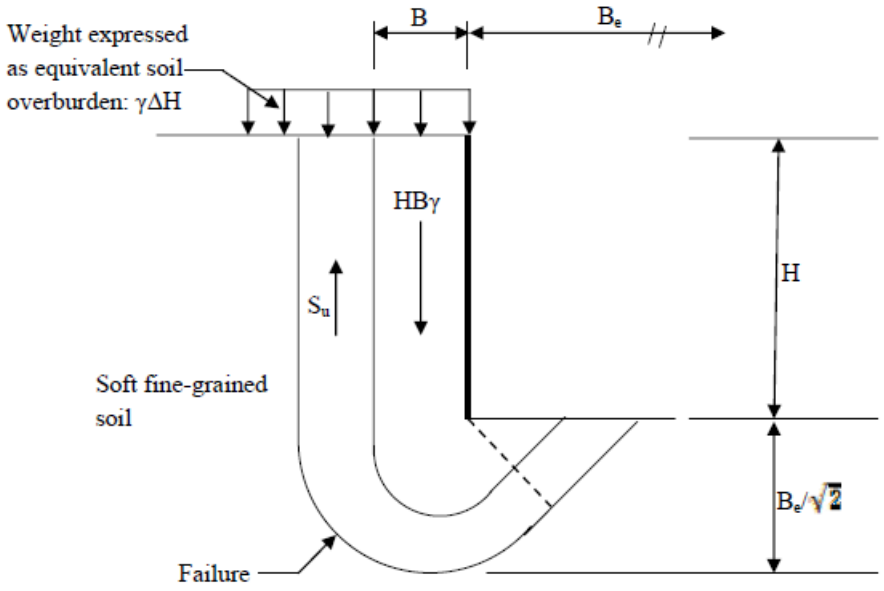

Figure 3. 13: Schematization of undrained bearing mechanism of braced excavation, schematics taken from [2]

3.4 Sliding stability

According to the FHWA [2], sliding stability is considered a special case of global stability and a minimum factor of safety of 1.5 is required for static loads and of 1.1 for dynamic loads. It is not present in most soil-nail designs. It may however arise in cases where a weak soil layer underlies the block of reinforced soil and when soil-nails do not contribute to stability. The later stability can be checked using

$$\phi_{LS} R_S = \gamma_{EH} P_a \cos\delta + \gamma_{ES} ES$$

in which

ϕ_{LS} is the resistance factor for lateral sliding,

R_S is the nominal soil resistance per unit width acting at the base of the soil block,

γ_{EH} is maximum load factor for horizontal earth loads (FHWA [2] recommends a value of 1.5),

γ_{ES} a maximum load factor for horizontal effect of permanent surcharge (FHWA recommends a value of 1.5),

δ is friction angle between the reinforced block and the retained soil which may be estimated depending on the back slope angle from horizontal, see Figure 3. 14,

ES is the horizontal component of the permanent earth surcharge, and

P_a is the lateral earth thrust.

The nominal soil resistance can be estimated as

$$R_S = c_b B_L + (W + P_a \sin\delta)\tan\varphi_{fb}$$

where

c_b is the effective soil cohesion strength along the base,

B_L is the length of the horizontal slip surface where c_b is acting,

W is the weight of reinforced soil mass, P_a,

φ_{fb} is the effective friction angle at the base.

P_a is the lateral earth thrust, the active force per unit width given by

$$P_a = \frac{1}{2} K_a \gamma_s H_1^2$$

where

k_a is the active earth pressure,

γ_s is the unit weight of the soil behind the wall,

H_1 is the effective height over which the earth pressure acts which is given by

$$H_1 = H + (B_L - H \tan\eta) \tan\beta_{eq}$$

in which

η is the face batter

and $\beta_{eq} = a \tan(\Delta H / H)$ for broken slopes (see Figure 3. 14) and the back slope angle from horizontal for infinite slope.

Assuming no cohesion in the soil behind the block, the active earth pressure can be obtained from Coulomb theory

$$K_a = \frac{\sin^2(\theta + \varphi)}{\sin^2\theta \sin(\theta - \delta)\left[1 + \sqrt{\frac{\sin(\varphi + \delta)\sin(\varphi - \beta)}{\sin(\theta - \delta)\sin(\theta + \beta)}}\right]^2}$$

where

θ is the inclination of the back of the wall face from horizontal,

φ is the friction angle of the soil-nail reinforced mass.

It may also be obtained from Rankine theory

$$K_a = \cos\beta \left[\frac{\cos\beta - \sqrt{\cos^2\beta - \cos^2\varphi}}{\cos\beta + \sqrt{\cos^2\beta - \cos^2\varphi}}\right]$$

When considering effect of inertia forces due to seismic loads, the active earth pressure coefficient can be estimated from modified formulas. One such formula is presented in Appendix C.

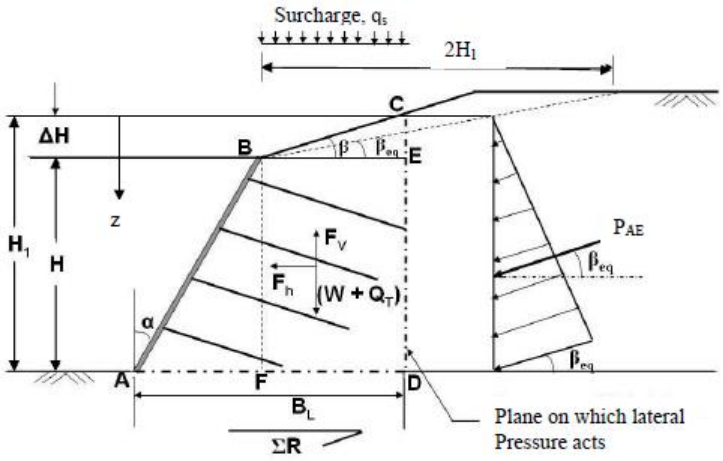

Figure 3. 14: Sliding stability of a soil-nail wall [3]

3.5 Recommended factors of safety

Different standards recommend different safety factors against the various failure modes. The required safety factors depend on the duration of the structures, the importance of adjacent structures and the degree of risk associated with the failure of the soil nail system. A table of recommended safety factors directly taken from [2] is presented in Table 3. 3.

Table 3. 3: Minimum Recommended Factor of Safety for the Design of Soil-nail Walls using ASD Method [2]

Failure Mode	**Resisting Component**	**Symbol**	**Minimum Recommended Factors of safety**		
			Temporary Structure	**Permanent Structure**	**Seismic Loads (Temporary and permanent structure)**
External Stability	Global stability (long term)	FS_G	1.35	1.5	1.1
	Global stability (excavation)	FS_G	1.2 – 1.3 (2)		NA
	Sliding	FS_H	1.3	1.5	1.1
	Bearing Capacity	FS_H	2.5(3)	3(3)	2.3 (5)
Internal stability	Pullout Resistance	FS_P	2		1.5
	Nail bar tensile strength	FS_T	1.8		1.35
Facing strength	Facing flexure	FS_{FF}	1.35	1.5	1.1
	Facing punching shear	FS_{FP}	1.35	1.5	1.1
	H-stud tensile (A307 Bolt)	FS_{HT}	1.8	2	1.5
	H-stud tensile (A325 Bolt)	FS_{HT}	1.5	1.7	1.3

Notes: (1) For non-critical, permanent structures, some agencies may accept a design for static loads and log-term conditions with FSG = 1.35 when less uncertainty exists due to sufficient geotechnical information and successful local experience on soil nailing.

(2) The second set of safety factors for global stability corresponds to the case of temporary excavation lifts that are unsupported for up to 48 hours before nails are installed. The larger value may be applied to structure that is more critical or when more uncertainty exists regarding soil conditions.

(3) The safety factors for bearing capacity are applicable when using standard bearing capacity equations. When using stability analysis programs to evaluate these failure modes, the factors of safety for global stability apply.

3.5 Application of the simple wage method for calculation of safety factor

Here, the application of one of the simplest methods of analyses of global stability-the plane wage method-is considered. The method is applied to investigate in what way do configuration parameters of a soil nail system influence the calculated safety factor. An initial configuration is assumed and one parameter is varied at a time to study its effect.

The wedge with the minimum factor of safety satisfies

$$\frac{\partial F_{SG}}{\partial \theta} = 0$$

$$= \left[(W + Q \pm F_V^a)\sin\theta - T_{EQ}\sin(\theta - i) - F_H^a \cos\theta\right]\begin{bmatrix} -F_H^a \cos^2\theta \tan\varphi_m - \\ (W + Q \pm F_V^a - F_H^a \sin\theta)\sin\theta \tan\varphi_m - T_{EQ}\sin(\theta - i) \end{bmatrix}$$

$$-\left[cL + (W + Q \pm F_V^a - F_H^a \sin\theta)\cos\theta \tan\varphi_m + T_{EQ}\cos(\theta - i)\right]\begin{bmatrix} (W + Q \pm F_V^a)\cos\theta \\ -T_{EQ}\cos(\theta - i) + F_H^a \sin\theta \end{bmatrix}$$

This is equation is non-linear and should be solved iteratively. It can be easily calculated using spreadsheet programs. What is implied in the equation is however clear. It can be seen that the size (or rather the angle) of the wedge mechanism depends on several factors such as

- the nail inclination,
- the nail capacity,
- inertial forces
- and the strength of the soil.

For finding the wedge angle (and hence the factor of safety) for this approach, a simple algorithm is given as follows.

- For given geometric properties, soil properties and loading conditions assume the wedge inclination angle θ.

- Calculate the factor of safety for the assumed wedge inclination angle θ.
- By changing the value of θ repeat the calculation. Plot the wedge inclination angle versus the factor of safety. A bowl shape plot is expected. The factor of safety to be reported is the minimum of the safety factors so calculated.

3.6.1 Base case

For the base case, geometry, nail parameters and soil parameters are presented in Table 3. 4. Figure 3. 15 shows the basic set-up of planar wedge method and the plot in Figure 3. 16 shows an example plot of the search for the wedge configuration that yields the minimum safety factor and hence the governing mechanism of the global stability. An examples of the various intermediate calculations are presented in Appendix D for the base case.

Table 3. 4: Base case parameters

Geometry			**Nail**				**Soil**			
		H	i	L	D	S_h, S_v			c	K_0
[°]	[°]	[m]	[°]	[m]	[14]	[m]	[kN/m³]	[°]	[kPa]	[-]
18	0	9	10	8	150	1.5	21	39	8.1	0.37

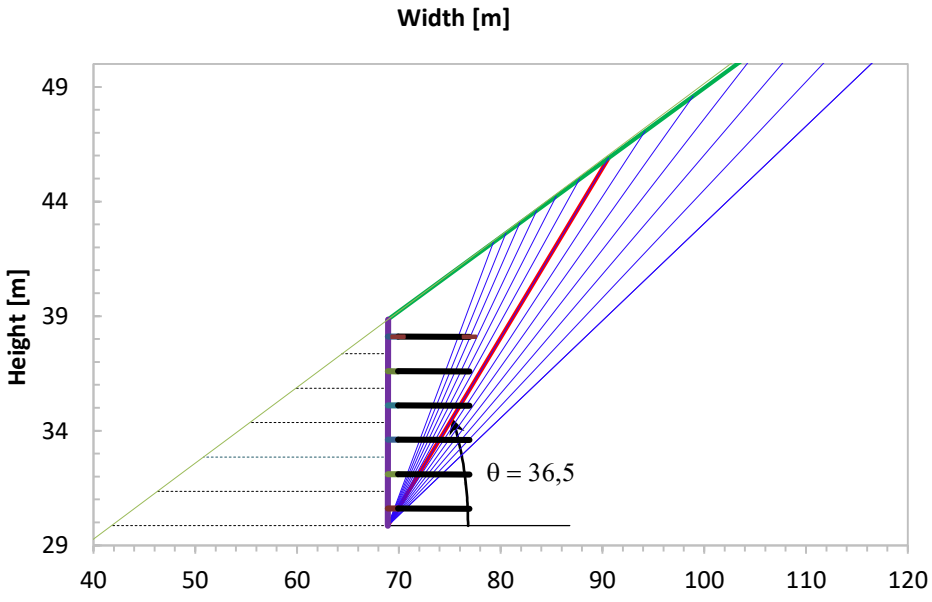

Figure 3. 15: Soil-nail system configuration, trial planar wedges, critical wedge

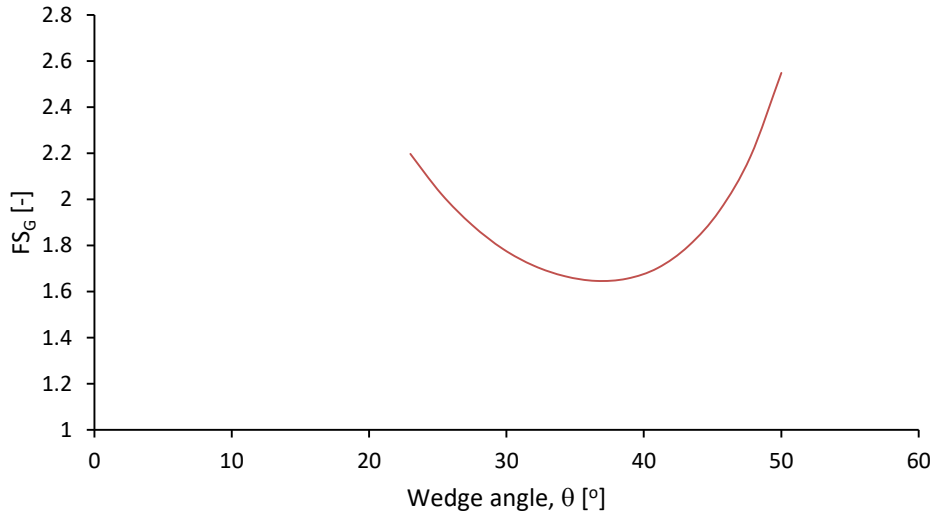

Figure 3. 16: Calculated safety factor versus wedge angle

3.6.2 Effect of nail inclination

The nail inclination is varied *citrus-paribus*. The calculated global safety factor is plotted against nail inclination and presented in Figure 3. 17. The global safety factor increases up until a nail inclination of 5 degrees and then decreases. The nail inclination at which the global safety factor is found to be the maximum is the *optimum nail inclination*. In this case, the optimum nail inclination.

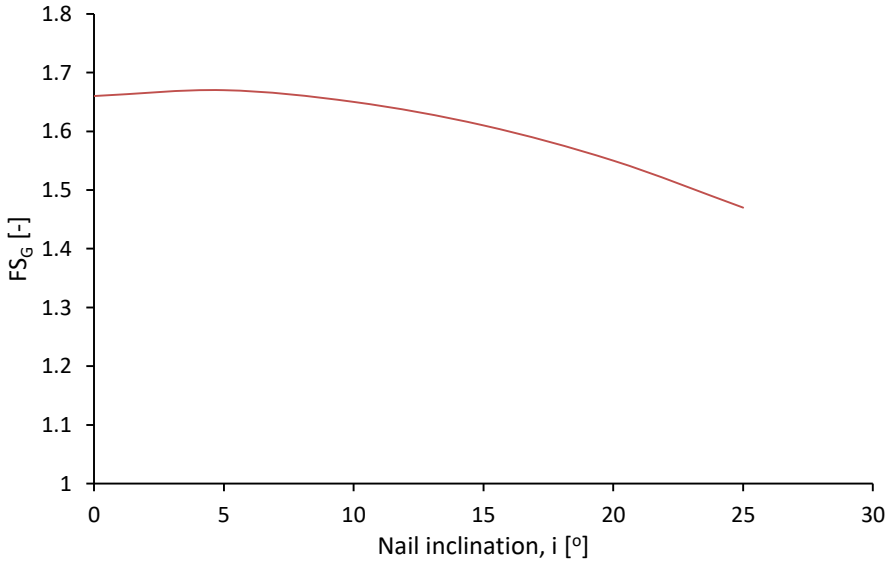

Figure 3. 17: Effect of nail inclination on the global safety factor

3.6.3 Effect of wall-batter

The wall-batter is varied *citrus-paribus*. The calculated global safety factor is plotted against wall-batter and presented in Figure 3. 18. The global factor of safety increases with increasing wall-batter. This is in line with intuition and observation.

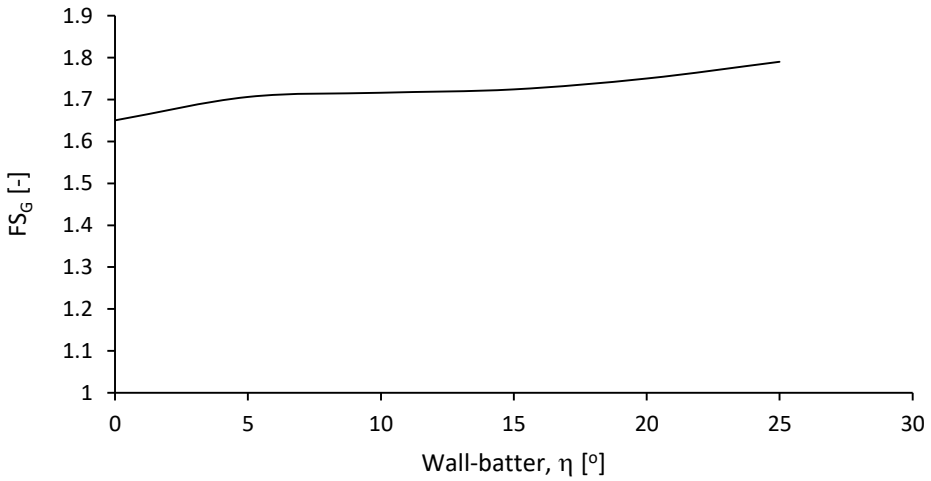

Figure 3. 18: Global factor of safety against wall-batter.

3.6.4 Effect of back terrain slope

The back slope is varied maintaining the other parameters as in the base case. The plot of safety factors versus back terrain slope is presented in Figure 3. 19. In the plot, the global safety factor decreases almost linearly with increase in back slope.

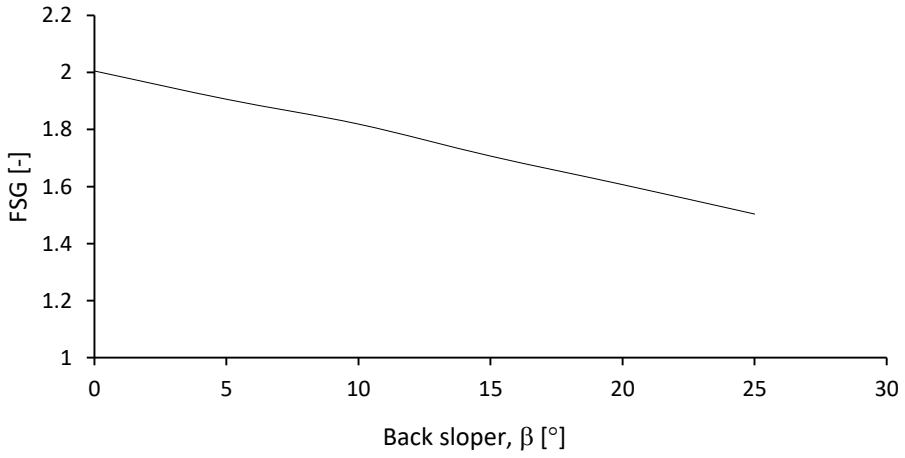

Figure 3. 19: Global factor of safety against back terrain slope.

3.6.5 Effect of nail spacing

The vertical and the horizontal spacing are assumed to be equal and they are varied citrus-paribus, while maintained equal amongst themselves. Factor of safety versus nail spacing plot is presented in Figure 3. 20. As can be seen, safety factor decreases with increasing nail spacing.

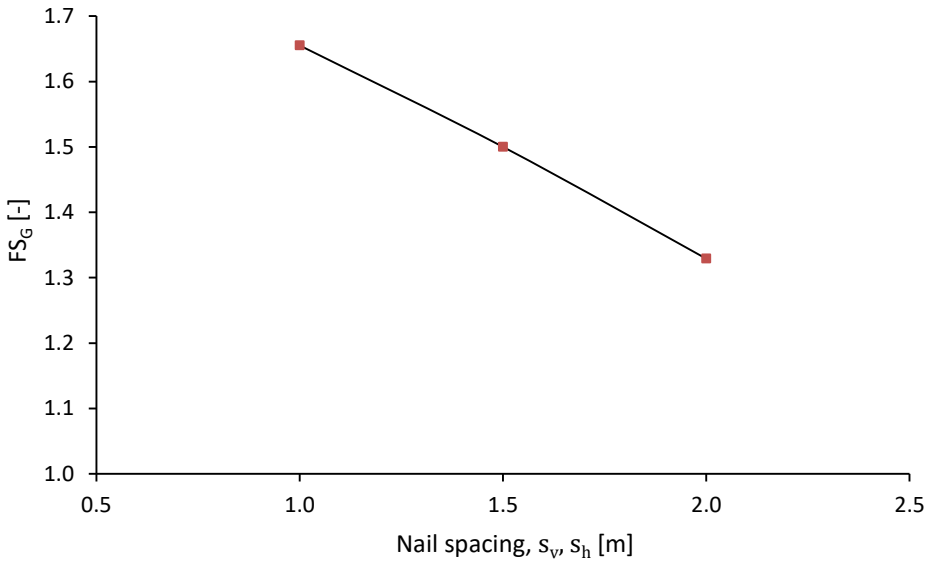

Figure 3. 20: Effect of nail spacing on global safety factor

3.6.6 Effect of various parameters on the critical angle of the wedge mechanism

Next, the effect of various parameters on the critical angle of the wedge mechanism is studied. In general, it is found that the critical angle

- is constant for smaller nail inclination angles and increases with increasing nail inclination for higher inclinations,
- decreases with increasing wall-batter,
- increases with increasing back slope,
- decreases with increasing cohesion and increasing friction, and
- does not depend on unit weight of soil.

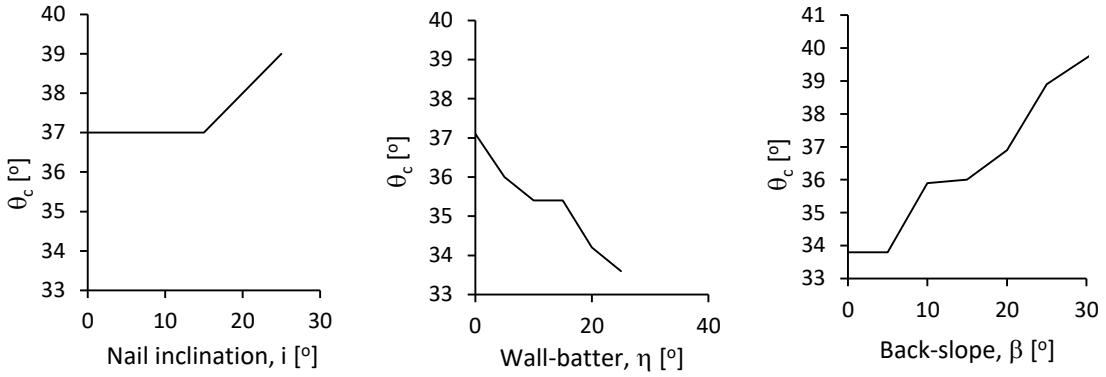

Figure 3. 21: Effect of nail and slope configuration on the critical angle of the wedge mechanism

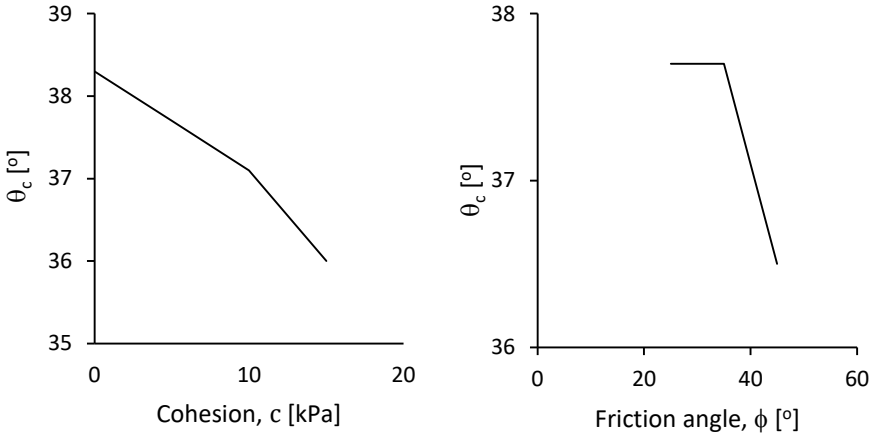

Figure 3. 22: Effect of strength parameters on the critical angle of the wedge mechanism

CHAPTER 4: Application of Geosuite

4.1 Introduction

In Chapter 3, several limit equilibrium methods that are extended to accommodate the analysis of soil-nail slopes are presented. Among the methods, the simple wedge method was employed to investigate effect of the different configuration parameters of a soil-nail system on global stability safety factor.

Several of the extended limit equilibrium methods are implemented in different software products. One such software product that is considered in this study is Geosuite. Geosuite has a series of computer programs especially developed for design and analysis of geotechnical problems, including stability, settlement, bearing capacity, pile and excavation calculations. It is widely used in Scandinavian geotechnical engineering firms. In this chapter, we will apply extended classical stability analysis methods using the GS stability module of the Geosuite software for studying the effect of various nail configuration parameters on safety factor. The user interface of the GS stability module is presented in Appendix A.

4.2 Base case soil-nail configuration and material parameters

A slope ground presented in Figure 4. 1 is considered as a base case. Then a soil cut with a steep slope, in for example cuts adjacent to road developments, is considered. For stabilizing the steep cut slope, a soil nailing technique is assumed. Starting from a base soil-nail configuration, the various configuration parameters such as nail slope, wall-batter and nail spacing are varied. The effect of their variation on the calculated safety factor is then studied. The base configuration is given in Table 4.1 and the soil parameters are given in Table 4. 2.

Table 4. 1 Configuration parameters

Ground slope [-]	Wall-batter [°]	Nail inclination [°]	Nail spacing[m]	Nail length [m]	Free length [m]	Drill hole diameter [mm]
1:3	0	10	1.5	8	1	150

Table 4. 2 Soil parameters

Unit weight [kN/m^3]	Friction angle ϕ' [°]	Cohesion c' [kPa]	Attraction [kPa]
21	39	8.1	10

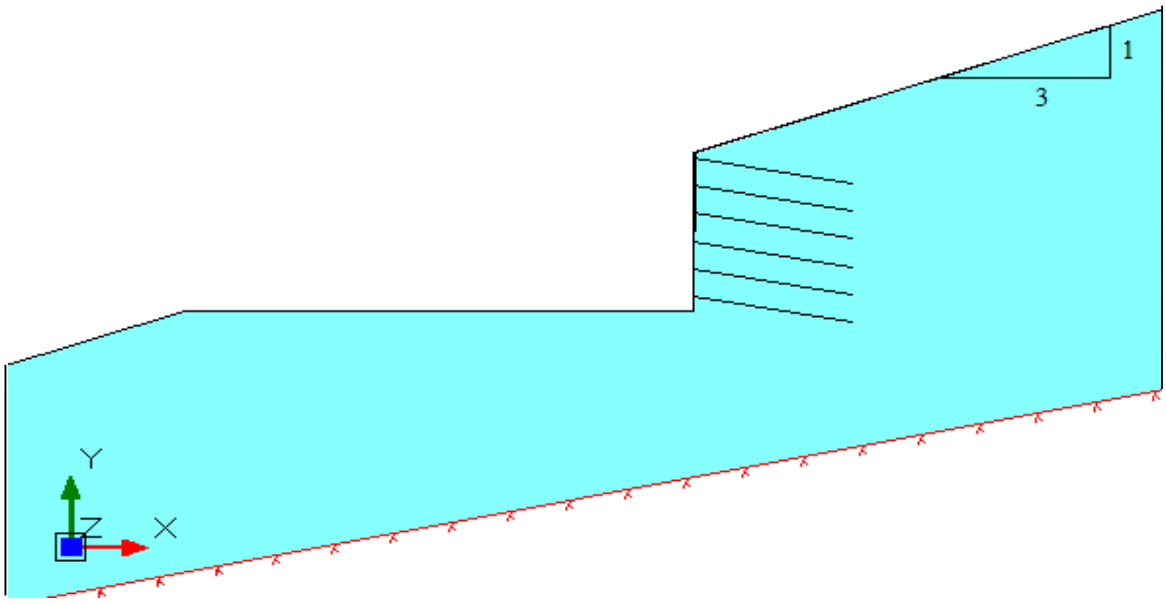

Figure 4. 1: The soil geometry for safety analysis from Geosuite software

4.3 Global slope stability safety analysis in GS stability

The GS Stability modules offers four different methods for the calculation of global slope stability. The four methods are the following.

1. *Force equilibrium*- this method satisfies force equilibrium only, not moment equilibrium. The calculations are carried out with the interslice roughness values. [15]
2. *Bishop Simplified*-a method among the method of slices. See section 3.2.2
3. *Bishop Modified*- One method among the method of slices. The difference between Bishop Simplified and Bishop Modified is that in the Bishop modified, the side forces are neglected and the produce FS is too low (conservative). Bishop modified assume side shear forces are zero but account for side normal forces.
4. *BEAST 2003* – is the default calculation method in the GS stability. The method can be used to analyze slope stability, bearing capacity and earth pressure problems by a general procedure of slices. The BEAST global slope stability analysis method is more flexible than the previous three. The features that are available in the BEAST [15]

    - Total or effective stresses may be used.
    - Shear surfaces may be planes, circles, combined surfaces or general surfaces specified point by point.
    - The solution method selected obtains force and moment equilibrium for each slice, with an automatic control of the quality of the solution obtained.
    - The geometry considered is plane strain with inclusion of end surface shear stresses if wanted.

GS Stability also offers different calculation strategies such as tangent, RTangent, points, RPoints, radius, plane, stretch and slope direction, see Appendix B. In this thesis, tangent calculation strategy is selected for safety analysis. In the tangent

calculation strategy, the user gives a probable center point for the critical shear surface, search area (quadratic), upper and lower tangential level and the number of levels. [15]

Application of the different methods may lead to small differences in the calculated safety factor. Table 4. 3 shows example results of safety factors calculated for the base case soil-nail configuration by applying the four safety analysis methods described here above.

For the base case, the failure mechanisms obtained from the four methods are presented in seen in Figure 4. 2 and Figure 4. 3. The methods produce nearly similar mechanisms. However, the Bishop modified method has a slightly different failure mechanism-unlike the others it goes bellow the wall toe. The BEAST calculation method and tangent calculation strategy is used for this study.

Table 4. 3 Example of safety factor analysis result for different methods

Calculation method	Force equilibrium	Bishop Simplified	Bishop Modified	Beast 2003
Factor of safety	1.77	1.82	1.92	1.8

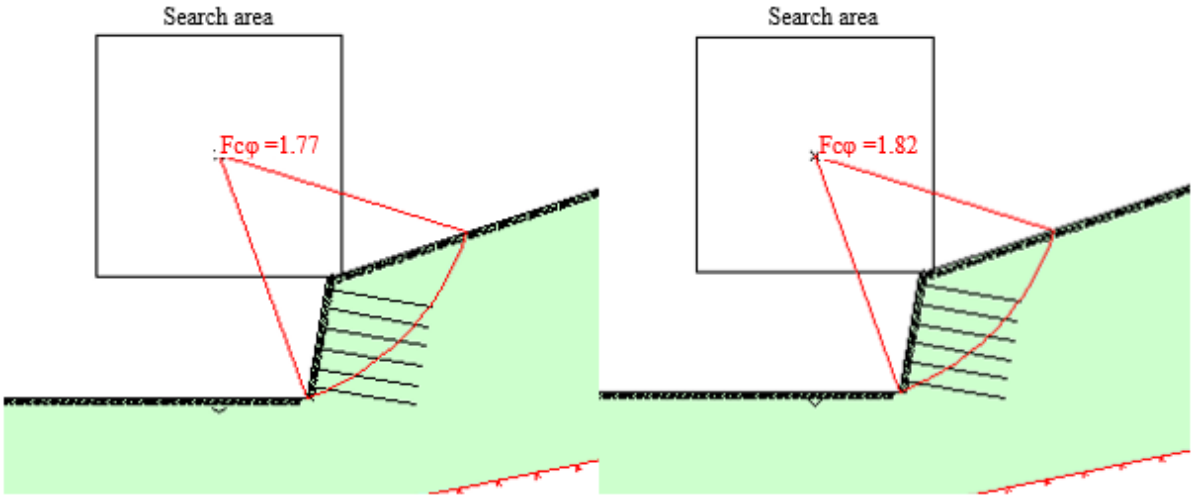

Figure 4. 4: critical shear surfaces for force equilibrium (left) and Bishop simplified (right)

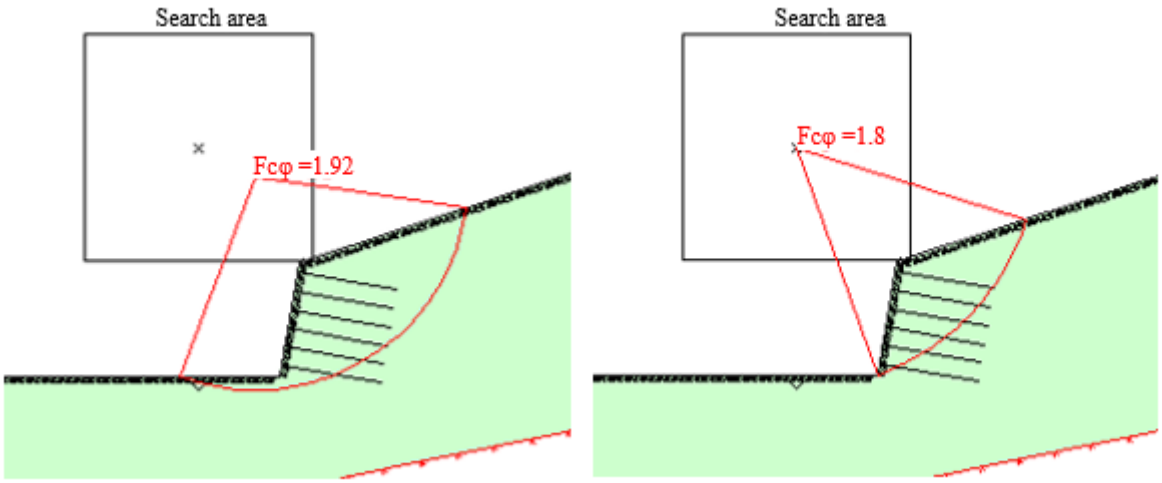

Figure 4. 5: Critical shear surfaces for Bishop modified (left) and Beast 2003 (right)

4.4 Effect of configuration parameters on safety factor

4.2.1Effect of nail inclination

In order to investigate the effect of soil-nail inclination on the safety factor, the nail inclination is varied between 5° and 25° with a 5° interval. Other soil-nail parameters such as wall-batter, nail length and vertical and horizontal spacing remain the same as in the base case. The relationship between nail inclination and safety factor is presented in Figure 4. 6.

As shown in Figure 4. 6 the value of the safety factor first increases with the increase of soil-nail inclination until an *optimum nail inclination*-where a maximum safety factor is reached. Further increase of nail inclination beyond the optimum leads to a decrease in safety factor. In this case, the optimum nail inclination is 20°. Between nail inclinations of 5° to 15° the safety factor increased almost linearly and between nail inclination of 15° to 20° the rate of increase is decreasing until it vanishes at the optimum nail inclination. Afterward, the value of safety factor starts to decrease. The finding is in accordance with literature, except the shape of the curve.

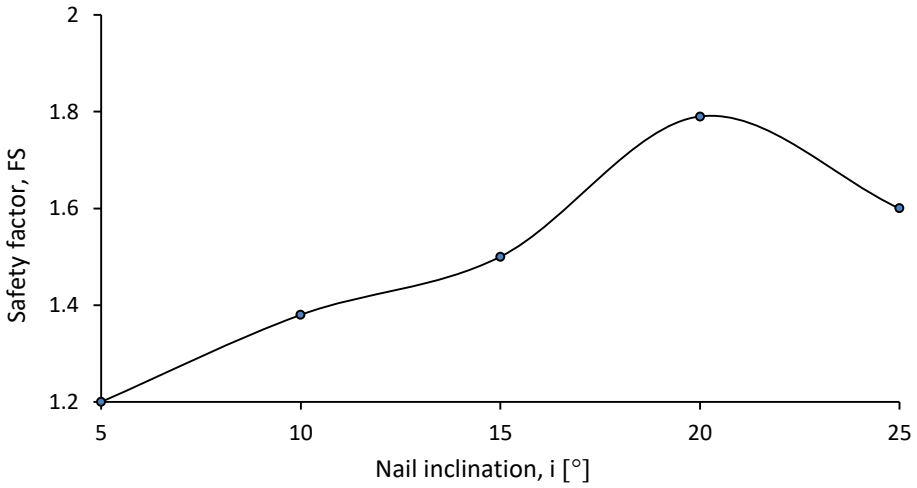

Figure 4. 6: Safety factor versus soil-nail inclination for s_v = 1.5 m

4.2.2 Effect of wall-batter

In order to investigate the effect of wall-batter on safety factor, the wall-batter is varied between 0° and 20° with a 5° interval. Other soil-nail parameters such as nail inclination, nail length and vertical and horizontal spacing are maintained the same as in the base case. The relationship between wall-batter and safety factor is presented in Figure 4. 7. According to the plot, an increase in wall-batter leads to an increase in safety factor. The lowest factor of safety is for vertical wall ($\eta = 0°$). The rate of increase is sharper at lower wall-batter. However, the amount of increase of the safety factor per unit degree of wall-batter is low for wall-batter greater than 10°.

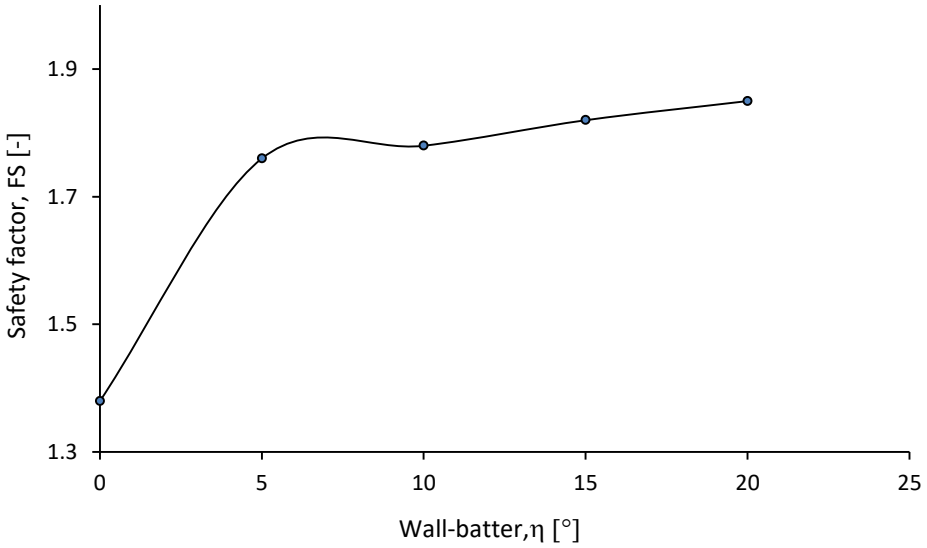

Figure 4. 7: Effect of wall-batter on safety factor

4.2.3 Effect of nail spacing

To study the effect of nail spacing, vertical and horizontal nail spacing varied as 1.2 m, 1.5 m, 1.8 m, 2.2 m and 2.5 m. Other soil-nail parameters are maintained the same as in the base case. The plot of safety factor versus vertical spacing is shown in Figure 4. 8. As can be seen in figure soil-nail vertical spacing has a significant effect on safety factor. For vertical nail spacing greater than after 1.8 the safety factor decreases rapidly.

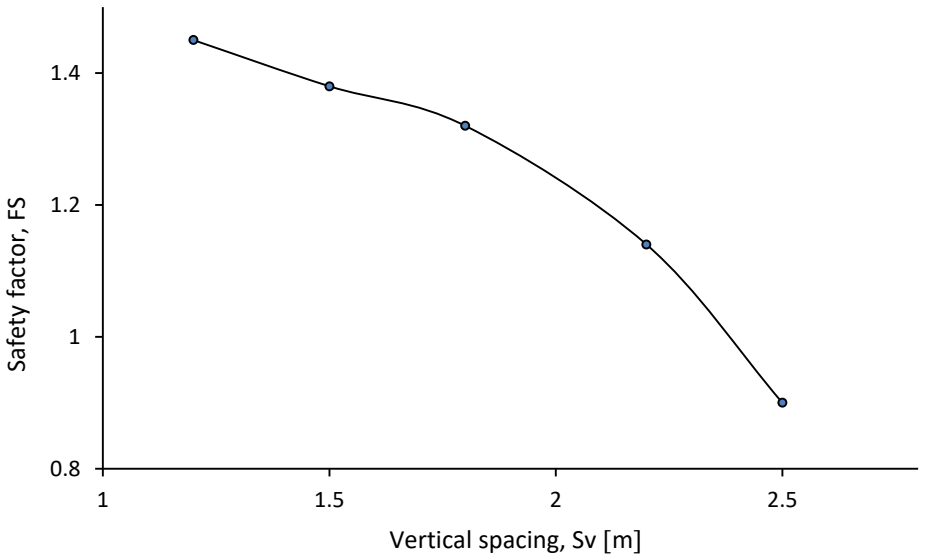

Figure 4. 8: Effect of vertical soil-nail spacing on safety factor

4.5 Limitations of the Geosuite global stability analysis

The limit equilibrium global stability analyses in Geosuite is easy to perform. Numerical issues are minimal and the presentation is well organized. However, the following limitations are noted

- The probable center of the critical shear surface is given by the user. This is seen to affect the result.
- The search area needs to be specified manually. This is time taking and finding the critical shear surface can be difficult.
- Geosuite allows input of a single value for the soil nail skin friction, q_s. The average value is considered in this case.

In general, due to lack of stress strain law, it is not possible to calculate deformations and mobilized nail forces.

CHAPTER 5: Application of Plaxis 2D

5.1 Introduction

So far, the effect of various *configuration parameters* on soil-nail slopes are studied using limit equilibrium methods. However, limit equilibrium methods have limitations in estimating the maximum loads in soil-nails accurately. The reasons are [16]:

- unrealistic stress distribution and
- lack of stress-strain constitutive relationship to insure displacement compatibility

Besides these two reasons, in limit equilibrium formulations convergence problems may arise when there are concentrated lateral loads due to nails, anchors, and so on. To have a better grasp of the condition, advanced finite element methods with realistic constitutive models should be employed. However, it is good practice to consider empirical methods and simple numerical methods prior to the use of any advanced numerical tool such as finite element methods as it is easy to be "lured by the colored outputs" of the later-treading into it with a prior understanding of the situation and some informative numbers is important. In this chapter, a two-dimensional commercial finite element (FEM) program, Plaxis 2D is used for performing numerical studies on the various parametric studies.

5.2 Base case-configuration parameters, material parameters and interaction parameters

The base case considered in this chapter is the same as the one investigated in Chapter 3, using the Geosuite analysis tools. This is to make comparison between the different results. One-layer soil and inclined soil surface with slope of 1:3 (V:H) are considered.

The model set-up, mesh and details of the soil-nail complex are shown in Figure 5. 4 and Figure 5. 5.

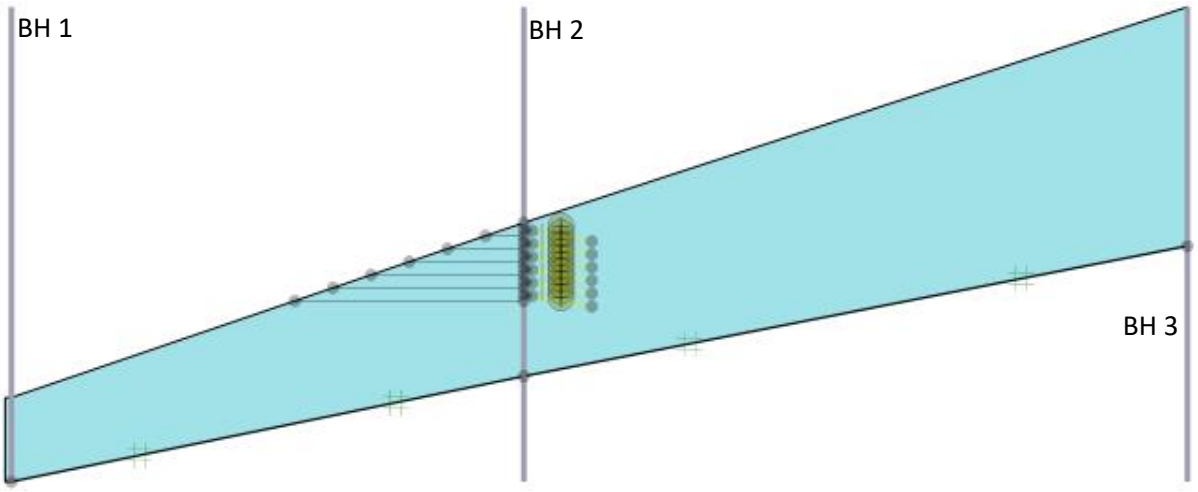

Figure 5. 1: Illustration of the soil geometry modelled in Plaxis 2D with boreholes

5.3 Plaxis 2D

Before proceeding into the numerical study of a soil-nail configuration in Plaxis 2D, we give a short introduction of the Plaxis 2D. The Plaxis 2D FEM package is a 2D finite element package. The package contains diverse structural elements and several soil models. In connection to this study,

- the simple elastic perfectly plastic Mohr-Coulomb model is used for modeling the soil,
- node-to node anchor is used for modeling the free length of the nails,
- embedded pile row is used for modelling the grouted part of the soil-nails, and
- plate elements are used for modelling the reinforced shotcrete facing.

5.3.1 The Mohr-Coulomb Model

In Plaxis, a variety of soil models are available. One can have the pleasure of choosing advanced soil models such as Hardening Soil (HS), Hardening Soil Small (HSS), etc. when one has the required soil data available. In this study, the Mohr-Coulomb drained soil model is considered. The so-called Mohr-Coulomb model in Plaxis is a simple *elasto-plastic* model that makes use of the Mohr-Coulomb criterion for establishing the limiting stress state. The Mohr-Coulomb

criterion encloses a six-sided conical region, Figure 5. 2. Each side is governed by the following function

$$f = \frac{1}{2}(\sigma_{\max} - \sigma_{\min}) + \frac{1}{2}(\sigma_{\max} + \sigma_{\min} + 2a)\sin\varphi \leq 0$$

where $\sigma_{\max}$ and $\sigma_{\min}$ are the major and the minor principal stresses, φ is the friction angle, a is the so-called *attraction* that relates to the cohesion, c, and the friction angle, φ, according to $a = c\cot\varphi$.

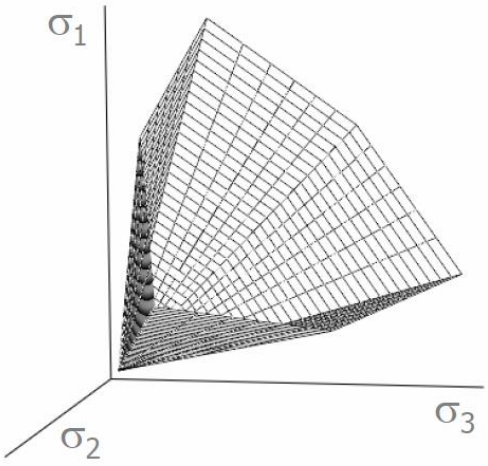

Figure 5. 2: The Mohr-Coulomb surface [17]

Within the Mohr-Coulomb region, the stress strain response is assumed to be linear elastic. Hooke's law is employed for modelling the linear elastic stress-strain relationship. Assuming isotropy, the stress (stress increment) is related to the strain (strain increment) according to

$$\sigma_{ij} = \frac{E\nu}{(1+\nu)(1-2\nu)}\delta_{ij}\delta_{kl} + \frac{E}{1+\nu}\delta_{ik}\delta_{jl}$$

where E and ν are two model parameters. They are called *Young's modulus* and *Poisson's ratio*, respectively. The young's modulus for soils is a positive number having a unit of stress. It can be estimated from various tests. Triaxial compression tests are commonly used. The Poisson's ratio defines the negative ratio of transversal strain to axial strain. Theoretically, Poisson's ratio ranges from -1 to 0.5 [18]. For soils, Poisson's

ratio is a non-negative value. However, in the linear elastic set-up, the Poisson's ratio determines the ratio of the lateral stress to the axial stress of the at rest condition. This will limit the realistic choice we have over the Poisson's ratio.

The ratio of the lateral stress to the axial stress for the at-rest condition is called at *rest lateral earth pressure coefficient* and is denoted by K_0. Suppose we know the K_0 value. The Poisson's ratio is then related to the K_0 value according to.

$$\nu = \frac{K_0}{1 + K_0}$$

Quite often, the K_0 value is estimated from empirical formulas. One of such formulas frequently used is Jaky's formula given as

$$K_0 = 1 - \sin\varphi\,.$$

Substituting $K_0 = 1 - \sin\varphi$ into $\nu = \frac{K_0}{1 + K_0}$ one finds

$$\nu = \frac{1 - \sin\varphi}{2 - \sin\varphi}.$$

This implies that, even though the linear elastic Mohr-Coulomb model appears a model with two stiffness parameters, namely the Young's modulus and the Poisson's ratio, basically the choice for the latter is very limited and practically it is a single stiffness parameter model.

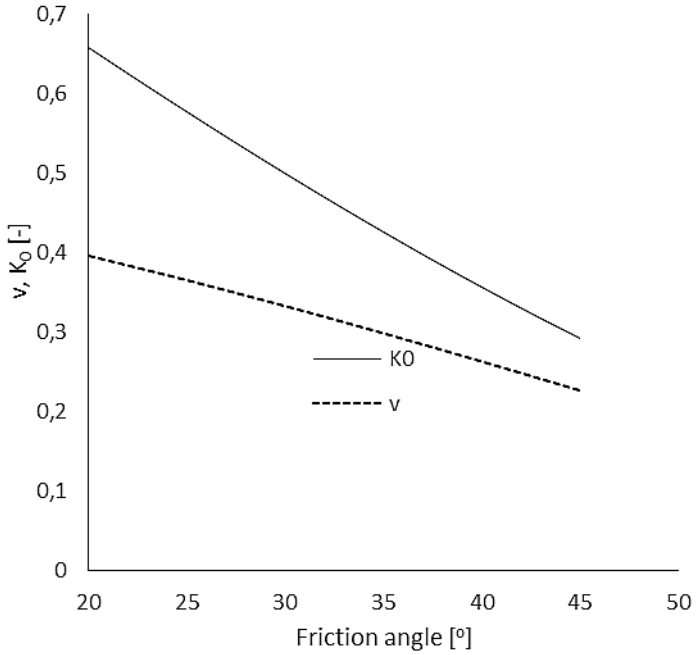

Once the stress state touches the Mohr-Coulomb failure envelope, it stays on the envelope. This is the so-called *consistency condition [18].* It gives us the magnitude of the plastic strain increment for an attempted stress increment beyond the failure envelope. The direction of the plastic strain increment is determined from the so-called plastic potential function. In the Plaxis Mohr-Coulomb model, the plastic potential function is established by replacing the friction angle in the Mohr-Coulomb yield function by the so-called *dilatancy angle.*

$$g = \frac{1}{2}(\sigma_{\max} - \sigma_{\min}) + \frac{1}{2}(\sigma_{\max} + \sigma_{\min})\sin\psi$$

The dilatancy angle tells us by how much plastic volumetric strain changes (contractive or dilative) for a given shear strain increment [18].

The parameters listed in Table 5. 1 are the Mohr-Coulomb model parameters that are assumed for the base case. The strength parameters will be varied and effect of each on the safety factor will be investigated.

Table 5. 1: Base case-soil parameters

Description			**Soil Layer**
General	Material set	Identification	
		Material Model	Mohr-Coulomb
		Drainage type	Drained
	General properties	γ_{unsat} [kN/m^3]	21
		γ_{sat} [kN/m^3]	12
Parameters	Stiffness	E' [-]	81000
		E_{oed} [-]	9.00E+04
		ν [-]	0.2
		c [kN/m^2]	8.1
	Strength	ϕ [^{0}]	39
		ψ [^{0}]	0
Initial		K_0 [-]	0.37
Interaction	Interface	r [-]	1

5.3.2 The embedded pile row

The embedded pile row is a newly introduced structural element in Plaxis [17] and is used for modelling the grouted part of the nail. The embedded pile row is a simplified approach to deal with a row of piles (or pile like structures such as soil-nails, anchors) in the out-of-plane direction in a 2D plane strain model [9].

The main parameters may be grouped into three-the parameters of the pile, parameters of the skin resistance and parameters of the foot resistance. The equivalent Young's modulus of the nail grout system is calculated as

$$E_{eq} = E_n\left(\frac{A_n}{A}\right) + E_g\left(\frac{A_g}{A}\right);\ A_n = A_n + A_g$$

where E_{eq} is the equivalent Young's modulus, E_n is the Young's modulus of the nail and E_g is the young's modulus of the cement mix grout. A linearly elastic stress-strain relation is assumed for the pile (in our case the nail).

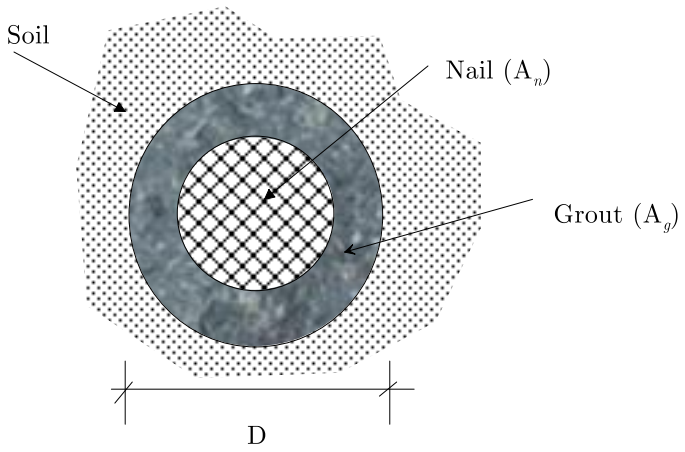

Figure 5. 3: Nail-grout cross-section

An elastic perfectly plastic model is used to model the traction along the embedded pile skin that is given as

$$t_s = K_s \delta_s^{ps} \leq T_{\max}$$

where

t_s is the traction force,

$T_{\max}$ is the maximum prescribed skin friction. The skin friction is assumed to be linearly varying in the grouted nail according to $T_{\max} = \pi\mu \frac{1+2K_0}{3} \gamma' z D$ in which D is the diameter of the dillhole.

K_s is the stiffness along the skin which is estimated from the shear modulus of the soil, G_{soil}, and the spacing between nails ($L_{spacing}$),

$K_s = ISF_{RS} \frac{G_{soil}}{L_{spacing}}$, in which ISF_{RS} an input parameter,

$\delta_s^{ps} = \delta_s^p - \delta_s^s$ is the displacement of the pile relative to the soil (δ_s^s) in the direction tangent to the embedded pile row.

In the direction normal to the embedded pile row, the stress-strain relation is assumed to be linearly elastic-

$$t_n = K_n \delta_n^{ps}$$

in which

t_n is the force normal to the tangent to the direction of the embedded pile row,

K_n is the stiffness in the same direction and

δ_n^{ps} is the displacement of the pile in the normal direction relative to the surrounding soil. The stiffness K_n is estimated from

$K_s = ISF_{RN} \frac{G_{soil}}{L_{spacing}}$, in which ISF_{RN} is an input parameter.

For describing the force-displacement relation at the foot of the pile, an elastic perfectly plastic model is used.

$$F_{foot} = K_{foot} \delta_{foot}^{ps} \leq F_{\max}$$

where

F_{foot} is the mobilized force at the embedded pile foot,

$F_{\max}$ is the maximum force allowed at the foot of the embedded pile (an input),

δ_{foot}^{ps} is the displacement of the foot of the pile relative to the surrounding soil,

K_{foot} is the stiffness at the embedded pile foot, which like the previous two is estimated from

$K_{foot} = ISF_{KF} \frac{G_{soil} \mathrm{R}_{eq}}{L_{spacing}}$, in which ISF_{KF} an input parameter, and

R_{eq} is an internally determined parameter and is the radius of the region bellow the foot that is assumed and elastic zone.

The default values of the parameters ISF_{RS}, ISF_{RN} and ISF_{KF} are in Plaxis estimated from the (nail) spacing and from the pile (grout) diameter. The values used in this thesis are given in Table 5. 2.

Table 5. 2: Basic input parameters for embedded pile row

Properties	**Unit**	**Value**
Equivalent Yong's Modulus (E_{eq})	[kN/m^2]	26E+06
Diameter	[m]	0.15
$L_{spacing}$	[m]	1.5
Axial skin stiffness factor ISF_{RS}	[-]	Default
Lateral skin stiffness factor, ISF_{RN}	[-]	Default
Pile base stiffness factor ISF_{KF}	[-]	Default

5.3.3 Node-to-node anchors

It is also assumed that there will be a not-grouted (ineffectively grouted) part towards the nail facing connection-about a meter length. This part of the nail is modelled as a *node-to-node anchor*. A linearly elastic perfectly plastic model is selected for the same. Until the compressive/tensile force in the node-to-node anchor reaches the maximum compressive and tensile strength (which are inputs), the axial force-axial displacement relation is assumed linearly elastic, which can be written as

$$N_{comp,tens} = \left|\frac{EA}{L}u\right| \leq \left|F_{\max,comp/tens}\right|$$

where $N_{comp,tens}$ is the tensile/the compressive force, E is Young's modulus, A is the cross-sectional area of the nail, L is the length of the nail, u is the displacement and $F_{\max,comp/tens}$ is the maximum compression/tensile strength of the nail.

Table 5. 3: Input parameters for node-to-node anchor

Properties	**Unit**	**Value**
EA	[kN]	1070
$L_{spacing}$	[m]	1.5
$F_{max,tens}$	[kN]	206
$F_{max,comp}$	[kN]	206

5.3.4 Plate elements

The reinforced shotcrete is modelled as an elastoplastic plate element. The shotcrete parameters are determined assuming a doubly reinforced shotcrete of thickness 120 mm. The parameters used in this thesis are given in Table 5. 4.

Table 5. 4: Material parameter for RSC facing

Properties	**Unit**	**Value**
Axial stiffness, EA	[kN/m]	2.42E+06
Flexural stiffness, EI	[kNm²/m]	2905
Weight, w	[kN/m/m]	3
Moment capacity, M_p	[kNm/m]	896
Axial capacity, N_p	[kN/m]	2427

5.3.5 ϕ-c reduction for safety analysis in Plaxis

The Plaxis safety calculation employs the so-called *ϕ-c reduction* method. The method finds the global safety factor by successively reducing the strength variables such as the friction angle and the cohesion until failure is approached. The total multiplier ΣMsf is used to define the value of the soil strength parameters at a given stage in the analysis:

$$\Sigma Msf = \frac{\tan\varphi}{\tan\varphi_{reduced}} = \frac{c}{c_{reduced}}$$

- When the friction angle has reduced so much that it becomes equal to the input dilatancy angle, any further reduction of the friction angle will lead to the same reduction of the dilatancy angle.
- The strength of interfaces is reduced in the same way.

- Optionally, the strength of structural elements such as plates and anchors can also be reduced in a Safety calculation.

The recommended practices are

- to use *Arc-length* control during safety calculations,
- that *tolerated error* should not exceed 1%, and
- to view the development of ΣMsf using the *Curves* option and check whether a constant value is reached while the deformation is continuing.

To apply strength reduction to soil clusters as well as structures and/or exclude particular soil clusters or structures from the strength reduction procedure, Plaxis adds the so-called *Enhanced safety* analysis. This facility makes it possible to exclude surficial soil clusters along a slope from the strength reduction procedure to avoid unrealistic shallow failure mechanisms.

5.4 Effect of soil-nail configuration parameters on factors of safety

Here, the Plaxis calculations are run by changing one of the soil-nail configuration parameters at a time and the factor of safety for the new configuration is registered. Based on the calculation results, different plots are then produced. In all calculations

- medium mesh size is used. According to studies conducted [11, 12], although mesh size has some influence on the global safety factor, it is not that significant. As expected, when mesh size decreases calculation time increases.
- drained condition is considered.

For all model runs, the different stages that were established in the Plaxis environment were such that to mimic the expected construction sequences in the field.

- First, an initial stress state is generated using gravity loading.

- Then, for the first course of excavation, nailing and application of a shotcrete, which were all activated in a single phase. This calculation is repeated for the next five phases.

An example model set-up at the last excavation stage is shown in Figure 5. 5.

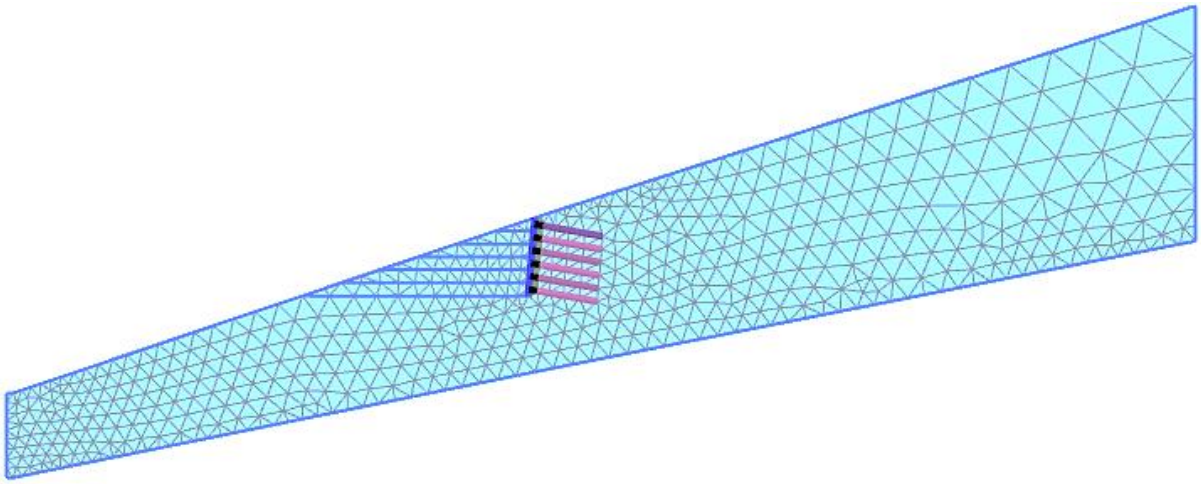

Figure 5. 4: A medium size mesh of the soil geometry

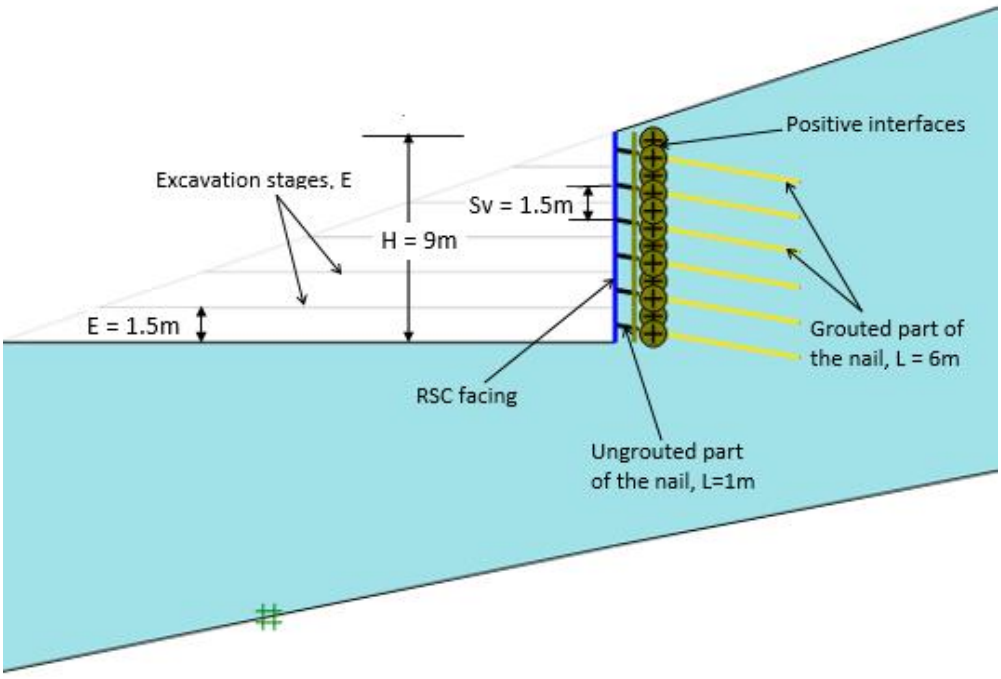

Figure 5. 5: Example of soil-nail geometry and excavation stage for vertical wall, i = 10° and sv = 1.5m.

5.4.1 Effect of nail inclination

The nail inclination is varied between 5° and 25° with a 5° interval. Other soil-nail parameters are maintained the same as in the base case. The relationship between nail inclination and safety factor is presented in Figure 5. 6.

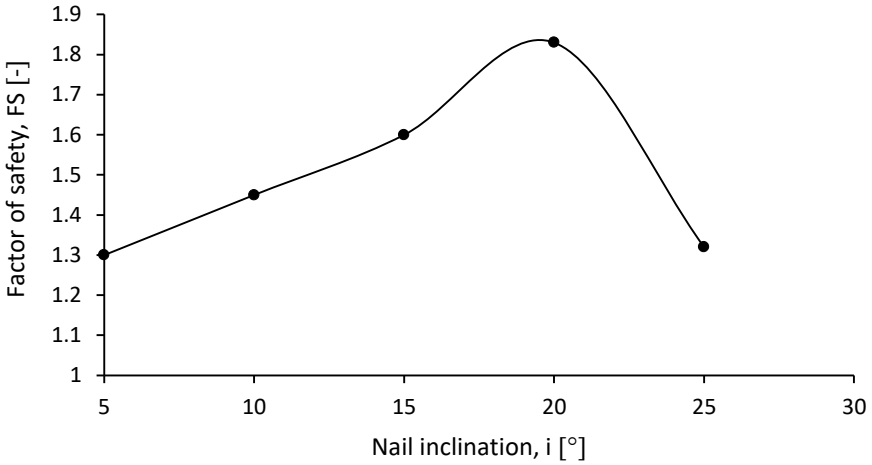

Figure 5. 6: Effect of nail inclination, i on factor of safety for s_v = 1.5 m.

Next, the amount of wall length required for achieving a specified factor of safety of 1.5 is investigated by varying the vertical nail spacing *citrus-paribus*. The results obtained are presented in Figure 5. 7. According to the plot, the required nail length to guarantee a given factor of safety decreases with increasing nail length. This is in agreement with literature [9].

Table 5. 5: Influence of nail inclination on total nail length.

i [°]	s_v [m]	FS [-]	s_v [m] for FS=1.5	∑L [m/ml]
5	1.5	1.3	1.2	52.5
	1.8	1.2		
	2.2	1		
10	1.5	1.5	1.5	42
	1.8	1.3		
	2.2	1.12		
15	1.5	1.6	1.68	37.5
	1.8	1.43		
	2.2	1.21		
20	1.5	1.8	1.8	35
	1.8	1.5		
	2.2	1.22		

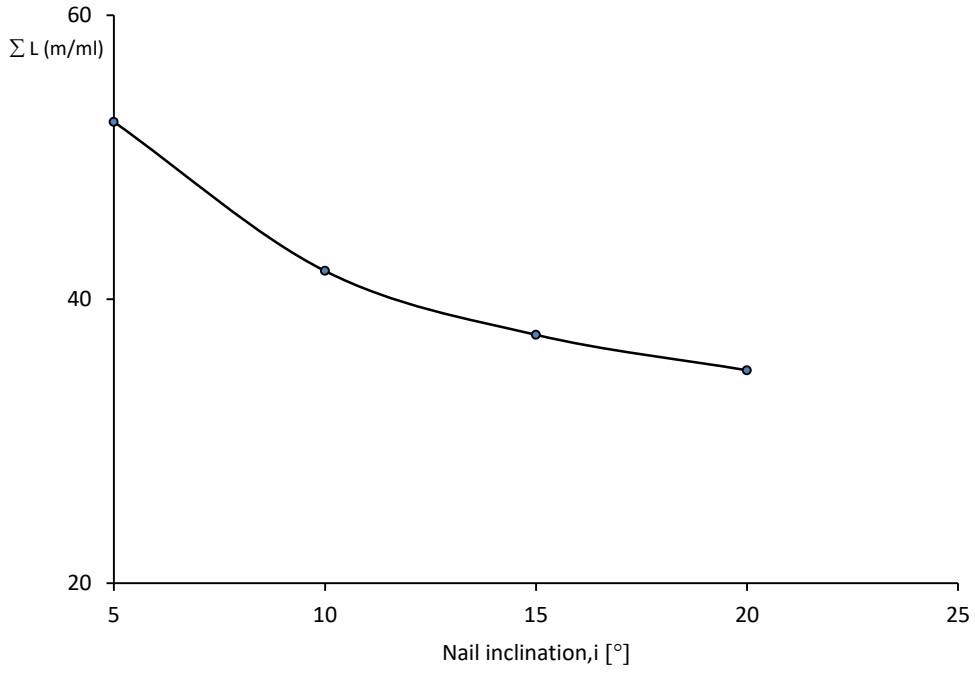

Figure 5. 7: Effect of nail inclination, i, on nail length [9]

5.4.2 Effect of wall-batter

The wall-batter is varied between 0° and 20° with a 5° interval. Other soil-nail parameters are maintained as in the base case. The relationship between wall-batter and safety factor is presented in Figure 5. 8 for variable wall-batter $\eta = 0°, 5°, 10°$ and 15°.

Next, the amount of wall length required for achieving a specified factor of safety of 1.5 is investigated by varying the vertical nail spacing citrus paribus. The results obtained are presented in Figure 5. 9. The plot shows that the wall-batter has a significant effect on nail length. The stepper the wall-batter the longer the total nail length required. This observation is in good agreement with literature [9].

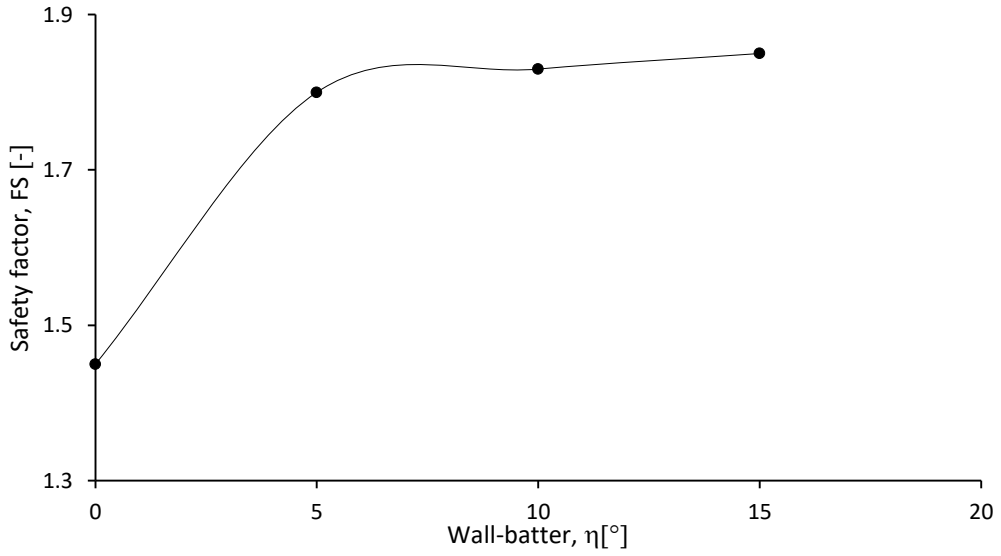

Figure 5. 8: Effect of wall-batter on safety factor.

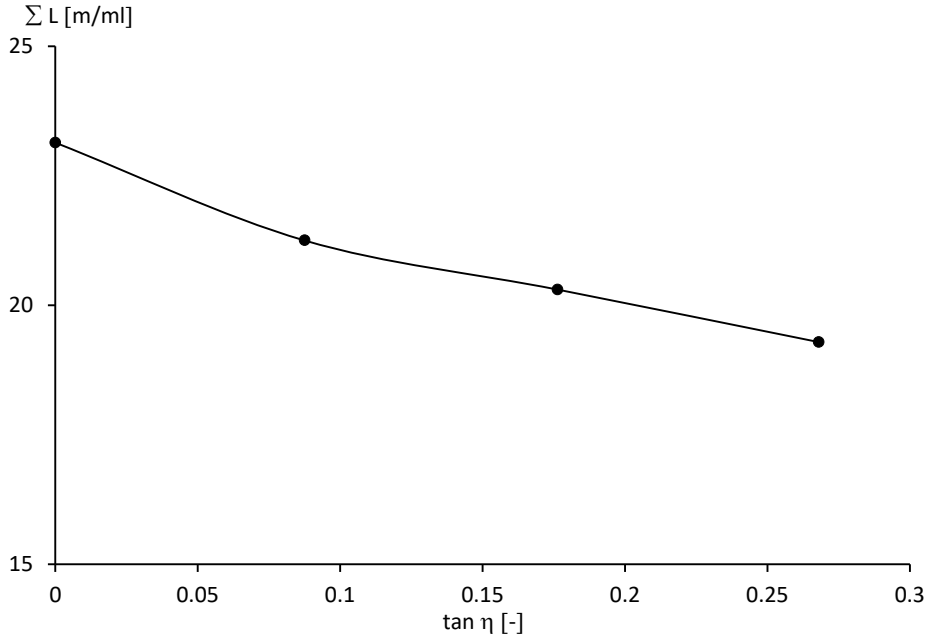

Figure 5. 9: Effect of wall-batter,η on nail length for variable vertical spacing from Plaxis 2D.

5.4.3 Effect of nail spacing

The effect of nail spacing is studied by varying and horizontal nail spacing between as 1.2 m and 2.5 m with an increment of 0.3 m. Accordingly, two different plots are produced.

- Figure 5. 10 shows plots of factor of safety for a nail inclination 10^{o} and four different wall-batter values.
- Figure 5. 11 shows plots of factor of safety for constant wall-batter $\eta = 0°$ and three different soil nail inclinations.

From the plots, the following observations are noted.

- Safety factor decreases almost linearly with increasing nail spacing. A similar result was found using the wedge approach. The rate of decrease found in the Geosuite analysis was nonlinear was found to be increasing with nail spacing.

- The rate of decrease is weakly influenced by both nail inclination and wall-batter.

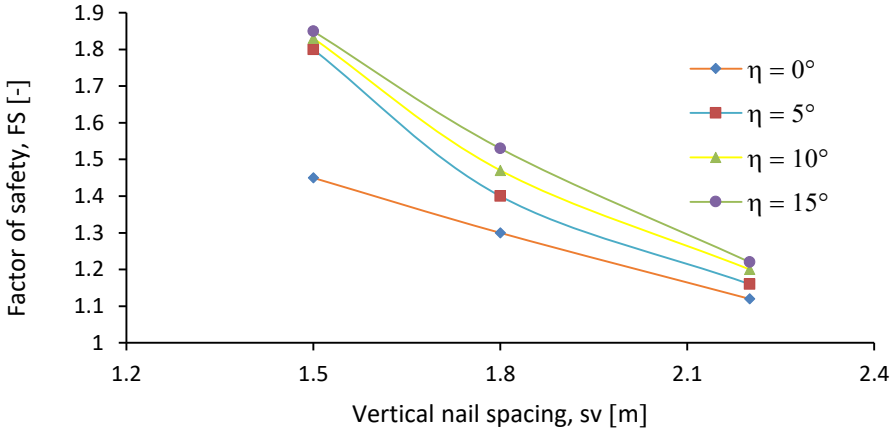

Figure 5. 10: Effect of vertical spacing on factor of safety for different wall-batter angle.

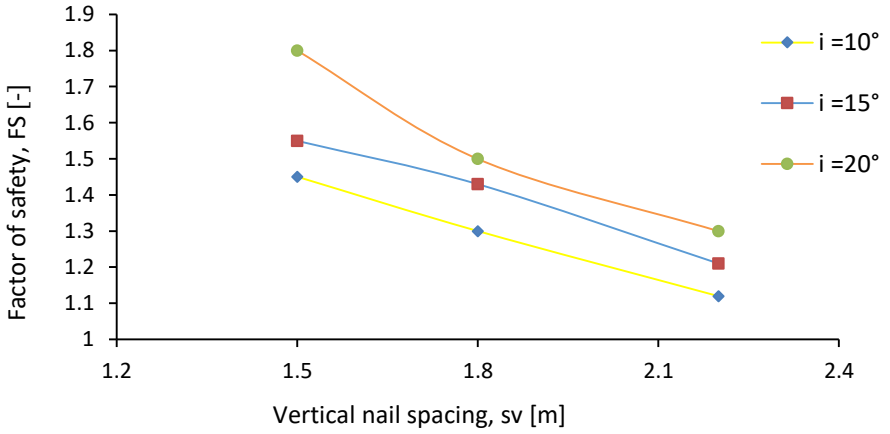

Figure 5. 11: Effect of vertical spacing on factor of safety for different soil-nail inclination.

5.5 Effect of some soil parameters on safety

In this section, the effect of friction angle and cohesion and dilatancy angle on safety factor is considered. Stiffness parameters are as defined elsewhere.

5.4.1 Effect of strength parameters (c and ϕ)

The cohesion c is set to 5 kPa, 12 kPa and 25 kPa while other parameters are maintained as in the base case. The plot of safety factor versus cohesion is presented in Figure 5. 12. Then, the friction angle ϕ is set to 26°, 30, 35° and 39° while other

parameters remain as in the base case. The relationship between friction angle and safety factor is presented in Figure 5. 13.

As expected both cohesion and friction angle have a positive contribution to the safety factor. For the studied domains, i.e., $c \in [5\,\text{kPa}, 25\,\text{kPa}]$ and $\phi \in [26^{\circ}, 40^{\circ}]$, the increase in safety factor is almost linear in both cases.

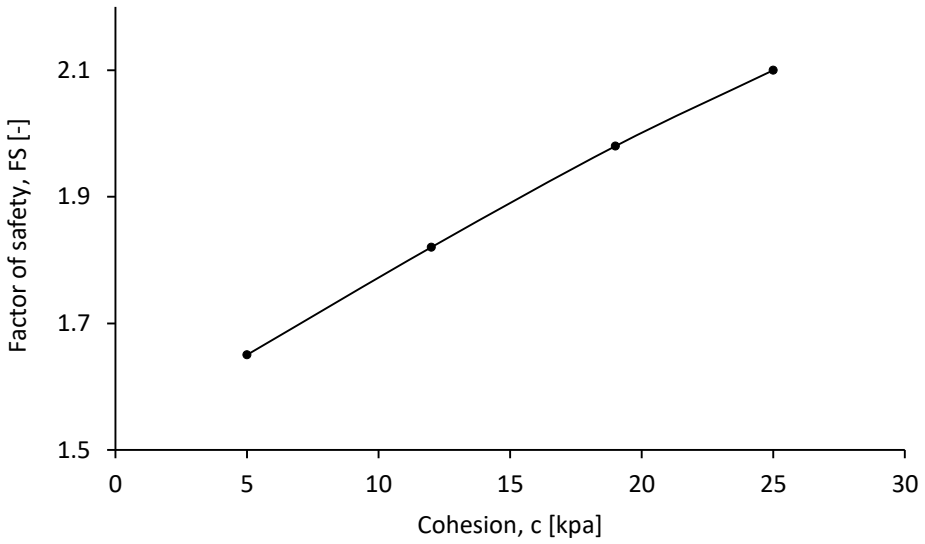

Figure 5. 12: Effect of cohesion on safety factor

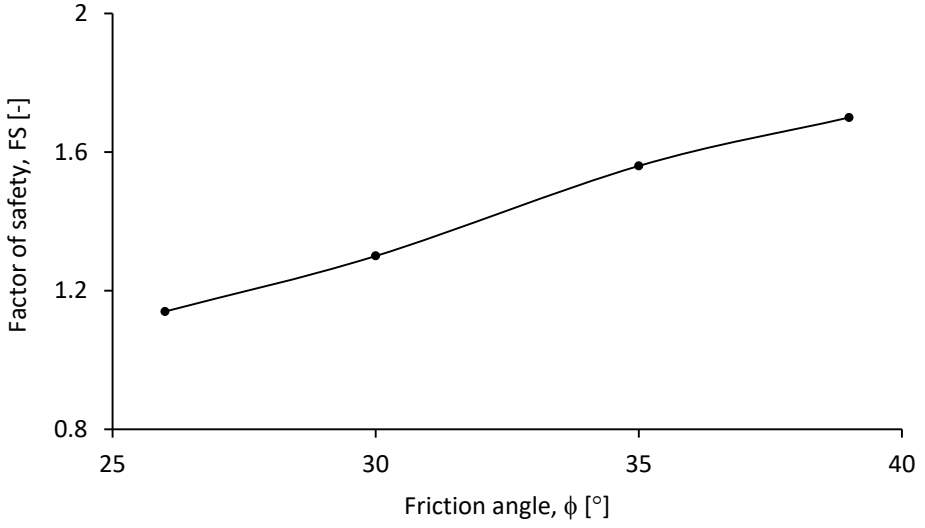

Figure 5. 13: Effect of friction angle on safety factor

5.4.2 Effect of dilatancy angle

The dilatancy angle ψ is set to -4°, 0°, 4°, 10°, 20°, 30° and 39° while other soil parameters are maintained as in the base case. The relationship between dilatancy angle and the calculated safety factor is presented in Figure 5. 14. It is seen that the safety factor weakly increases with the increasing dilatancy angle. The increase is almost linear beyond the dilatancy angle of 4°.

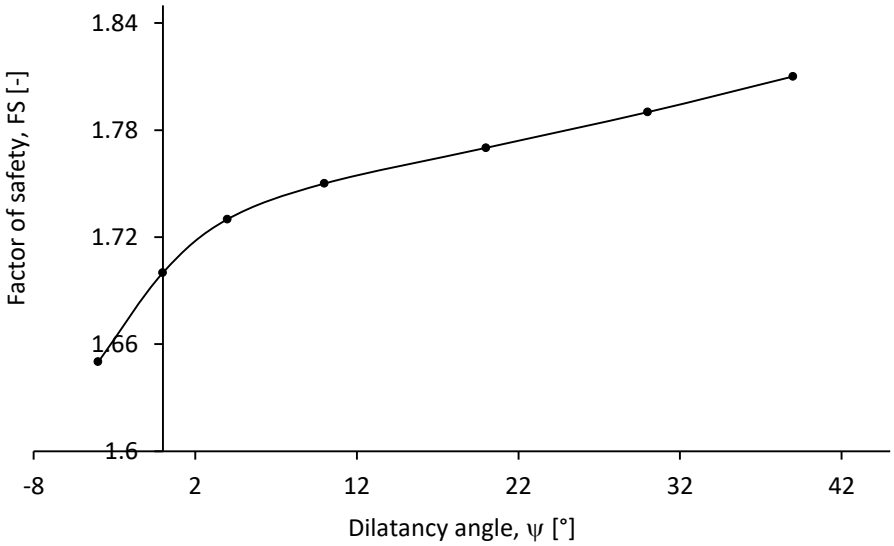

Figure 5. 14: Dilatancy angle effect on safety factor

5.6 Failure mechanism

Examples of the incremental displacement shading and the incremental shear strain shading after the *c-ϕ reduction* analysis are shown in Figure 5. 15 and Figure 5. 16 respectively. The figures illustrate the expected failure mechanism. The failure mechanism is closer to bilinear.

The effect of wall-batter and nail inclination on the failure mechanism are studied, Figure 5. 17 and Figure 5. 18. It is seen that both nail inclination and wall-batter affect

the size and shape of the failure mechanism. The influence pattern however is not consistent.

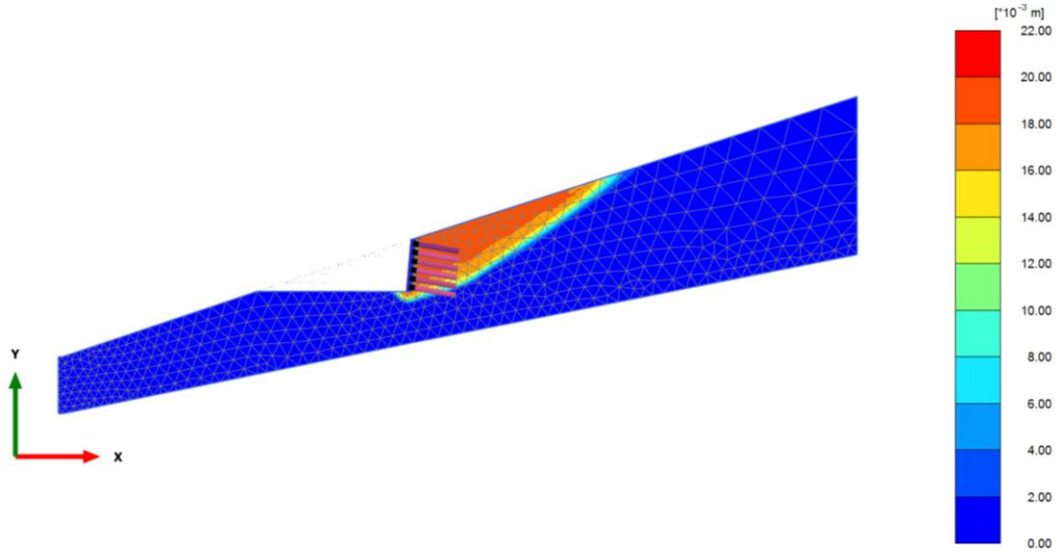

Figure 5. 15: Example of failure mechanism as increamental displacment sheading (i = 10°, η = 5°, and sv= 1.5m)

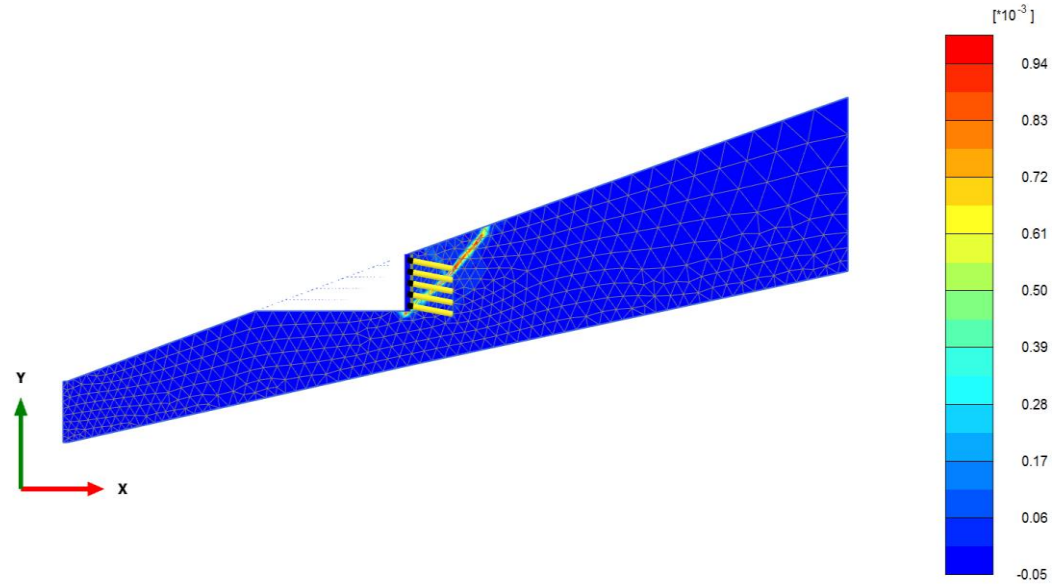

Figure 5. 16: Example of failure mechanism as incremental shear strain sheading (i = 10°, η = 0°, and s_v= 1.8 m)

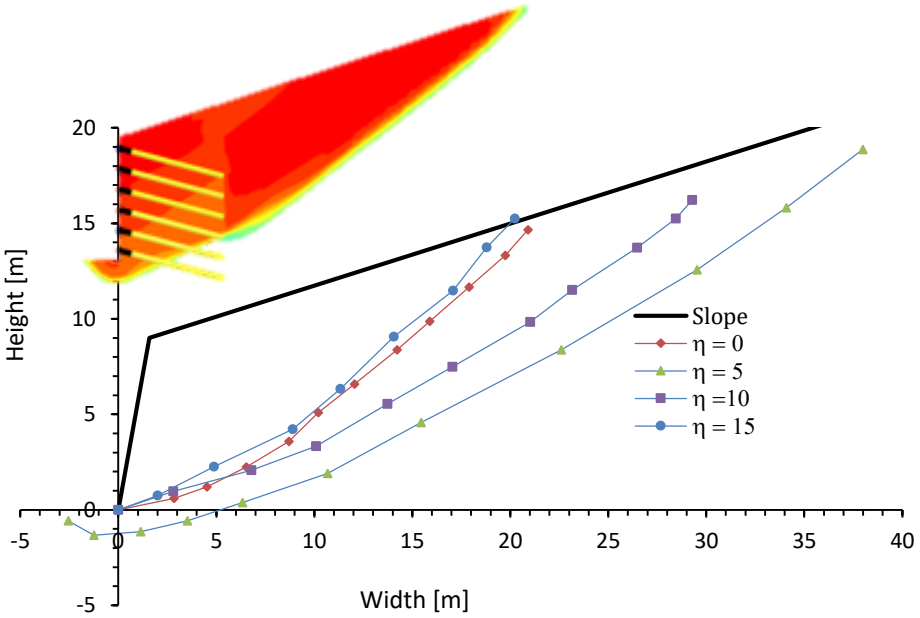

Figure 5. 17: The influence of wall-batter on the geometry of the failure mechanism.

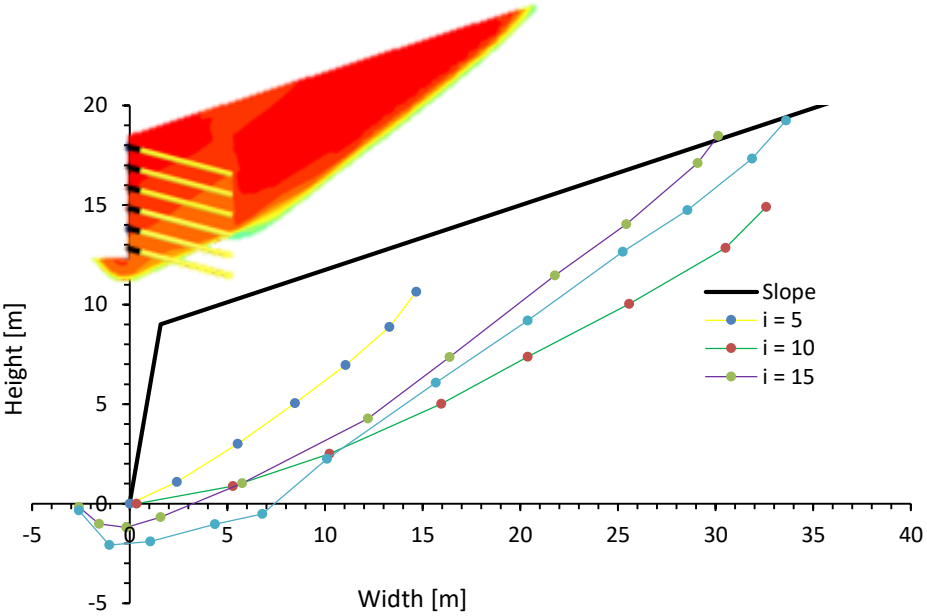

Figure 5. 18: The influence of nail inclination on the geometry of the failure mechanism.

5.7 Structural forces in the nail

The maximum axial forces on each soil-nail is presented in Figure 5. 19 for various nail inclinations. As can be seen, trend shows that the maximum nail axial forces on the nail increase with the increase in the depth of excavation. The maximum axial forces experienced by the free length of each nail during the whole excavation process are

studied for different nail inclination and wall-batter. The results are presented in Figure 5. 20 and Figure 5. 21. The trend shows that both nail inclination and wall batter have a significant effect on the maximum axial forces on the free length although the trend lacks consistency. This implies that the nail head axial forces are not only the function of spacing but also nail inclination and wall-batter. This is contrary to some suggested empirical equations in literature.

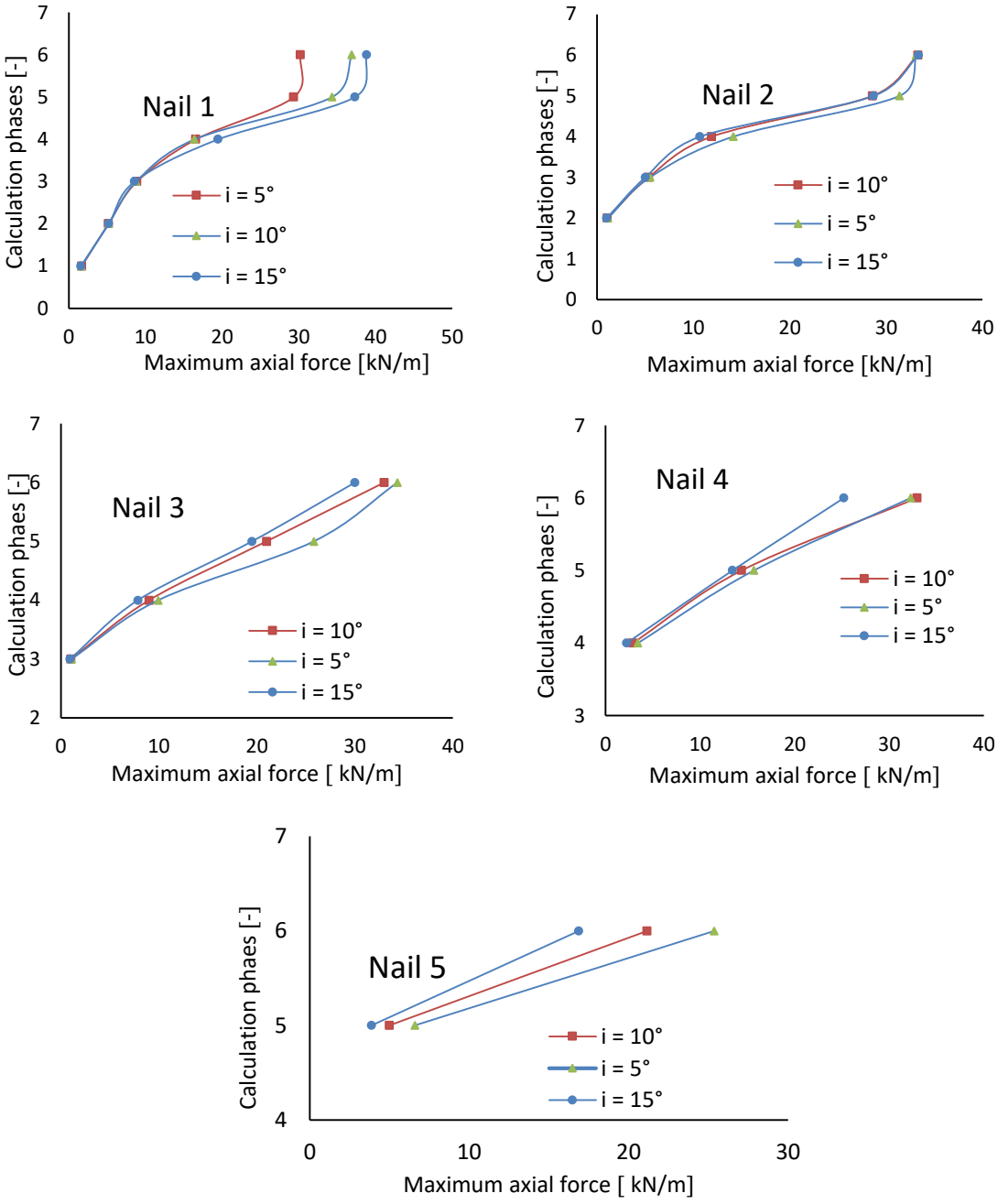

Figure 5. 19: Maximum axial nail forces for different calculation phases

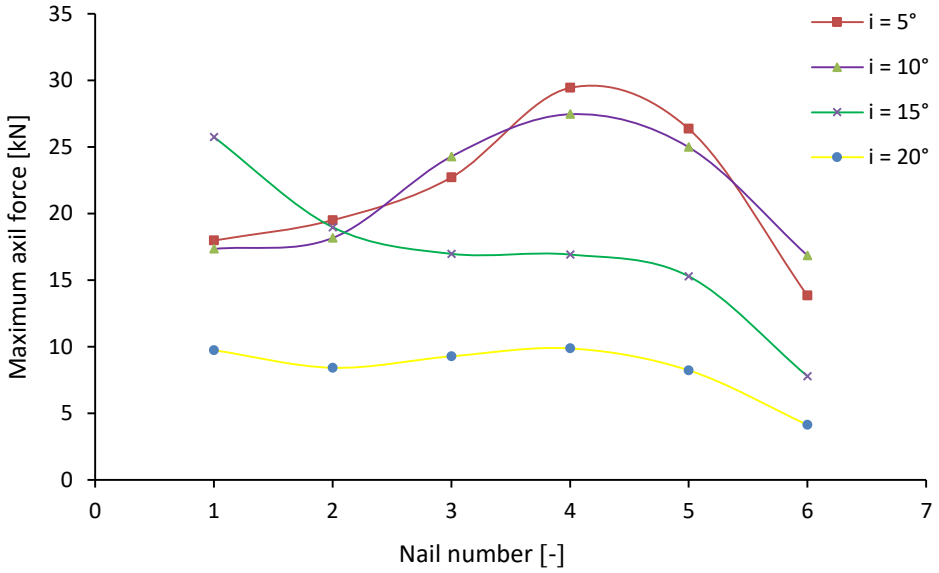

Figure 5. 20: Axial forces on the free length for different nail inclination

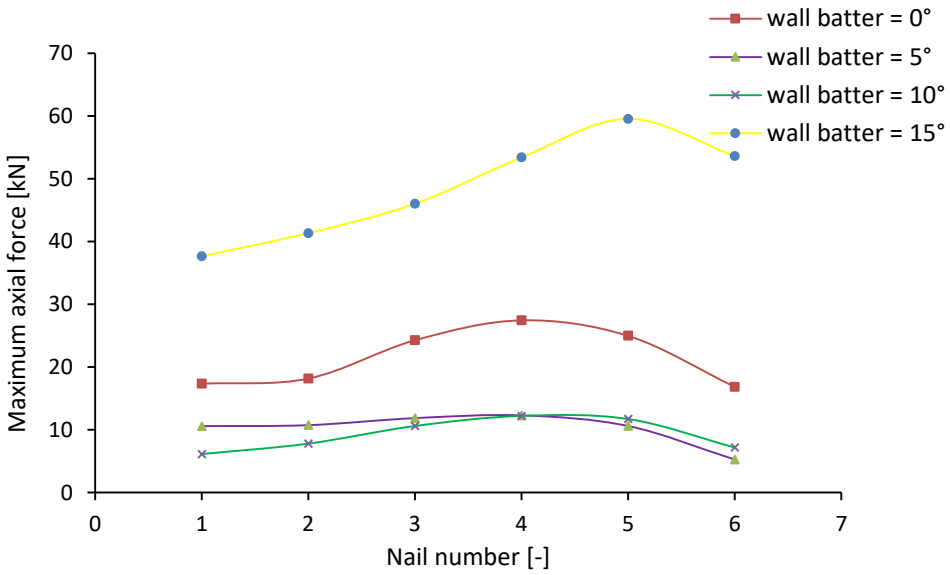

Figure 5. 21: Axial forces on the free length for different wall-batter

5.8 Structural forces in the facing

The effect of wall-batter on structural forces (shear forces and bending moments) of the facing wall was studied by varying the wall-batter while maintaining the other parameters as in the base case. The moments and the shear forces in the facing are shown respectively in Figure 5. 22 and Figure 5. 23. Generally, the bending moments

are small and are found to decrease consistently with increasing wall-batter. The wall-batter also affects the shear forces in some way but with an inconsistent pattern.

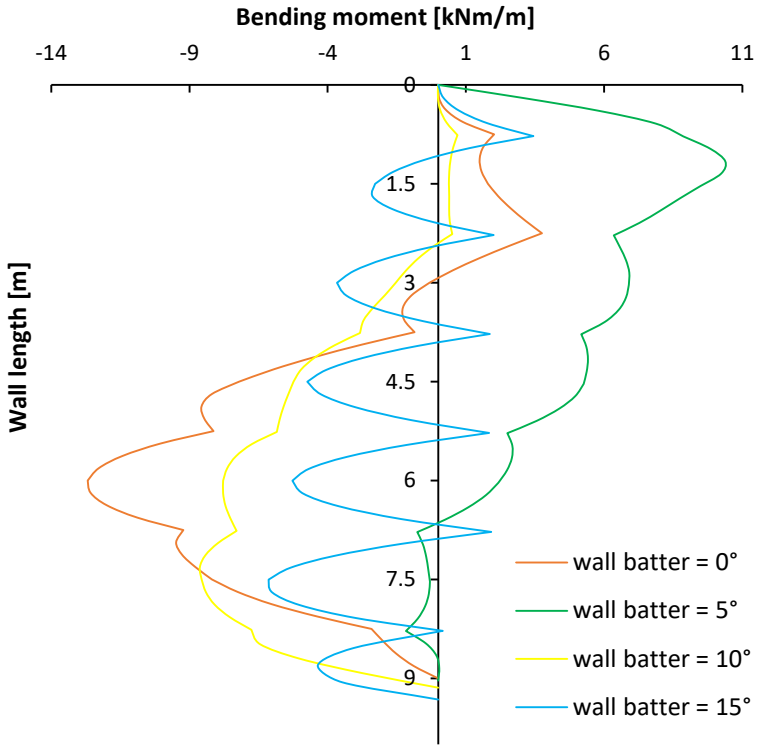

Figure 5. 22: Bending moment diagram for different wall-batter

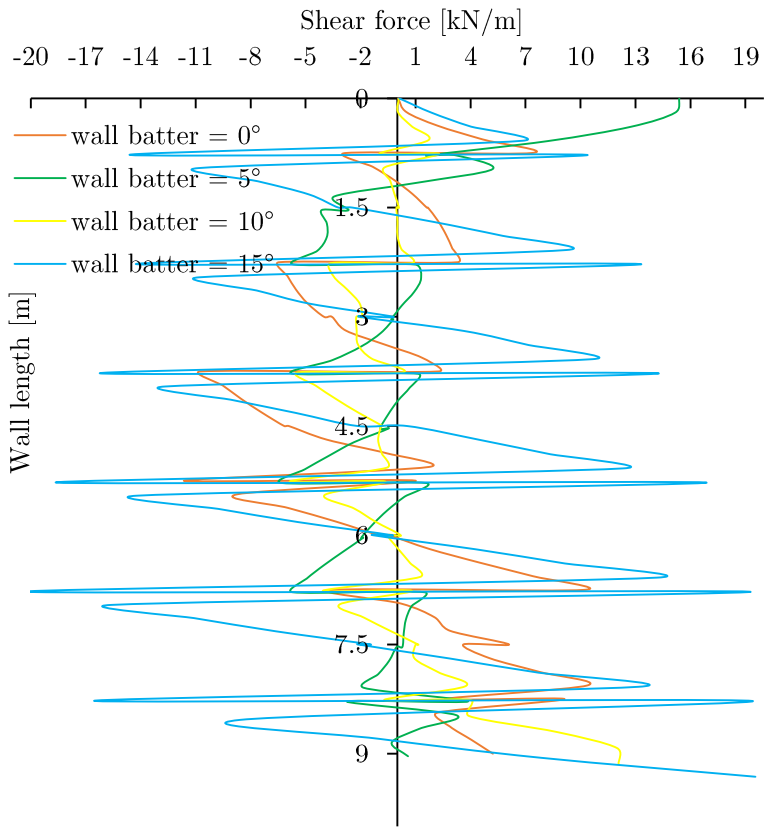

Figure 5. 23: Shear force diagram for different wall-batter

5.9 Earth pressure on wall

To study the variation of the earth pressure along the RCS facing the wall-batter is varied between 0° and 15° with a 5° interval. The results of earth pressure along the wall is presented in Figure 5. 24. As seen, wall-batter has some influence on the magnitude and distribution of earth pressure. However, the influence pattern however is not consistent. It is also noted that stress concentrations occur around the nail positions.

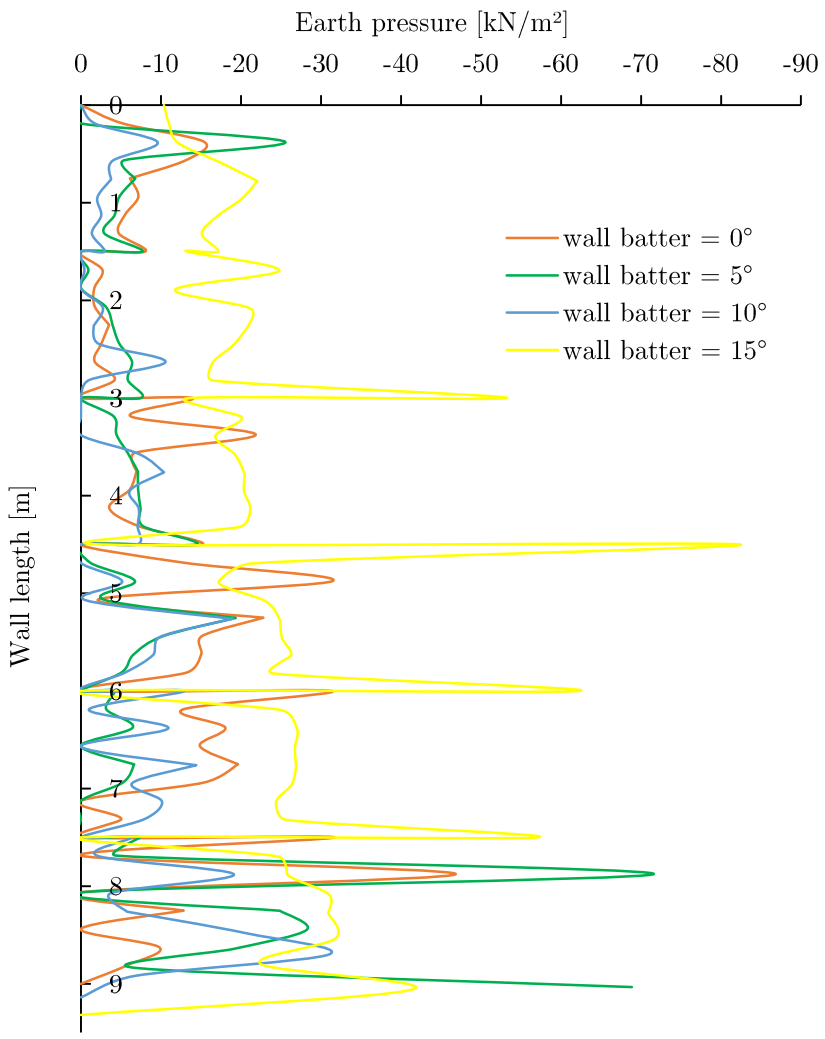

Figure 5. 24: Earth pressure along the facing for different wall-batter

5.10 Wall deformation

In Figure 5. 25 the horizontal displacement is plotted for different wall-batter. The maximum horizontal deformations is also plotted against wall-batter in Figure 5. 26. The trends show that the value of horizontal wall deformation decreases with increasing wall-batter.

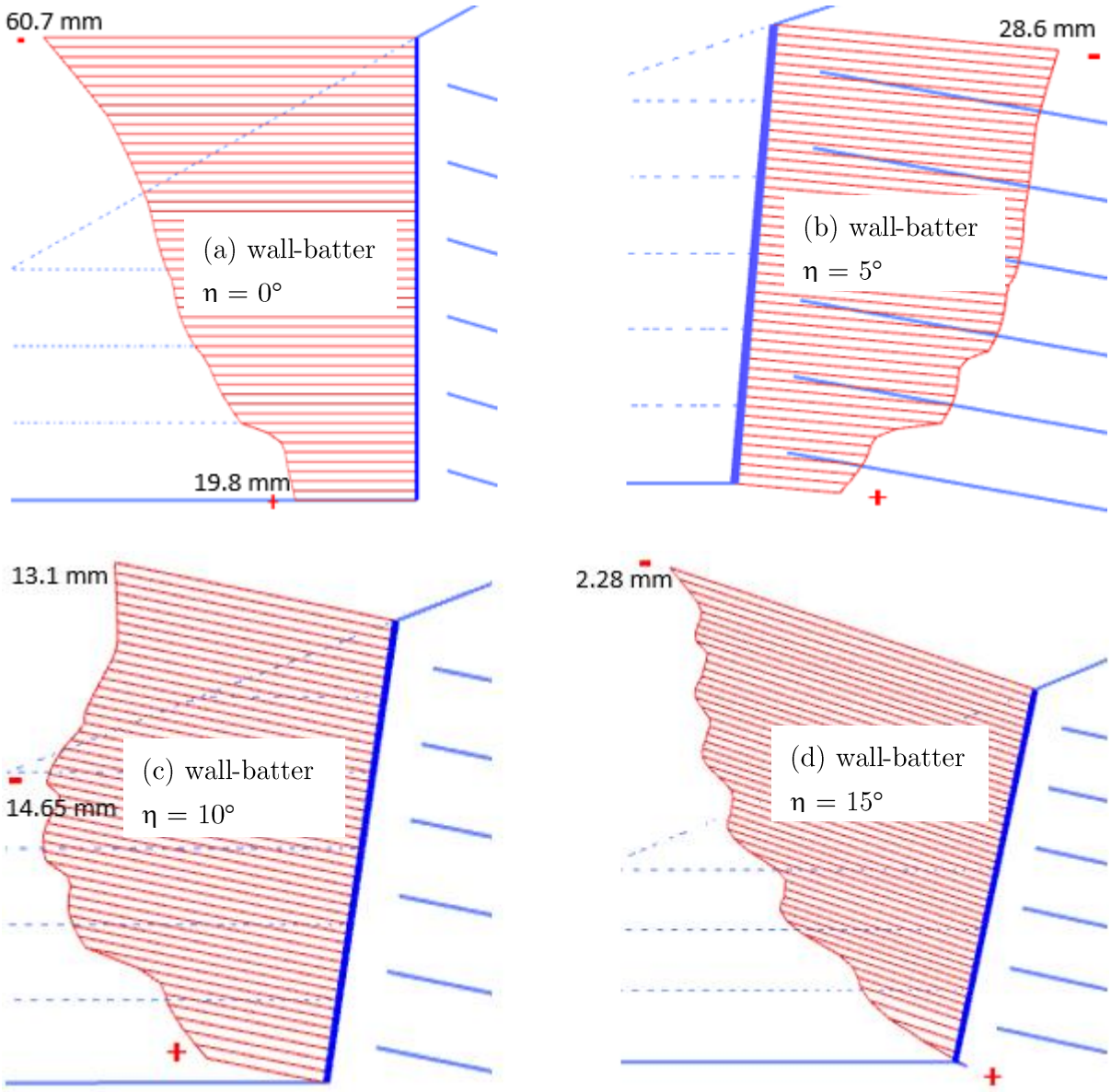

Figure 5. 25: Horizontal wall deformation for different wall inclination

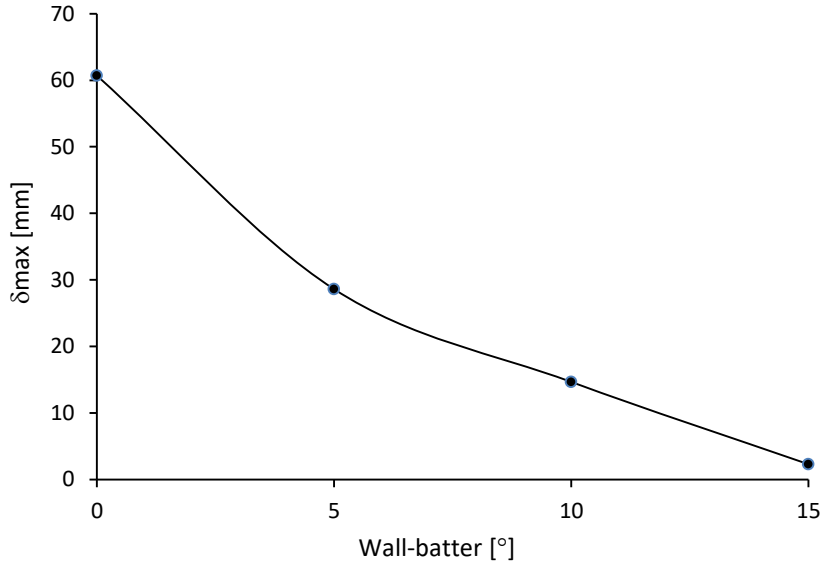

Figure 5. 26: Maximum horizontal deformation versus wall-batter plot

5.11 Comparison of Plaxis 2D and Geosuite calculation results

For the same soil domain and soil-nail configuration system, the factor of safety obtained in Geosuite and Plaxis 2D are presented in Table 5. The information in Table 5 is also shown in plots in Figure 5. 27 and in Figure 5. 28. It can be seen that, mostly, safety factors obtained in Plaxis-2D are a bit higher than the safety factors obtained from Geosuite analyses. However, for the 25° nail inclination the safety factor value obtained from the Geosuite limit equilibrium analysis is higher. As can be seen in the figure, between soil-nail inclination 10° and 15° the plot of safety factor versus nail inclination obtained from plaxis-2D is linear, however the plot obtained from Geosuite is non-linear.

An example comparison of the shape and size of the failure mechanism for a soil-nail configuration with wall-batter 10^{o} and nail inclination 10^{o} is shown in Figure 5. 29. The shapes have some difference. Their size is comparable. The mechanism obtained from the Geosuite BEAST analysis is circular and shorter in comparison to the others. The mechanism obtained from the Plaxis 2D analysis is more extended than the mechanism obtained from the Geosuite BEAST analysis. The wedge method gave a longer sliding

plane (failure plane) compared to the failure mechanisms obtained from both Geosuite and Plaxis 2D.

Table 5. 6: Factor of safety results obtained from Plaxis-2D and Geosuite

		FS-plaxis-2D	FS-geosuite
i (°)	5	1.3	1.2
	10	1.45	1.38
	15	1.6	1.45
	20	1.83	1.79
η (°)	0	1.45	1.38
	5	1.8	1.76
	10	1.83	1.77
	15	1.85	1.82

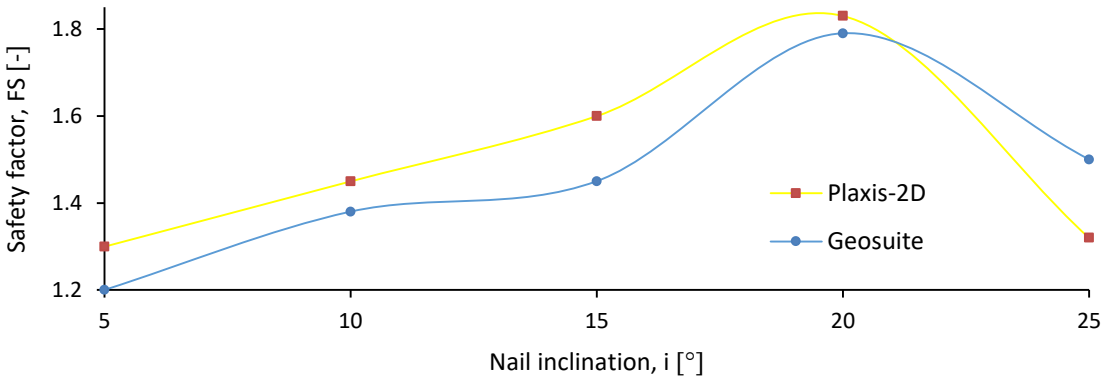

Figure 5. 27: Effect of soil-nail inclination on safety factor

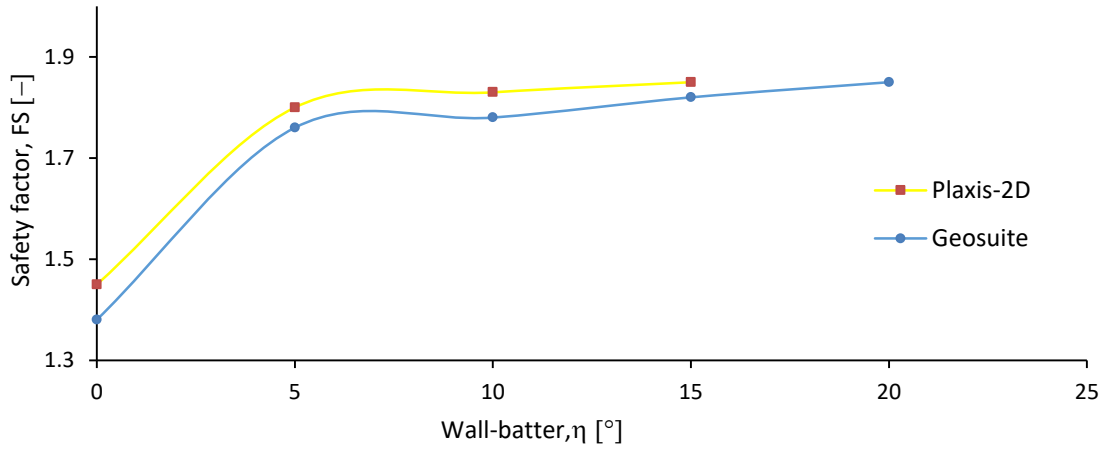

Figure 5. 28: Effect of wall-batter on safety factor.

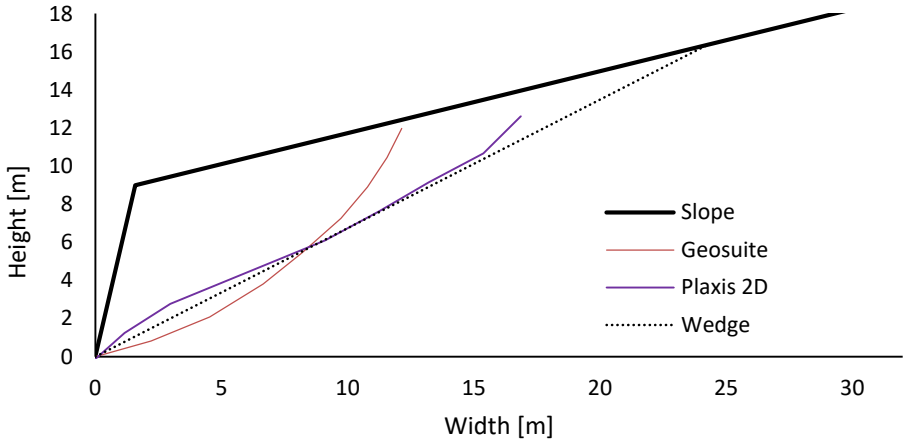

Figure 5. 29: Example comparison of size and shape of failure mechanisms.

CHAPTER 6: Application of Plaxis 3D

6.1 Introduction

In practice, the two dimensional analysis of slopes is more accepted since lower factors of safety result from ignoring the side effects of the 3D slide masses in the limit equilibrium methods [19].

There are unrealistic assumptions in engaging problems such as soil nailing in 2D. The nails do not extend infinitely in the *in-plane* direction-perpendicular to the plane of the slopes. A non-uniform pattern of nails can be chosen for various reasons. The 2D assumption cannot handle such configurations. When opportunities are available, it can be worthwhile to engage the problem in a 3D environment.

In this chapter, the Plaxis 3D finite element program is considered. The base case soil-nail system that was studied in the previous chapters is reconsidered here. The aim is

1) to study the effect of nail pattern of safety factor. *Uniform* and *staggered* nail patterns are considered.
2) to study the influence of the in-plane direction on the safety factor. This is done by considering one nail column (one spacing thickness) and five nail columns (six spacing thickness).
3) to compare safety factor obtained from Plaxis 3D with safety factor obtained from Plaxis 2D.

6.2 Base configuration and material parameters

Here too, a ground slope considered as base case in the previous chapters is considered. Configuration parameters are given in Table 6.1. The soil parameters used for the Mohr-

Coulomb material model are same as the one used in Plaxis-2D. A medium mesh size is generated and six excavation stages are considered. The RSC facing is modelled as elastic plate. As previously assumed, the first one meter of the nails is considered ineffectively grouted and modelled as a *node-to-node anchor*. The remaining nail length is assumed to be effectively grouted and modelled as *embedded pile row*. The skin friction between the grout and the soil is assumed to vary linearly along the nail length. Suppose the point on the nail is at depth z from the terrain, the skin friction is determined according to

$\frac{q_s}{z} = 4.9 \text{ kN/m}^3$.

Table 6. 1: Configuration parameters

Ground slope [-]	Wall-batter [°]	Nail inclination [°]	Nail spacing[m]	Nail length [m]	Free length [m]	Drill hole diameter [mm]
1:3	10	10	1.5	8	1	150

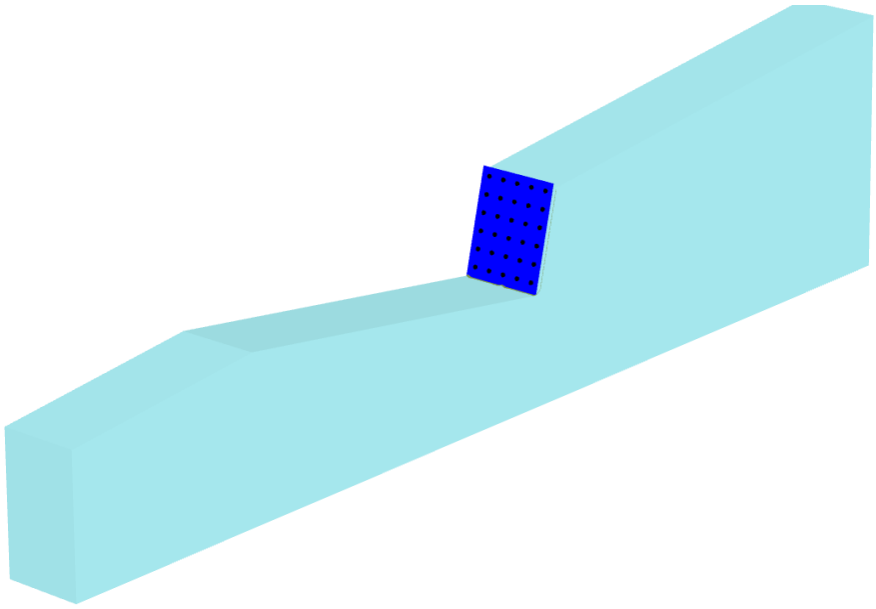

Figure 6. 1: The base case soil-nail wall configuration.

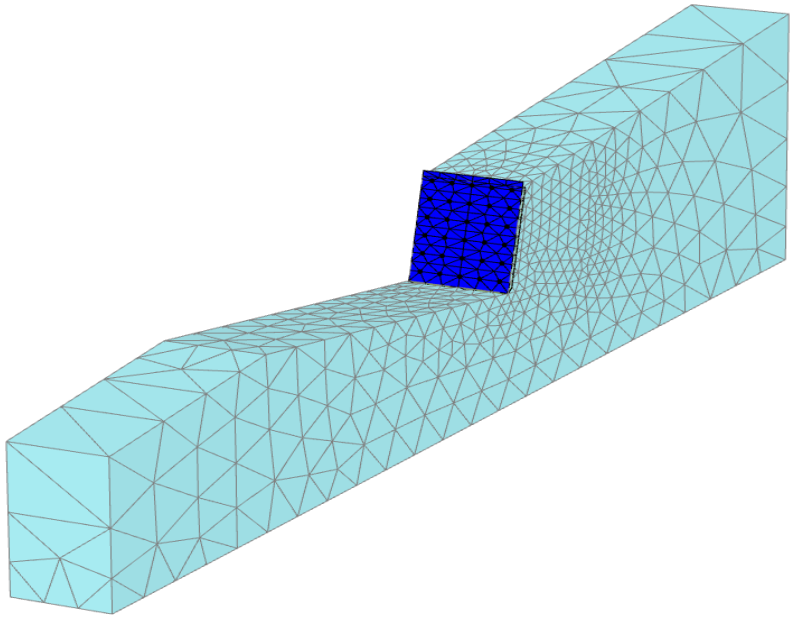

Figure 6. 2: A medium size mesh of the soil geometry

6.3 Nail pattern

Here, two soil-nail patterns, *uniform* and *staggered* nail patterns are considered. See Figure 6. 3. The safety factor result is presented in Figure 6. 7. It can be seen from the plots that the factor of safety obtained from uniform and staggered nail pattern are almost the same. The horizontal wall deformations are also nearly equal. The axial nail forces obtained in the staggered and uniform nail pattern are nearly equal and exhibit the same trend. In fact, for homogeneous soil medium as in the example considered here, the two patterns are not expected to have much difference. The result can be different if the soil is non-homogeneous. This can be studied by introducing non-structured weak soil layers. An example of axial force of the soil nail is shown in Figure 6. 6.

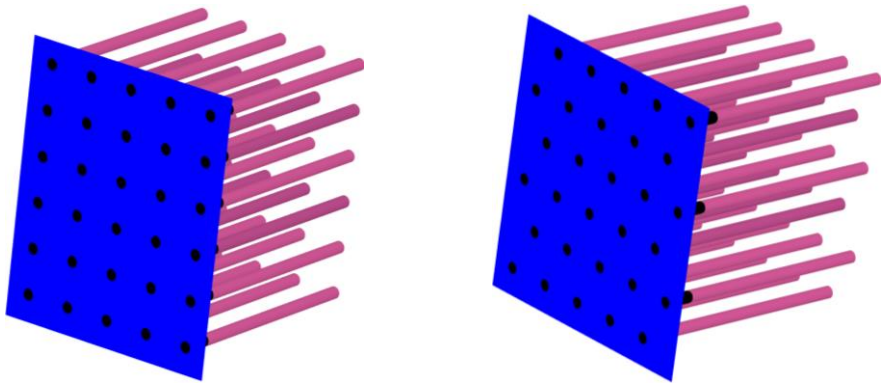

Figure 6. 3: Soil-nail patterns (left) uniform and (right) staggered

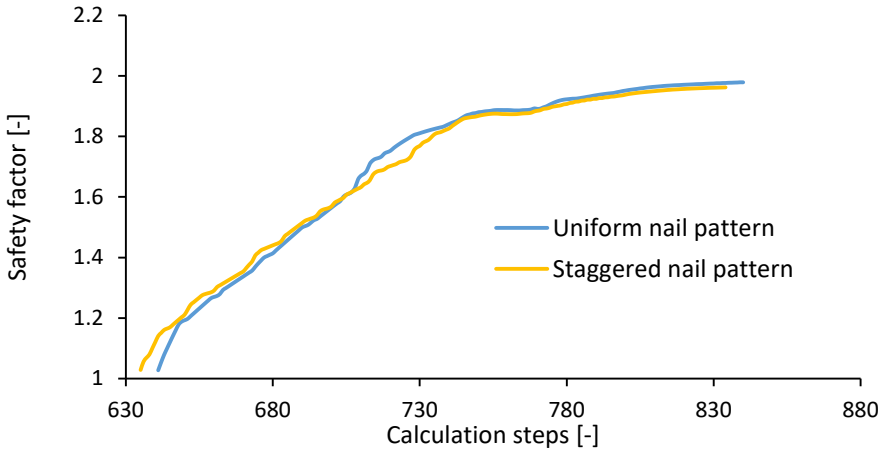

Figure 6. 4: Factor of safety results for staggered and uniform nail patterns

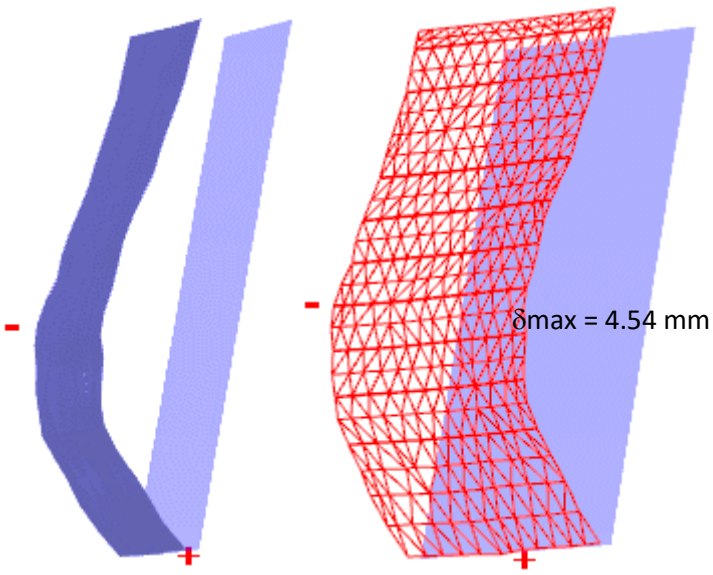

(a) Staggered nail pattern

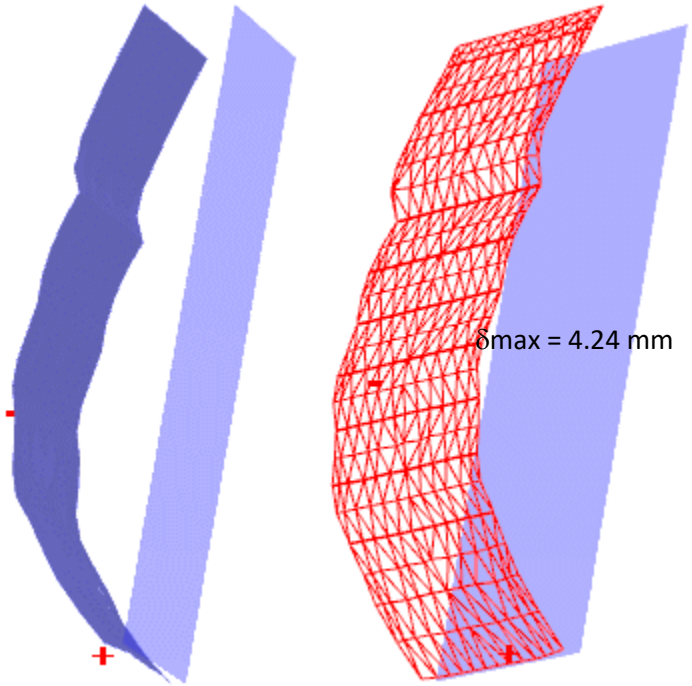

(b) Uniform nail pattern

Figure 6. 5: Horizontal wall deformations

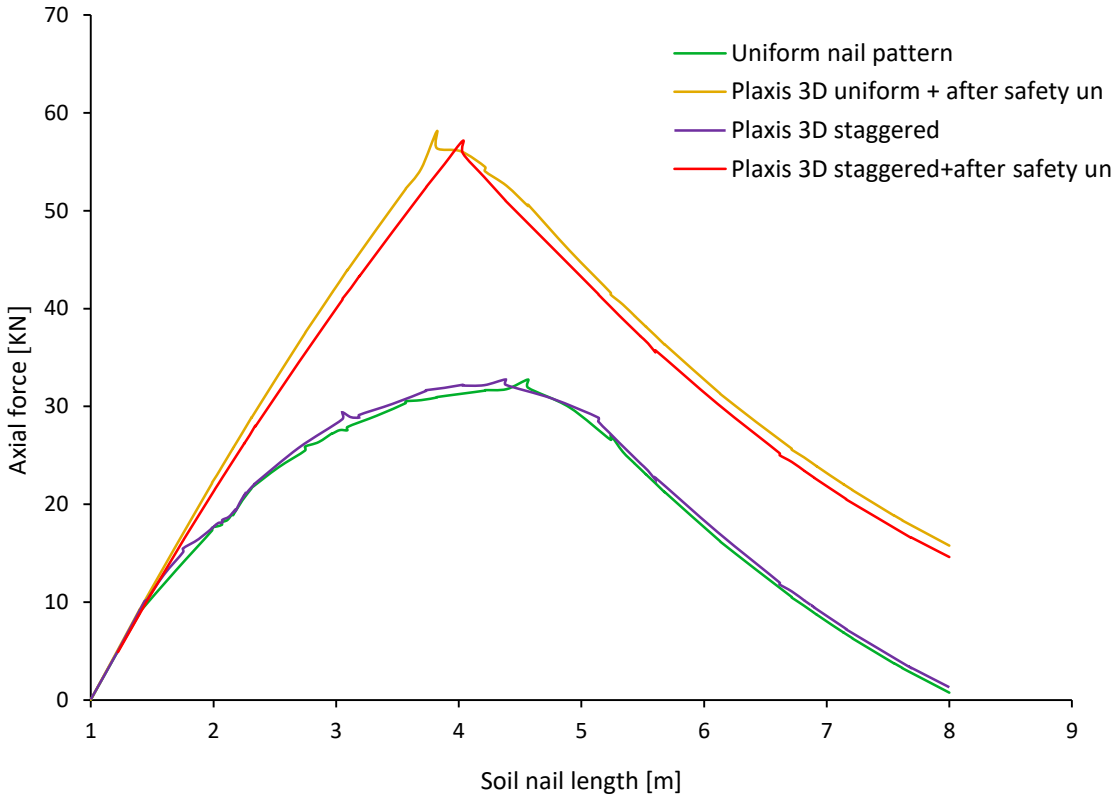

Figure 6. 6: Example of axial soil-nail force for nail 1

6.4 Effect of the in-plane dimension

Assuming a uniform nail pattern, one spacing and six spacing dimensions are considered in the direction perpendicular to the slope plane-*in-plane direction*. The safety factors are compared in Figure 6. 7. The results imply that the safety factor obtained in six spacing dimension is a bit higher.

The wall deformation for the one nail spacing thickness and the six nail spacing thickness models are presented in Figure 6. 8. A slightly higher deformation is obtained in the case of the single nail spacing thickness model. The difference however is not significant in this particular case.

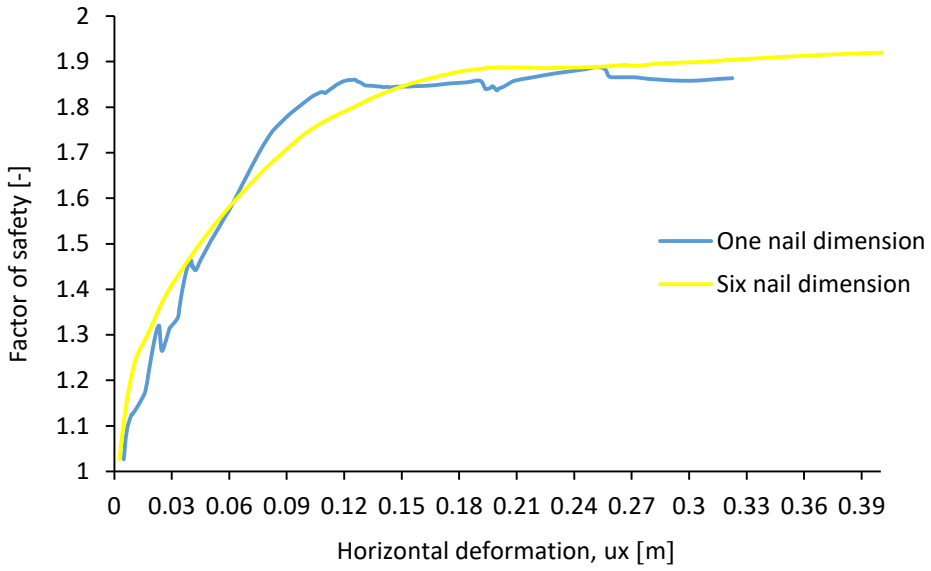

Figure 6. 7: Factor of safety results obtained in Plaxis-3D

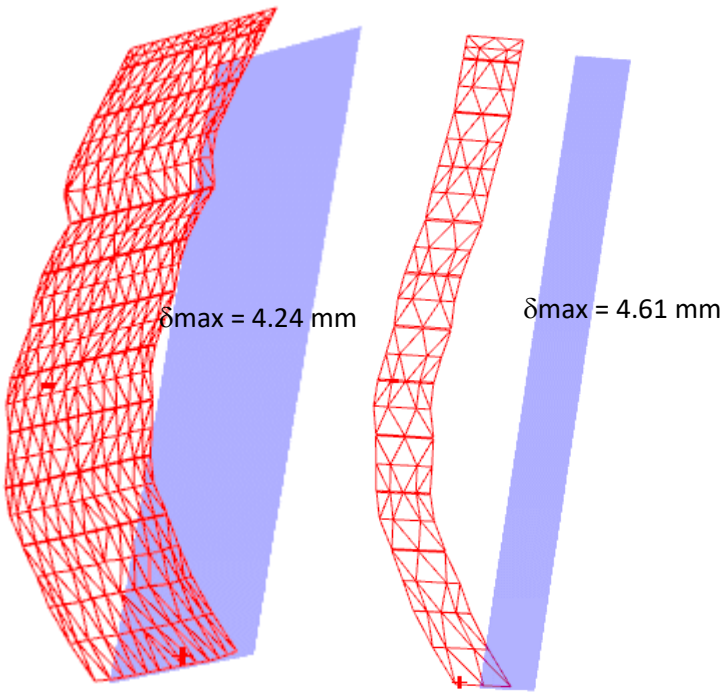

(a) (b)

Figure 6. 8: Wall deformation for a) six spacing thickness-five nail columns b) one spacing thickness-one nail column|

6.5 Illustration of failure mechanisms

The failure mechanism referred from the incremental displacement shading are plotted

a) For staggered, five spacing thickness, Figure 6. 9
b) For uniform, five spacing thickness, Figure 6. 10 and
c) For one spacing thickness, Figure 6. 11

The mechanisms obtained are similar among each other and similar to the ones observed in the Plaxis 2D analyses. They resemble the bilinear failure mechanism.

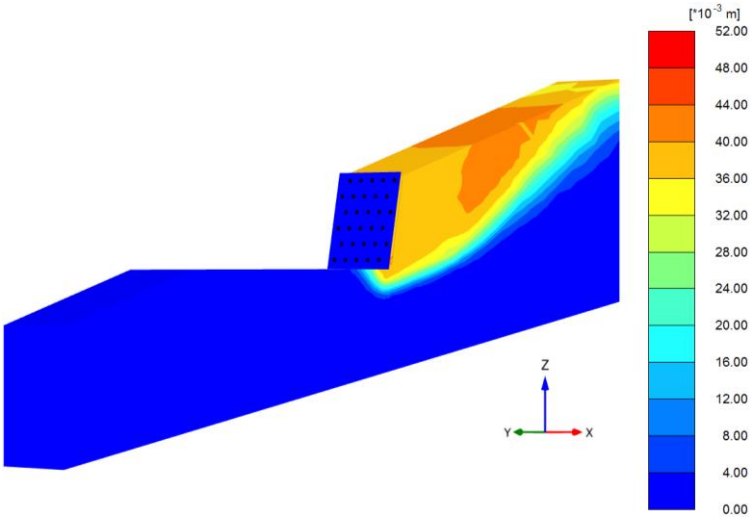

Figure 6. 9: Failure mechanism as incremental displacement plot for staggered nail pattern

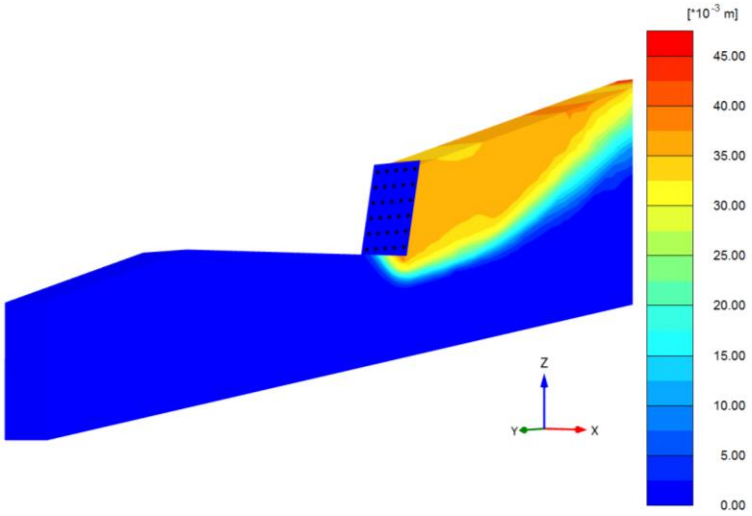

Figure 6. 10: Failure mechanism as incremental displacement plot for uniform nail pattern

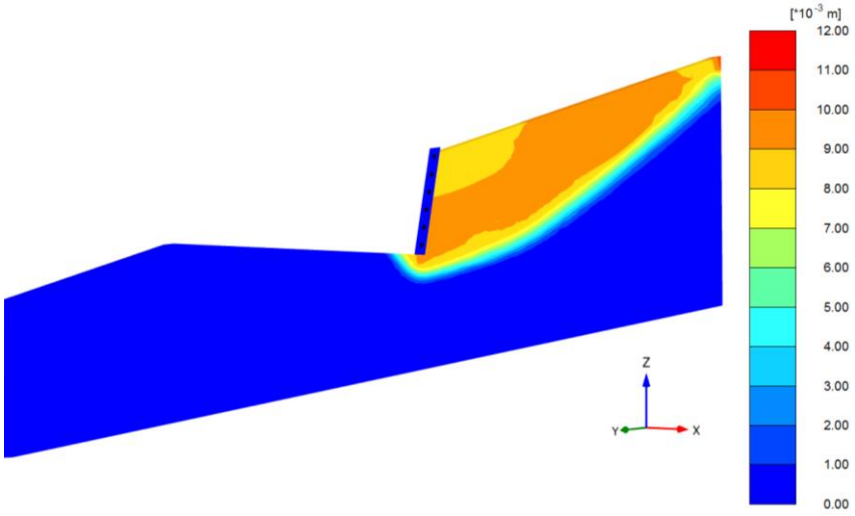

Figure 6. 11: Failure mechanism as incremental displacement plot for single column nail

6.6 In comparison with Plaxis 2D

Here, the safety factors obtained from Plaxis 3D are compared with Plaxis 2D results. As can be seen in Figure 6. 12 the safety factor obtained from Plaxis 2D is 1.7 and 1.84 from Plaxis 3D. Both the staggered and the uniform five spacing thickness Plaxis 3D analyses give higher safety factors than those safety factors obtained from both Plaxis 2D and single spacing thickness Plaxis 3D calculations.

Furthermore, the resulting nail forces and wall deformation outputs of Plaxis 2D and 3D calculations are compared. A relatively higher maximum axial nail forces are obtained in the case of the 3D calculations. The position of the maximum forces is also closer to the nail head in the case of the Plaxis 3D than the Plaxis 2D analyses results. A sample plot is shown in Figure 6. 13. Whereas the wall deformation pattern is the same in both cases, the magnitude of wall deformation obtained from the Plaxis 3D analyses is smaller than the 2D equivalent, see Figure 6. 14. The differences in the obtained results may be due to

'3D effect'. However, there are also basic difference between the Plaxis 2D and 3D than simply being 2D and 3D.

1) The elements in the two are different. The Plaxis 2D has *six noded* and *fifteen noded* elements. The latter is often used as is also used in this study. Whereas the Plaxis 3D has only tetrahedral element.
2) For a qualitatively defined mesh size-say medium, the sizes of the mesh in both cases can be different.

The differences due to element difference may be studied systematically. This may be done by modelling "plane strain" in Plaxis 3D by considering a considerably long domain perpendicular to the slope direction. It is difficult to study and quantify the differences in the mesh size. One possibility is to compare the number of elements and divide them by the average number of elements perpendicular to the slope direction and compare them with the number of elements generated in the Plaxis 2D. If the number of elements are then comparable, we may have reduced the potential differences due to the mesh size. To single out the '3D effects', these two prior investigations are essential. These studies are not done here and are suggested for further studies.

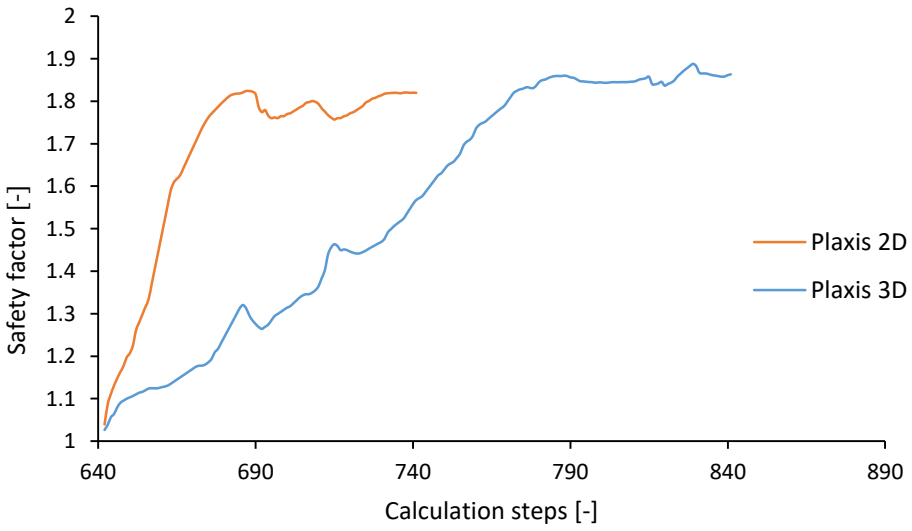

Figure 6. 12: Safety factor results obtained from Plaxis-2D and Plaxis-3D.

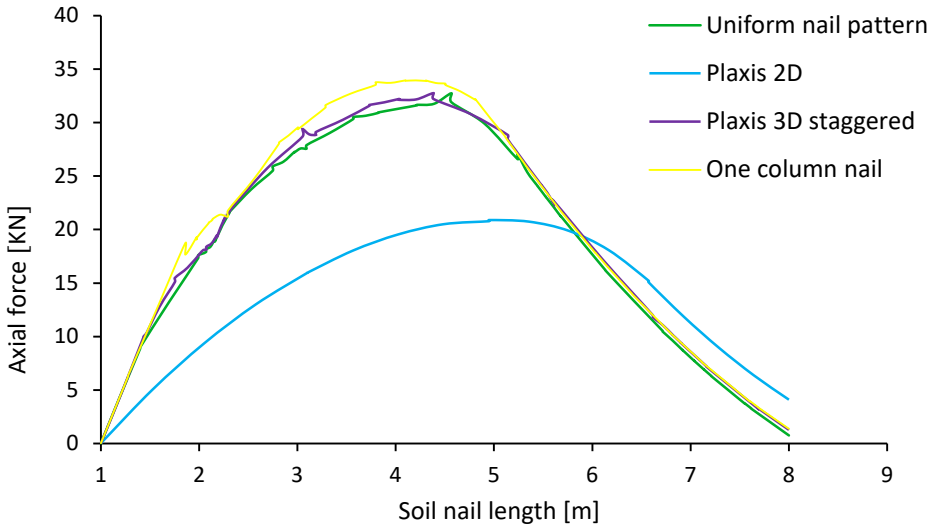

Figure 6. 13: Axial force along the nail versus soil-nail length

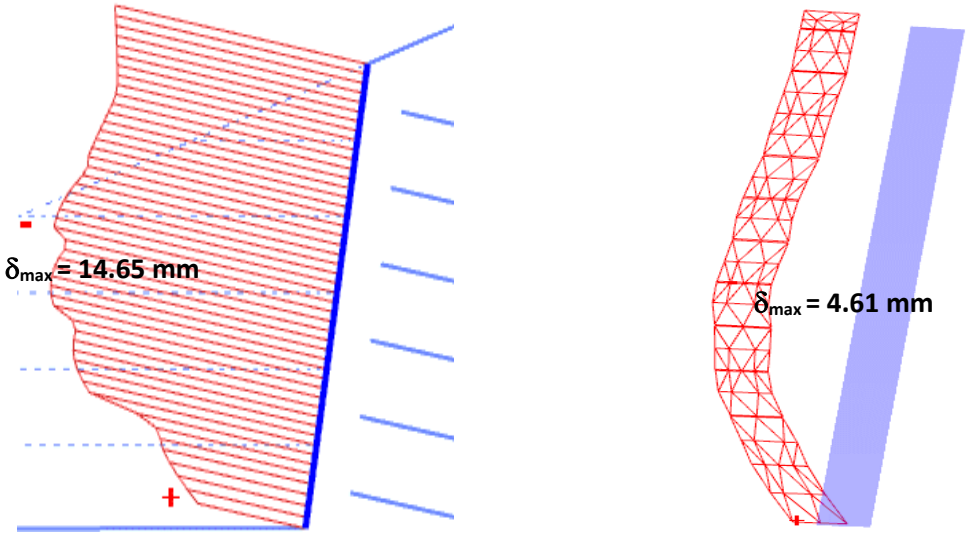

Figure 6. 14: Facing 2all deformation, Plaxis-2D (left) and Plaxis-3D (right)

CHAPTER 7: Case study

7.1 Introduction

In this chapter, preliminary design and analysis of a soil nailing system is carried out. The case project is to be implemented at a project site. The case is provided by the Multicosult AS.

The chapter starts out presenting the terrain profile and geotechnical characterization of the site. Then a rough sketch of the layout of a soil nail system is produced for which deformation analysis and stability analysis are performed using the Plaxis 2D FEM package.

7.2 About the case

A road construction close to Trondheim, from Espeneset in the south to Geithamrane in the north is being carried out. Along parts of the road construction, a steep cut is to be made as making self-stable gentler slopes would require a massive excavation work which can be costly. The soil nailing system is chosen for stabilization of the steep cut. See the Figure 7. 1 below.

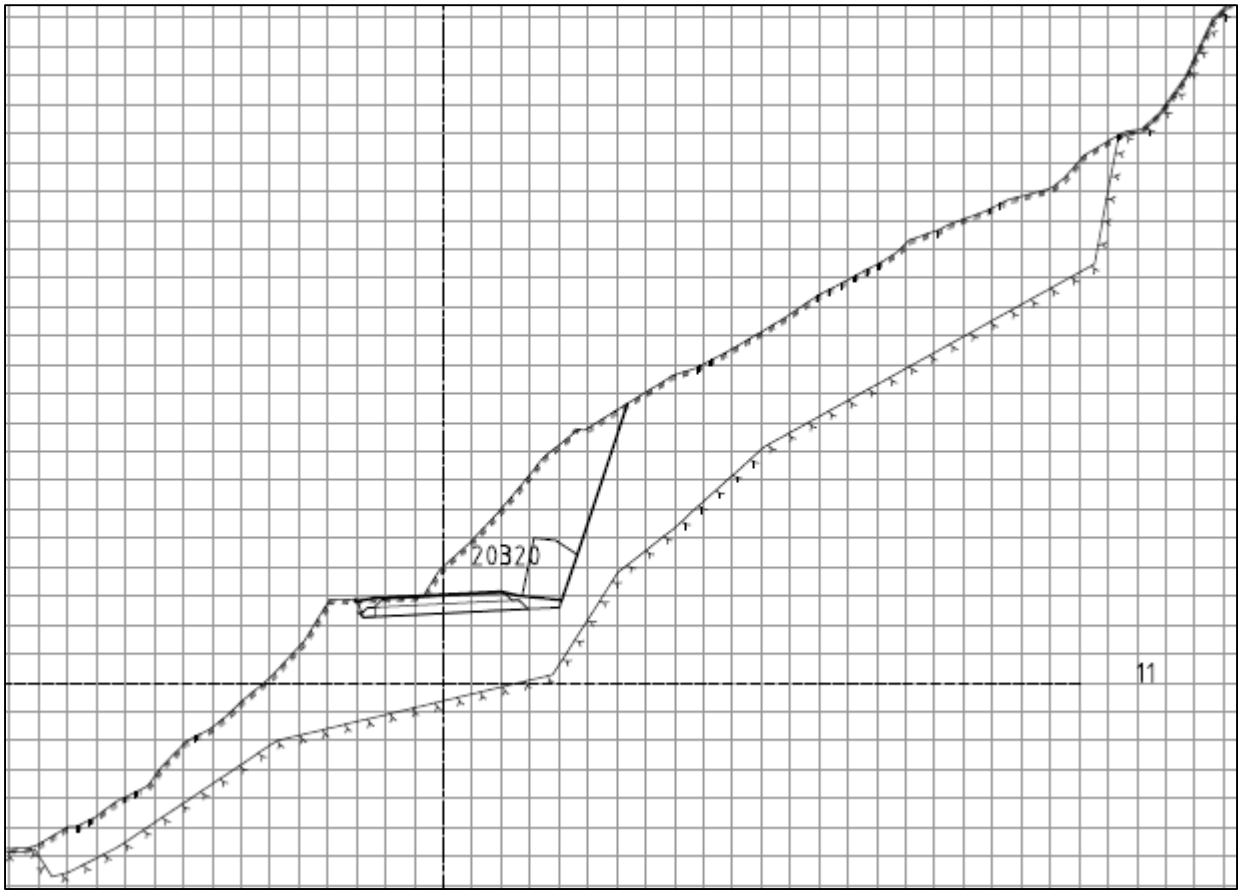

Figure 7. 1: Terrain profile

The particular profile along the roadside that is considered in this study is given in Figure 7. 1. To minimize the amount of cut volume, a two level soil nailing is proposed.

- The lower cut starts at the right edge of the road shoulder and continues with a slope of V: H = 3:1 for a 9 m height.
- The second cut starts at the top of the first cut and continues with a slope of V: H = 1.5: 1 until it intersects the terrain, see Figure 7. 2.

7.3 Soil-nail configuration

A preliminary design of the soil-nail configuration is done based on experiences gained in this study and suggestions in literature. With an initial choice of configuration parameters, nail length, drill hole dimeter and vertical and horizontal nail spacing are decided, Table

7. 1. The sketch of the soil-nail configuration and the corresponding excavation plan are shown in Figure 7. 2.

Table 7. 1: Geometric properties

Slope	H [m]	L [m]	D [m]	S_v [m]	S_h [m]
1-lower	9	11	0.12	1.5	1.5
2-upper	8.9	10	0.12	2	2

Table 7. 2: Comparison with ranges and values suggested in literature

Parameter	Unit	Bored and grouted Upper slope	Bored and grouted Lower slope	Bored and grouted (Gravel and sand)-Guidelines
Nail inclination	[°]	18	18	10-20*
Nail spacing, s_v	[m]	2	1.5	1.25-2**
Nail spacing area	[m^2]	4	2.25	<=4
Length ratio	[-]	1.1	1.2	0.5-0.8***
Friction ratio	[-]	0.30	0.59	0.3-0.6
Strength ratio	[-]	3.6E-03	6.4E-03	$0.4x10^{-3}$-$0.8x10^{-3}$
Deformation ratio	[-]			0.001-0.003

* Compared to the nail inclination range proposed in literature, this choice is on the maximum side. In our study, an optimum nail inclination around 20 degrees was found. This chosen value is a couple of degrees lower than the optimum. This is to maximize the positive contribution of the nail inclination as well as to be on the safe side for possible placement variations during construction. Coincidentally, the chosen angle happens to be perpendicular to the facing of the lower slope.

** Statensvegvesen manual [1]

*** Due to inclined back slope, a larger length ratio is chosen.

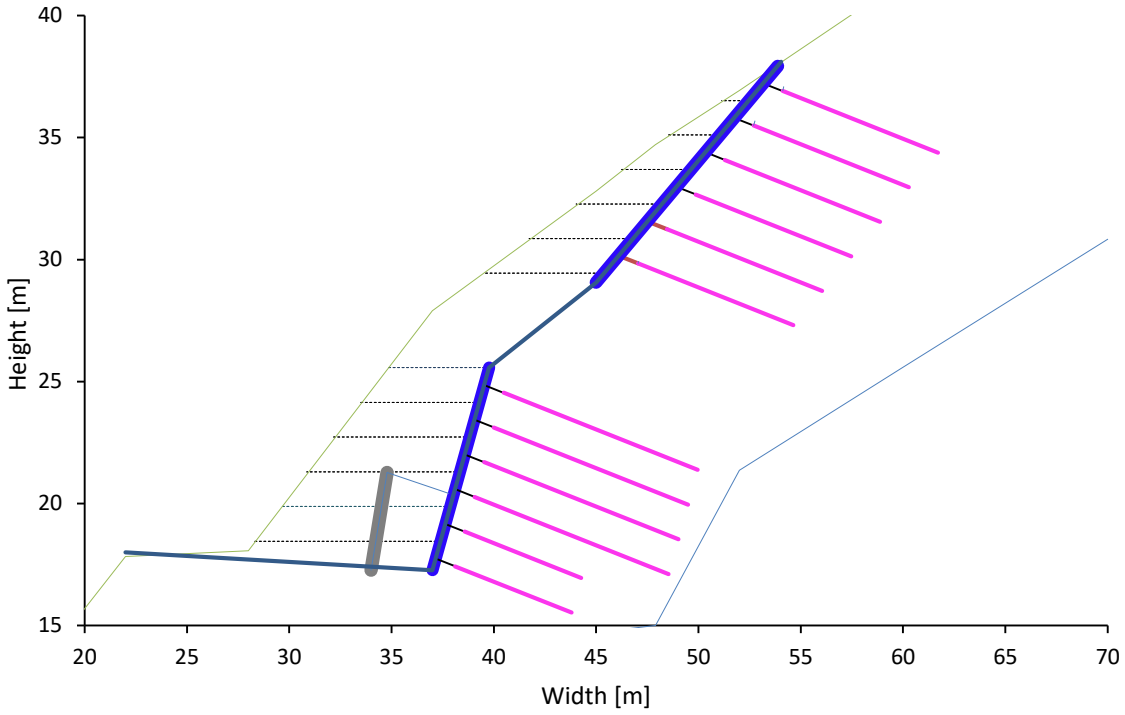

Figure 7. 2: Sketch of the preliminary soil-nail configuration and excavation plan.

7.4 Material parameters

7.3.1 Soil parameters

By the start of this project, except a visual inspection of the site, detailed site investigation was not carried out. We are therefore to rely on the engineering estimates of various parameters provided by Multiconsult AS. Very steep slopes are standing; there must be some cohesion in the soil. Furthermore, from the site inspection, it is evident that there are no structural utilities behind the proposed wall. The ground water table is assumed to be lower than the bottom of the cut.

Figure 7. 3: Site condition

Table 7. 3: Material parameters

Description			**Layer1**	**Layer2**
General	Material set	Identification		
		Material Model	Mohr-Coulomb	Mohr-Coulomb
		Drainage type	Drained	Drained
	General properties	γ_{unsat} [kN/m^3]	21	21
		γ_{sat} kN/m^3]	12	12
Parameters	Stiffness	E_{50}^{ref} [-]	81000	
		E_{oed}^{ref} [-]	9.00E+04	
		ν_{ur} [-]	0.2	0.2
	Strength	c_{ref} [kN/m^2]	8.1	12.2
		φ [^{0}]	39	39
		ψ [^{0}]	0	
Initial		K_0 [-]	0.37	0.37
Interaction	Interface parameter	r [-]	0.65	0.65

7.3.2 Nail parameters

The soil- nail is a structural steel along with grout. Threaded steel tubes 52/26 (with an external diameter of 52 and an internal diameter of 26) and 40/16 (with an external diameter of 52 and an internal diameter of 16) are selected. The grout is a mortar mix. Referred as nail parameters are the stiffness and strength of the soil nail along with the grout and the grout-soil interaction parameters.

Based on assumed efficiency of the grouting, the nail is distinguished into grouted and free. The first one meter of the soil nail is assumed to be ineffectively grouted and is modelled as an elastoplastic *node-to-node anchor* in Plaxis. The rest of the nail length is assumed effectively grouted and is modelled as *embedded pile row*. See section 5.3.2. The parameters for the nod-to-node anchor is presented in Table 7. 4. The skin resistance due to the grout-soil interface is assumed to be linearly increasing with depth according to

$$\frac{q_s}{z} = 20 \text{ kN/m}^3$$

where q_s is the skin resistance and z is the depth of the nail surface from the terrain.

The integrated skin friction, that is the skin friction multiplied by the drill hole perimeter is presented in Figure 7. 4. The rest of the parameters for the *embedded pile row* is presented in Appendix E.

Table 7. 4: Anchor parameters

Properties	Unit	Lower cut	Upper cut
Type	[-]	52/26	40/16
f_{sd}	[kPa]	227273	227273
A	[m^2]	0.001337	0.00879
I	[m^4]	3.36E-07	3.36E-07
EA	[kN]	304	1998
$L_{spacing}$	[m]	1.5	2
$F_{max,tens}$	[kN]	525	525
$F_{max,comp}$	[kN]	525	525

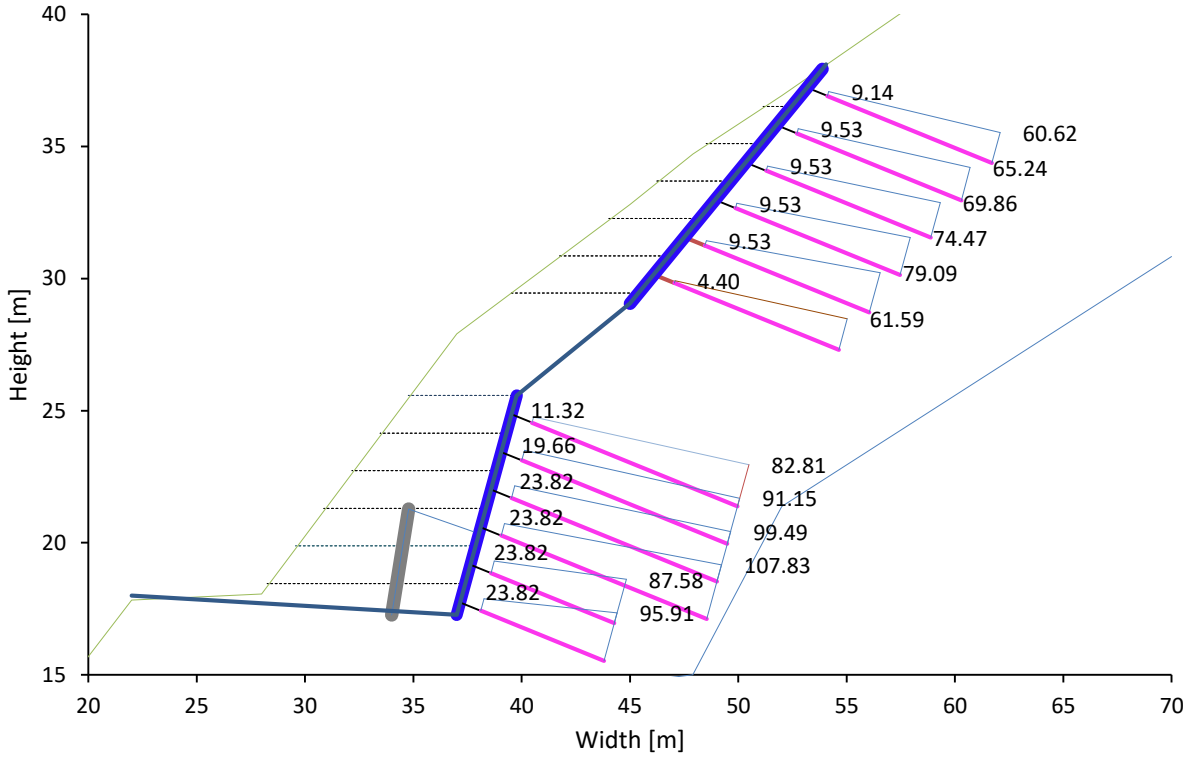

Figure 7. 4: Estimated nail skin resistance at the grout-soil interface

7.3.3 Reinforced shotcrete parameters

The front face is constructed often of a reinforced shotcrete. The corresponding parameters are estimated assuming a double reinforcement of 5 mm and spacing 120 mm with a cover of 30 mm and a distance between the upper and lower reinforcements of 90 mm. Table 7. 5 gives the estimated material parameters for the reinforced shotcrete.

Table 7. 5: Plate parameters for the reinforced shotcrete facing

Properties	**Unit**	**Value**
Axial stiffness, EA	[kN/m]	2.42E+06
Flexural stiffeness, EI	[kNm²/m]	2905
Weight per unit length, w	[kN/m/m]	3
Moment capacity, M_p	[kNm/m]	896
Axial force capacity, $N_{p,1}$	[kN/m]	2427

7.5 Results and discussions

A domain of width about 50 m and height about 60 m is discretized in the Plaxis 2D FEM environment. A medium mesh size of 3622 elements with 30648 nodes is generated. The following calculation stages are specified.

- The initial stress state is generated in a gravity loading.
- The first excavation phase is defined. The corresponding wall front and nail structure is activated at the same time.
- The first phase is repeated for the next eleven phases until the last excavation stage of the lower cut is completed.
- Under each excavation stage, a safety calculation phase is specified.

All the calculations are carried out under drained condition, assuming the water table is lower than the soil nail configuration and the side is adequately drained.

7.4.1 Deformations

The maximum horizontal and the maximum vertical front wall displacement found from the Plaxis calculation are 21 mm and 12 mm respectively. The deformation ratio is thus:

$$d_r = \frac{\delta_h}{H} = 0.0023$$

This is within the recommended range, see Table 2.2

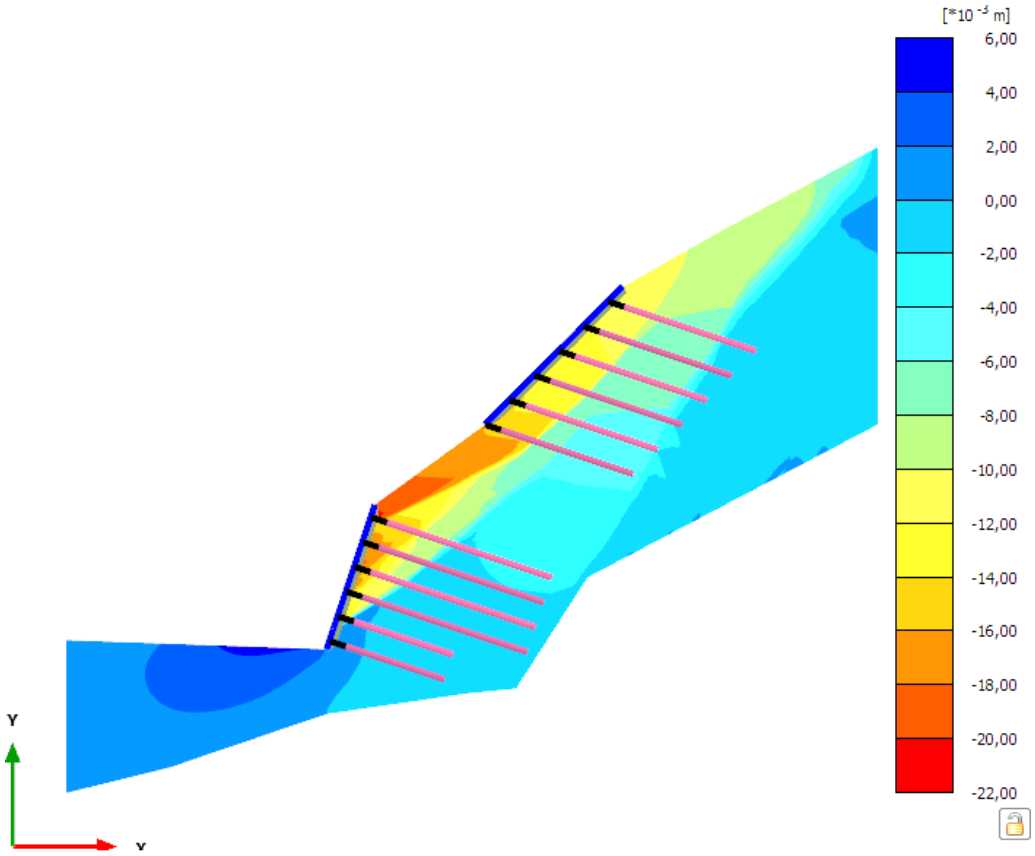

Figure 7. 5: Field of displacement

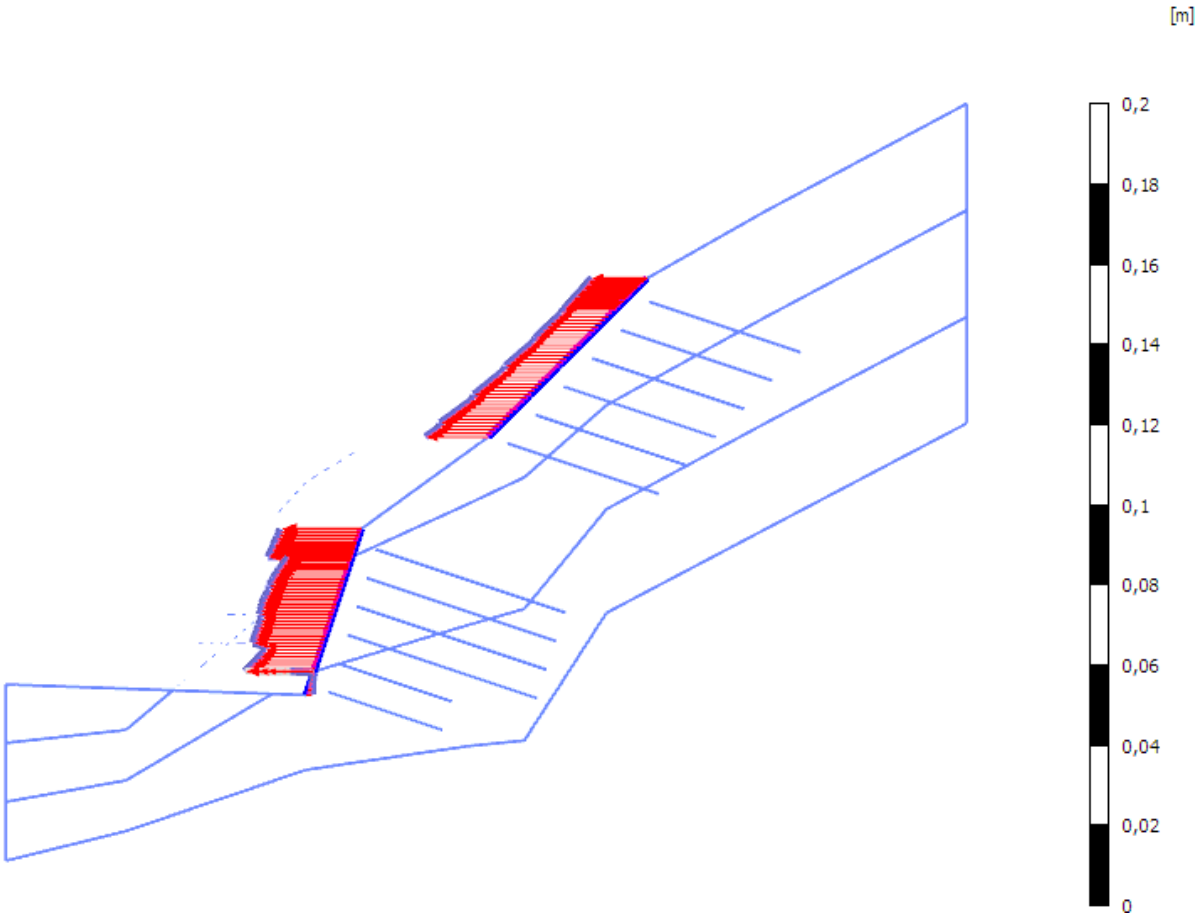

Figure 7. 6: Horizontal displacement of the front facing. Scale 200

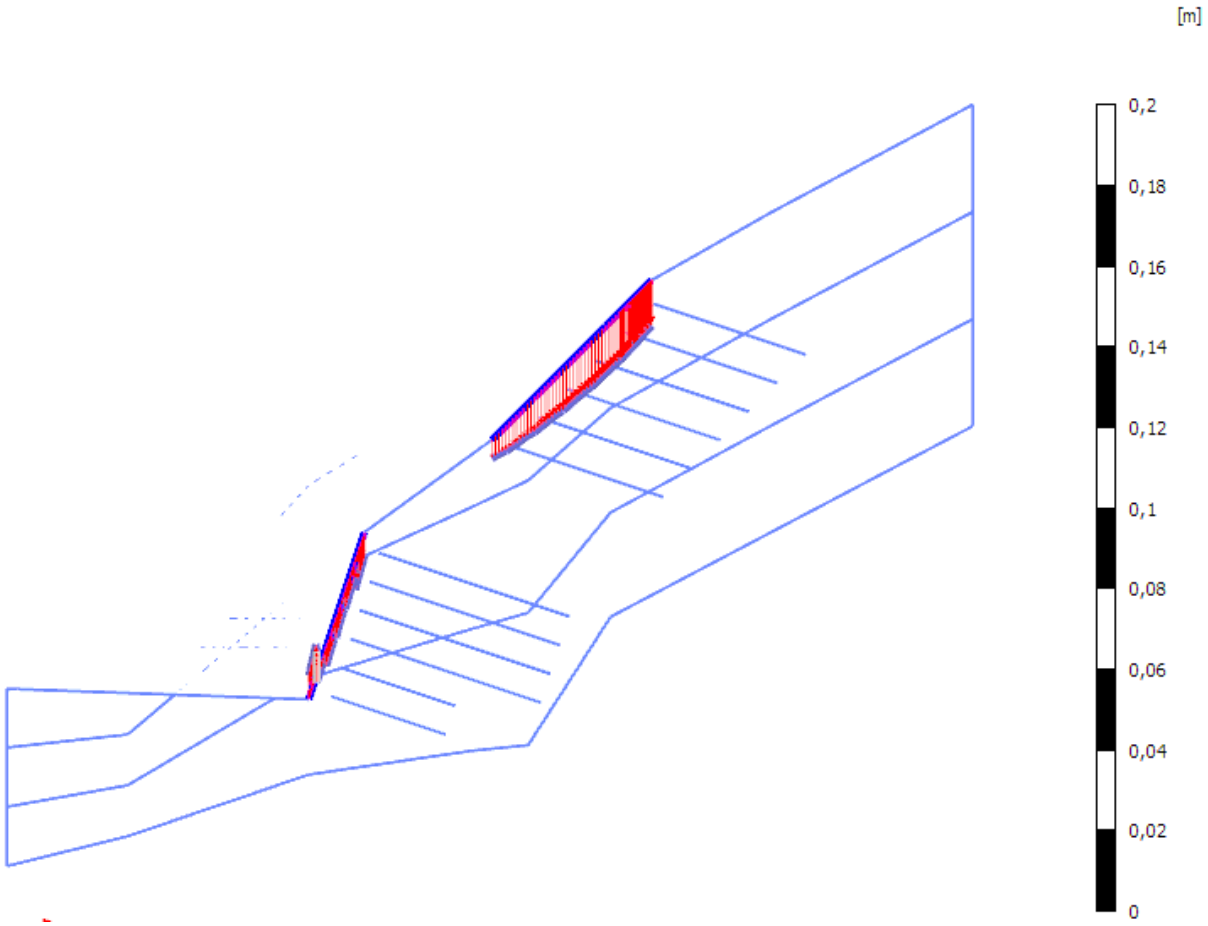

Figure 7. 7: Vertical displacement of front facing. Scale 200.

7.4.1 Safety factor and failure mechanism

The safety factor is presented and the associated mechanism is shown in Figure 7. 7. A factor of safety of 1.5 is found. This is a satisfactory value in many codes of practice. The factor of safety of each slope is separately checked using the wedge method and a safety factor of around 1.4 for the lower cut and a safety factor of around 2.6 is found for the upper cut.

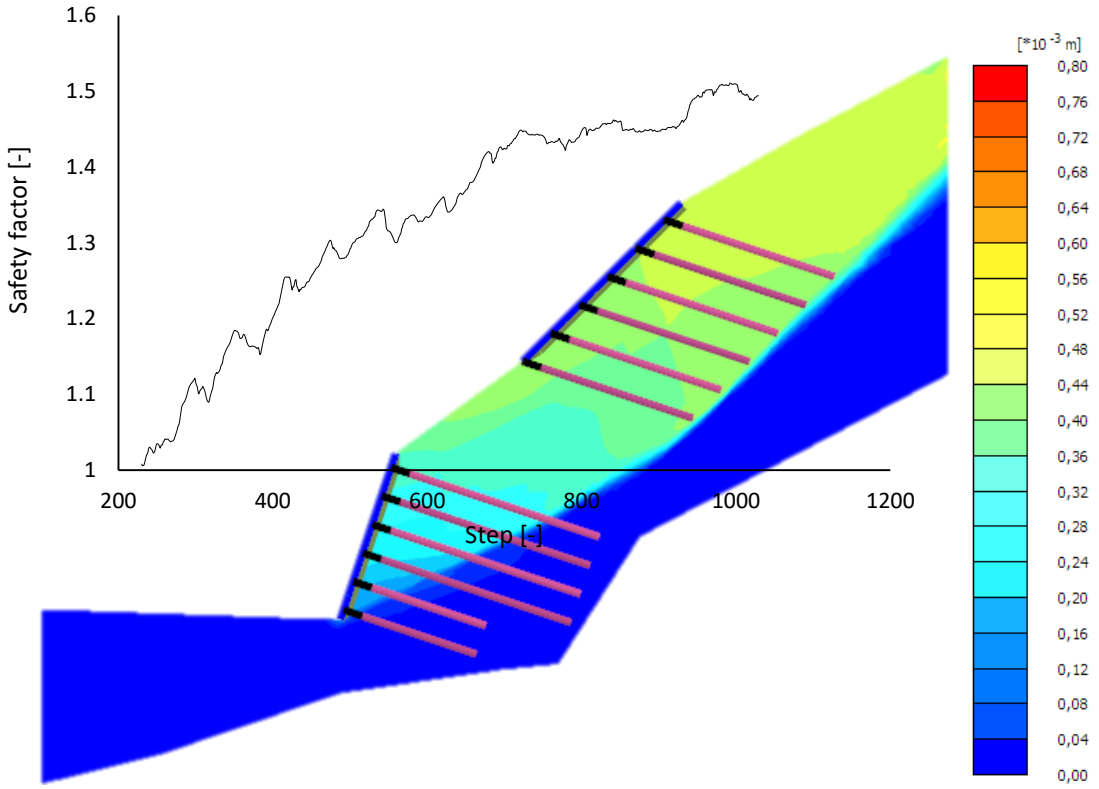

Figure 7. 8: Illustration of failure mechanism with the plot of field of incremental displacements and the safety factor plot for the last excavation.

7.4.2 Structural nail forces

The mobilized axial nail forces are shown in Figure 7. 9 for the last excavation stage. It can be easily shown that the axial forces do not exceed the nail structural capacity, the nail grout slip strength and the grout nail frictional strength.

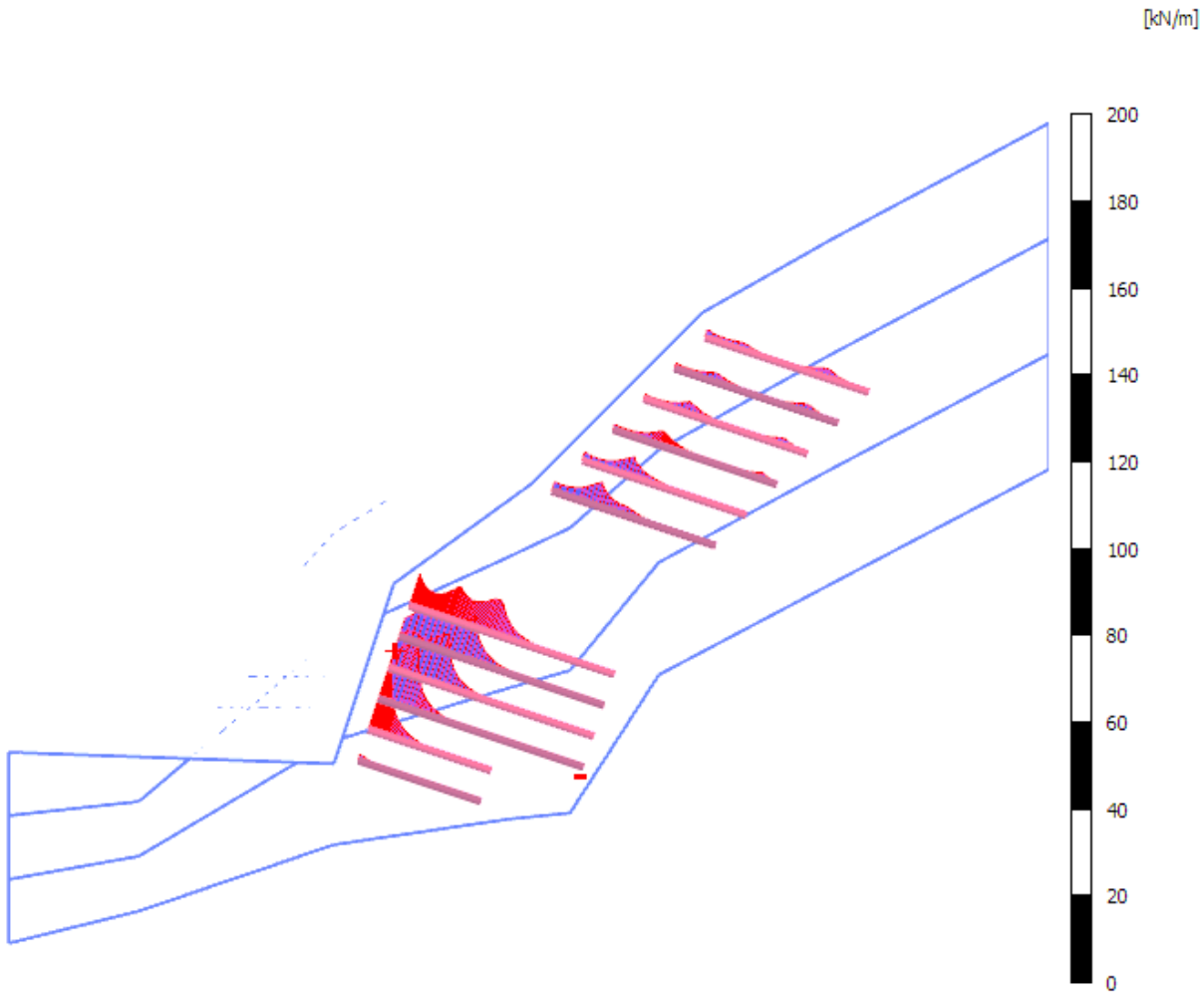

Figure 7. 9: Axial forces on the nails at the last excavation stage.

7.4 Summary

In this chapter a two level soil-nail slope proposed for stabilization of a sharply inclined soil slope adjacent to a new road construction is analyzed. The initial soil-nail configuration is decided based on experience based ranges and experiences gained in this study. The proposed soil nail configuration is shown, using Plaxis 2D analyses, to give adequate safety and tolerable deformation of the wall front.

CHAPTER 8: Summary, conclusions and recommendations

8.1 Summary

Literature review was conducted on the state-of-the art and the state-of-the practice of the soil nailing technique. The literature review focused on design analysis and constructional aspects of the soil nailing technique and effects of the most important soil-nail system configuration (geometric) parameters such as nail spacing, nail inclination, wall-batter, back terrain slope and nail length. Some classical methods of analysis of internal and external stability of a soil-nail system were also presented and discussed.

After conducting the literature review, numerical investigations were conducted on the effect soil-nail system configuration parameters and some soil parameters on the degree of stability and deformation of a soil-nail system. The numerical investigations were carried out using an own implemented simple wedge method followed by analysis using the Geosuite software product and the Plaxis 2D and 3D finite element packages. The different analysis results were then compared. In addition, in the finite element analyses, the effects of the different configuration parameters on the structural forces in the soil-nail system were investigated. Finally, a preliminary design and analysis of a soil-nail system was carried for a steep cut adjacent to a road construction.

8.2 Conclusions

Numerical studied conducted in this thesis show that:

- the safety factor of a nailed slope decreases almost linearly with increase in nail spacing.

- nail inclination influences the safety factor of a soil-nail slope. The trend obtained in Geosuite and Plaxis 2D calculations are nearly the same. They both show an increase in factor of safety until an inclination of 20° from the horizontal. Then, with further increase of the inclination, the safety factor starts to decline. The soil-nail inclination where the safety factor is the highest is called the *optimum nail inclination*. For the particular setup considered in this study, this turns out to be about 20°. This is just the maximum nail inclination recommended in both Statensvegvesen manual and FHWA. The optimum inclination obtained from the simple wedge analysis is different. It happened a bit earlier. It is about 5°. How this difference arises is unclear and should be investigated further. The simplified wedge geometry might have a role.
- the safety factor increases with an increase in wall-batter. The rate of increase is high at lower angles of wall-batter. An increase in wall-batter also means an increase in soil-nail construction material and hence an increase in cost.
- with an increase in back terrain slope the safety factor decreases almost linearly. The effect of back slope is studied only using the wedge method.
- with an increase in the strength parameters, cohesion and friction angle, the safety factor of a soil-nail system increases, perhaps a foreseen conclusion. It is further seen that with an increase in the dilatancy angle the safety factor weakly increases.
- the failure mechanism is influenced by a number of factors. In the wedge analysis the wedge angle is seen to be influenced by several factors. The wedge angle
    - is constant for smaller nail inclination angles and increases with increasing nail inclination for higher inclinations,
    - decreases with increasing wall-batter,
    - increases with increasing back slope,

- decreases with increasing cohesion and increasing friction, and
- does not depend on unit weight of soil.

Higher wedge angle implies smaller wedge area. In the Plaxis analysis, from the incremental displacement contours, the possible failure mechanism and the effect of wall-batter and nail inclination were studied. It is found that the shape of the failure mechanism is similar to a bilinear wedge. Wall-batter and nail inclination influence the geometry of the size of the mechanism formed at failure. The pattern of influence is however a bit complex.

- The nail inclination and the wall-batter have some influence on the structural forces in the front wall and in the nails and the earth pressure on facing. The influence does not have a consistent pattern.
- The safety factors obtained in both Geosuite and Plaxis 2D analyses are comparable. The safety factors obtained in the Plaxis 2D analyses are a little bit higher than the corresponding safety factors obtained from the Geosuite analyses for the same configuration and soil parameters.
- The Geosuite calculations are based on limit equilibrium methods. The state of deformation of the structure and the structural forces are not calculated and thus cannot be collected. The Plaxis calculations give the state of deformation of the structure and the structural forces in the nails and in the front wall. Furthermore, in the case of the Geosuite calculations the input soil-grout interaction parameter (the skin resistance) is a single value. Whereas, in the Plaxis the input can be constant, linearly varying or tabulated which allows the user to input a more realistic distribution. With a choice of an elastoplastic model for the *embedded pile row*, the moment and axial force structural capacities can be direct inputs. The utilities in the Plaxis 2D and 3D are almost the same. The Plaxis 3D relives the

unnecessary assumption that the slope is self-similar and continues infinitely in the in-plane direction.

- The staggered and the uniform nail patterns give almost the same analyses results in the Plaxis 3D calculations. The possible differences can be truly analyzed considering a nonhomogeneous soil domain.
- The in-plane thickness has some effect on calculated safety factors, wall deformations and nail axial forces. In the particular example studied in this chapter lower factor of safety was obtained when the in-plane thickness was one nail spacing.
- The safety factors obtained from Plaxis 3D-one nail spacing in-plane thickness are nearly the same as the safety factors obtained from Plaxis 2D analyses. However, significant differences are noted on axial nail forces. The axial nail forces obtained from the Plaxis 2D analyses are smaller and the location of the maximum axial force is further from the nail head than the location of the maximum axial nail force obtained from the Plaxis 3D analysis.

8.2 Recommendations for further work

In this study, the influence of several parameters on the degree of stability of the soil-nail slopes. However, some factors need to be further investigated. Some of these are:

The effect of back terrain slope has been investigated in the wedge analysis. It should be investigated in both Geosuite and Plaxis such that comparison is possible.

In this study, the Mohr-Coulomb model has been used. For a more realistic study of deformation related issues of the soil-nail system, other advanced models should be employed. It is also worthwhile to investigate effect of stiffness paramerts.

In this thesis effects of the different parameters are numerically investigated. This should be supplemented by an experimental investigation. Experience can be shared from several experimental setups that were conducted in France in the 1980's.

References

1. Statensvegvesen, *Publikasjon nr. 99, Jordnagling,*. 2002: Oslo.
2. Lazarte, C.A., et al., *GEOTECHNICAL ENGINEERING CIRCULAR NO. 7: Soil Nail Walls*. 2003.
3. Prashant, A. and M. Mousumi, *Soil Nailing For Stabilization of Steep Slops Near Railways Tracks*. 2010.
4. Pheat, A., et al., *Soil nailing - best practice guidance.* 2005.
5. C. A. Lazarte, V.E., R. D. Espinoza,P. J. Sabatini, *GEOTECHNICAL ENGINEERING CIRCULAR NO. 7: Soil Nail Walls*. 2003.
6. Elias, V. and I. Juran, *Soil Nailing for Stabilization of Highway Slopes and Excavations*. 1991.
7. Schlosser, F., *Analogies et differences dans le comportement et le calcul des ouvrages de soutements en terre armee et par clouage du sol.* 1983.
8. Clouterre, *Additif 2002 aux recommandations Clouterre 1991 (Trans: Addenda to Recommendations Clouterre 1991).* 2002.
9. Administration:, F.H., *Recommendations Clouterre 1991 = Soil Nailing Recommendations (English translation).* 1991 Springfield, VA 1993.
10. ZLENDER.B, J.P., *SOIL-NAIL WALL STABILITY ANALYSIS USING ANFIS.* 2013.
11. Lazarte, C.A., et al., *GEOTECHNICAL ENGINEERING CIRCULAR NO. 7, Soil Nail Walls Reference Manual* 2015.
12. Bruce, D.A. and R.A. Jewell, *Soil Nailing: Application and apractice.* 1986.
13. Gässler, G., *Vernagelte Geländesprunge - Tragverhalten und Standsicherheit, Reports of Institut für Bodenmechanik und Felsmechanik,UniversitätvFridericana.* 1987.
14. Kirkgard, M.M. and A.K. Hammock, *Monitoring Performance of a Soil-Nail Shoring System in Holocene Alluvium.* Retaining Structures, 1993: p. 609-617.
15. AB, V.G., *Novapoint GeoSuite Toolbox,* , in *Stability help*. 2015.
16. manual, G., *Stability Modeling with SLOPE/W 2007 Version*. 2010.
17. *Plaxis 2D manual, anniversary edition*. 2014.
18. Tsegaye, A.B., *On the modelling of state dilatancy and mechanical behaviour of frictional materials*, in *Department of Civil and Transport Engineering*. 2014, Norwegian University of Science and Technology.
19. Stark, T.D. and H.T. Eid, *Performance of three-dimensional slope stability methods in practice.* Journal of Geotechnical Engineering Division, ASCE, 124(11), 1049-1060., 1998.

Appendices

Appendix A: The main components of Geosuite-stability module

GS stability has three main components - a user interface, a calculation engine and a report generator. The user interface helps the user to define the calculation. BEAST is the calculation engine performing the analyze of the model. [15]

The user interface contains Calculation Data, Soil layers, C Profile, GW/ Pore Pressure, Loads and Model data.

Calculation data contain an information like project name, notes, calculation name, description, etc.

Different soil layers' geometry and properties, soil and rock surface and pore pressure settings are defined in the Soil layer panel. See Figure A. 2

Soils with variable undrained shear strength are modeled by using shear strength profiles - C profiles. Multiple C profiles are used for defining variable undrained shear strength in both vertical and horizontal direction. With multiple C profiles the actual undrained shear strength used in the calculations is interpolated/extrapolated from the profiles. [15]

Different loads such as point load, distributed load and shear loads are defined in Load panel.

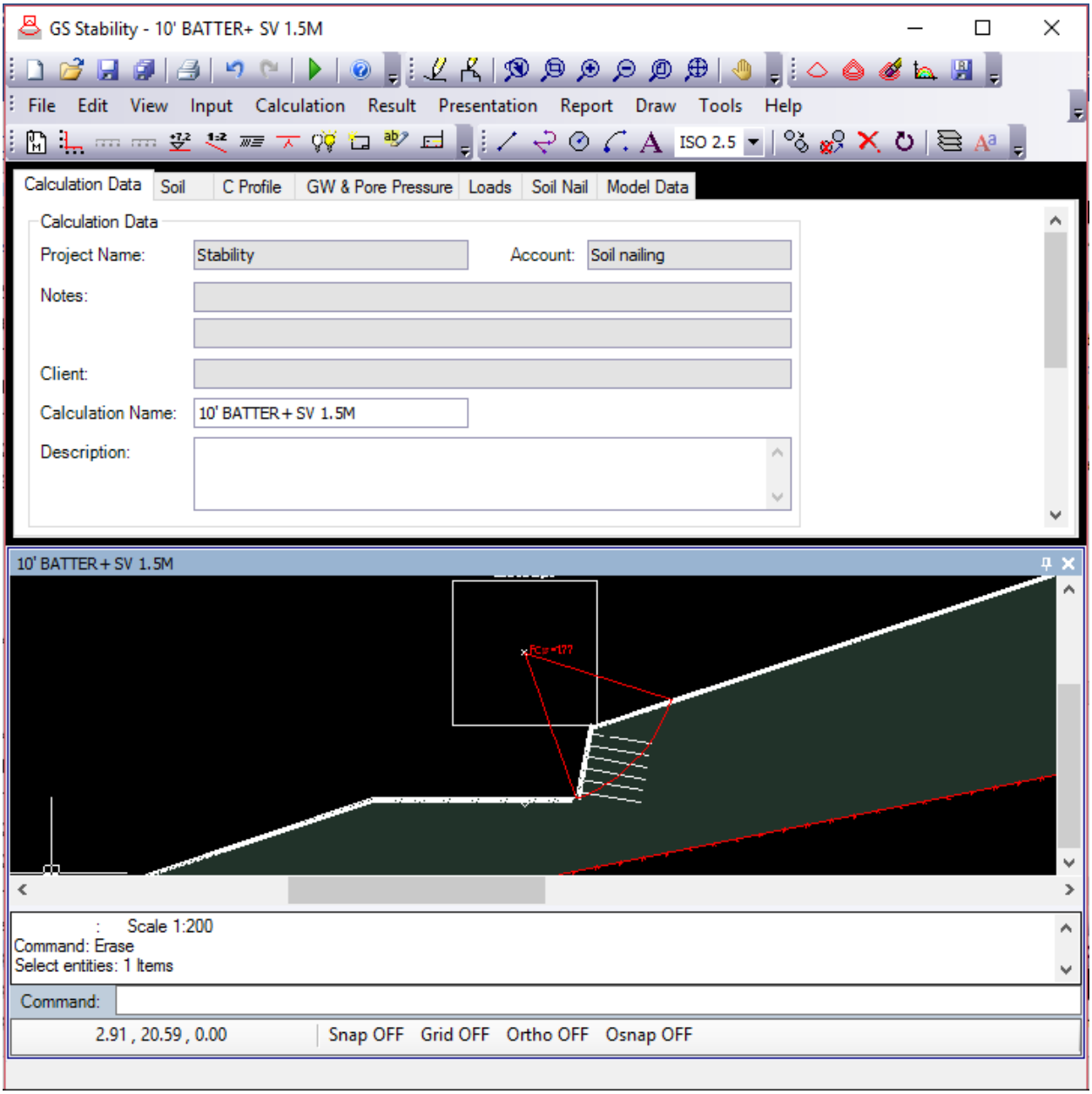

Figure A. 1: The user interface of GS stability module

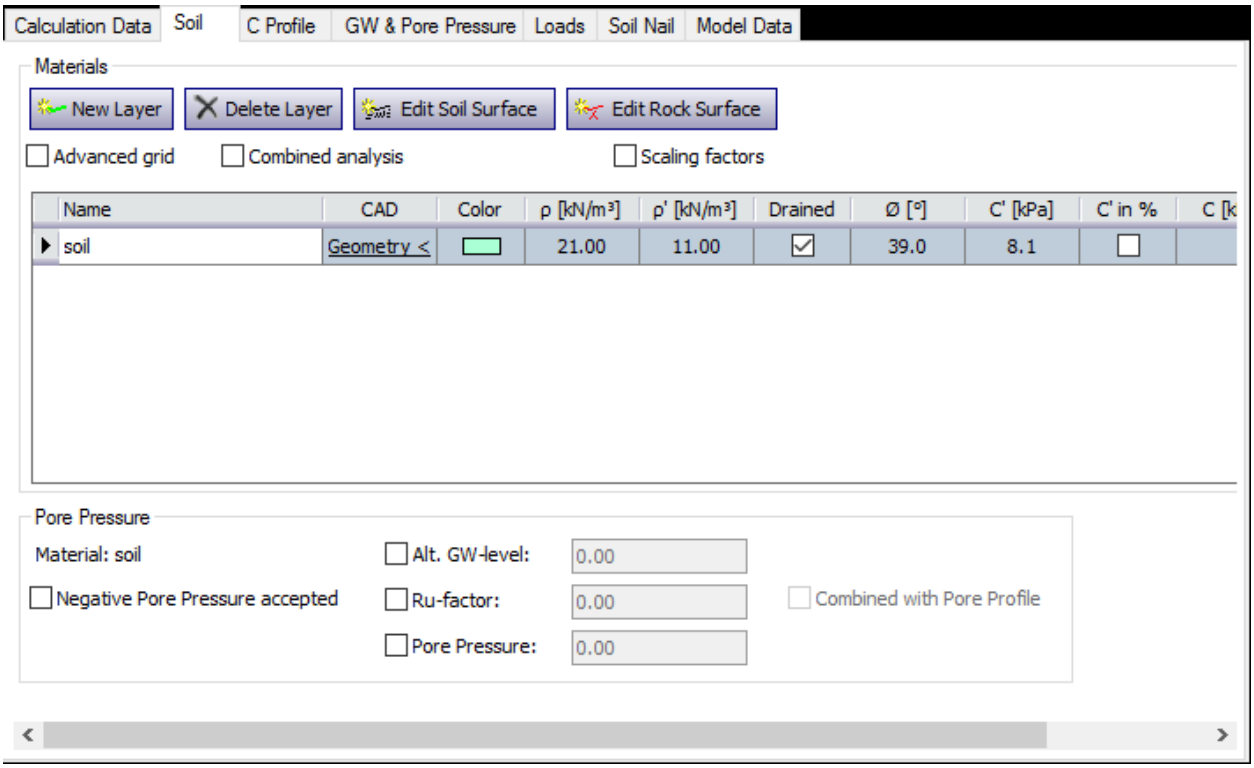

Figure A. 2: GS stability soil layer panel

In GS stability soil-nail parameters are defined in the input menu. As shown Figure A. 3 soil-nails are defined in terms of soil-nail diameter, centre-to-centre distance between the nails in the Y direction, nail capacity, nail axial structural capacity and bearing capacity of the plate/beam at the nail head.

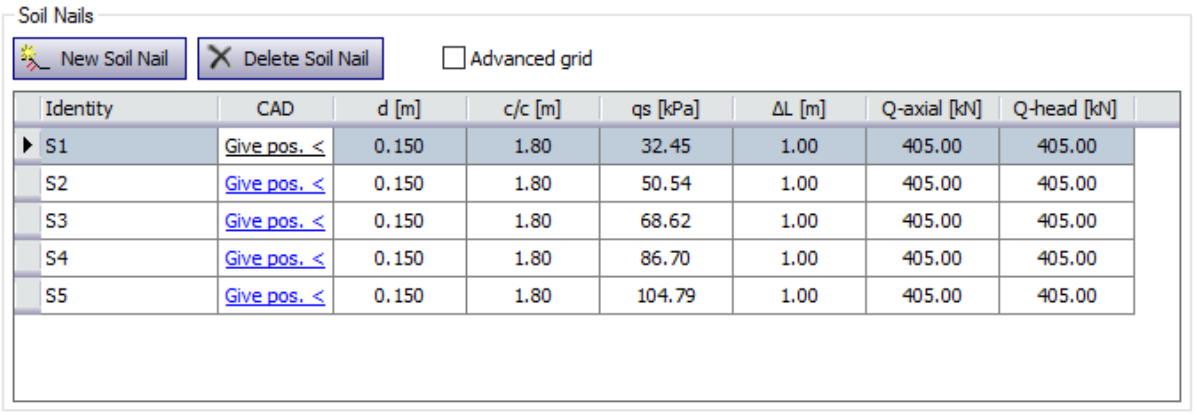

Identity	CAD	d [m]	c/c [m]	qs [kPa]	ΔL [m]	Q-axial [kN]	Q-head [kN]
S1	Give pos. <	0.150	1.80	32.45	1.00	405.00	405.00
S2	Give pos. <	0.150	1.80	50.54	1.00	405.00	405.00
S3	Give pos. <	0.150	1.80	68.62	1.00	405.00	405.00
S4	Give pos. <	0.150	1.80	86.70	1.00	405.00	405.00
S5	Give pos. <	0.150	1.80	104.79	1.00	405.00	405.00

d [m] = Soil-nail diameter.
c/c [m] = Centre-to-centre distance between the nails in the Y direction.

qs [kPa] = Soil-nail capacity.
ΔL [m] = Distance from the nail head to where the soil/nail skin friction starts.
Q-axial [kN] = Soil-nail axial structural capacity.
Q-head [kN] = Bearing capacity of the plate/beam at the nail head.

Figure A. 3: Example of soil-nails parameter and properties

Appendix B: Calculation stratagies in GS Stability software

GS Stability offers different calculation strategies such as tangent, RTangent, points, RPoints, radius, plane, stretch and slope direction. In this thesis, tangent calculation strategy is selected for safety analysis. In tangent calculation strategy the user gives a probable center point for the critical shear surface, search area (quadratic), upper and lower tangential level and the number of levels. [15]

Tangent- In this calculation strategy the user gives a probable center point for the critical shear surface, search area (quadratic), upper and lower tangential level and the number of levels. [15]

RTangent- The calculation strategy is similar to tangent but the search area is rectangular. [15]

Points- - In this calculation strategy the user gives a probable center point for the critical shear surface, search area (quadratic), and an arbitrary number of points through which the critical shear surface must pass. [15]

RPoints- It is similar to points but the search area is rectangular. [15]

Radius- The user calculates a single shear surface and give a center point and a radius. [15]

Plane- In this calculation strategy the shear surface is defined by giving a number of points. [15]

Strecth- Takes a circular shear surface as starting criteria. The shear surface will be "strecth" decided by a given starting and ending point. The number of steps is given. This strategy is suitable to use for long, not so deep, critical shear surface. For instance, in order to follow a local, thin, soil layer with critically low shear strength. [15]

Slope direction- The user select the direction of the critical shear surface will follow. [15]

Optimize- The optimization strategy performs an automatic search for a shear surface which has a lower safety factor than the original shear surface. [15]

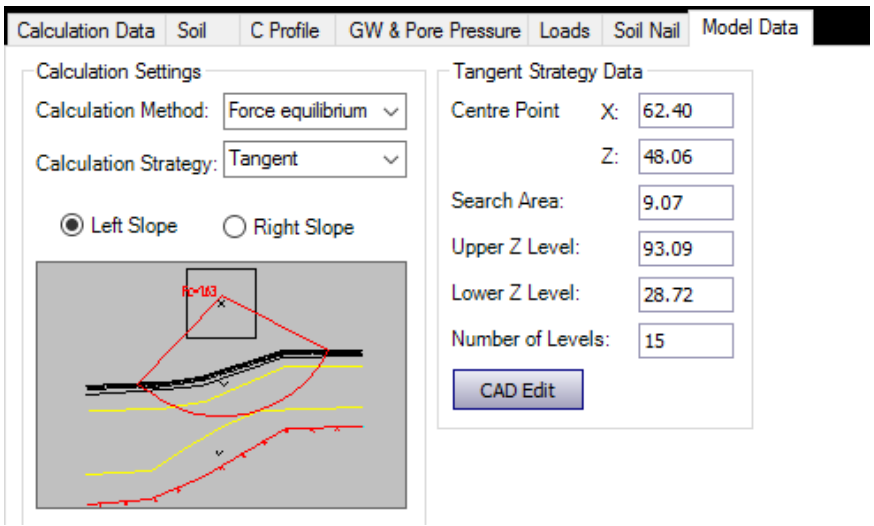

Figure B. 1: Model data panel

Appendix C: Sliding stability and coefficient of active earth pressure [3]

Determination of total active thrust P

$$P = \frac{\gamma H_1^2}{2} K(1-k_v)\left\{1+\frac{2q_s}{\gamma H_1}\left[\frac{\cos\alpha}{\cos(\beta-\alpha)}\right]\right\} \quad (4.8)$$

Where, K = coefficient of lateral active earth pressure which can be determined using Eq. 4.9

$$K = \frac{\cos^2(\phi-\alpha-\omega)}{\cos\omega\cos^2\alpha\cos(\alpha+\beta+\omega)\left[1+\sqrt{\frac{\sin(\phi+\beta)\sin(\phi-\beta-\omega)}{\cos(\alpha+\beta+\omega)\cos(\beta-\omega)}}\right]^2} \quad (4.9)$$

Where: ω [degrees]=an angle relating the horizontal and vertical seismic coefficients such that $\phi-\beta \geq \omega$, given by Eq. 4.10

$$\omega = \tan^{-1}\left(\frac{k_h}{1-k_v}\right) \quad (4.10)$$

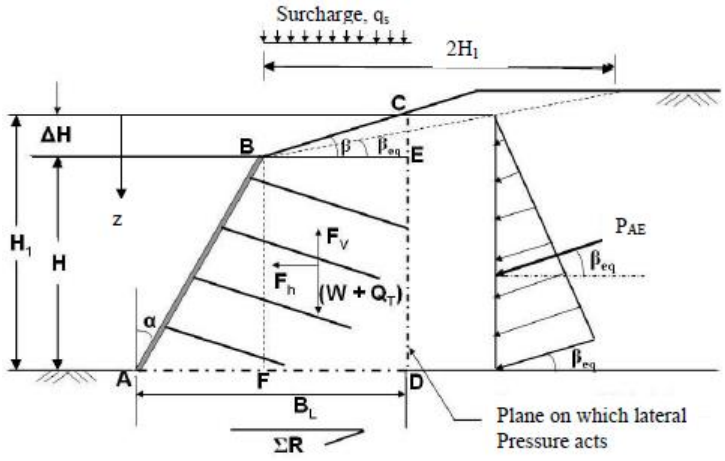

Figure C. 1: Sliding stability of a soil-nail wall [3]

Appendix D: An example of wedge analysis

Table D. 1: Example input for the wedge analysis

Input	**Geometry**		
			18
			0
	H	[m]	9
	Nail		
	i		10
	L	[m]	8
	D	[14]	150
	S_v	[m]	1.5
	s_h	[m]	1.5
	Soil		
		[kN/m3]	21
			39
	c	[kPa]	8.1
	K_0	[-]	0.37
	Surcharge		
	Q	[kN/m]	0
	Seismic		
		[-]	0.057
	s	[-]	1.3
	vertical	[-]	up
	horizontal	[-]	right
Shift origin	x_0	[m]	68.9
	y_0	[m]	29.9
	Tune		5

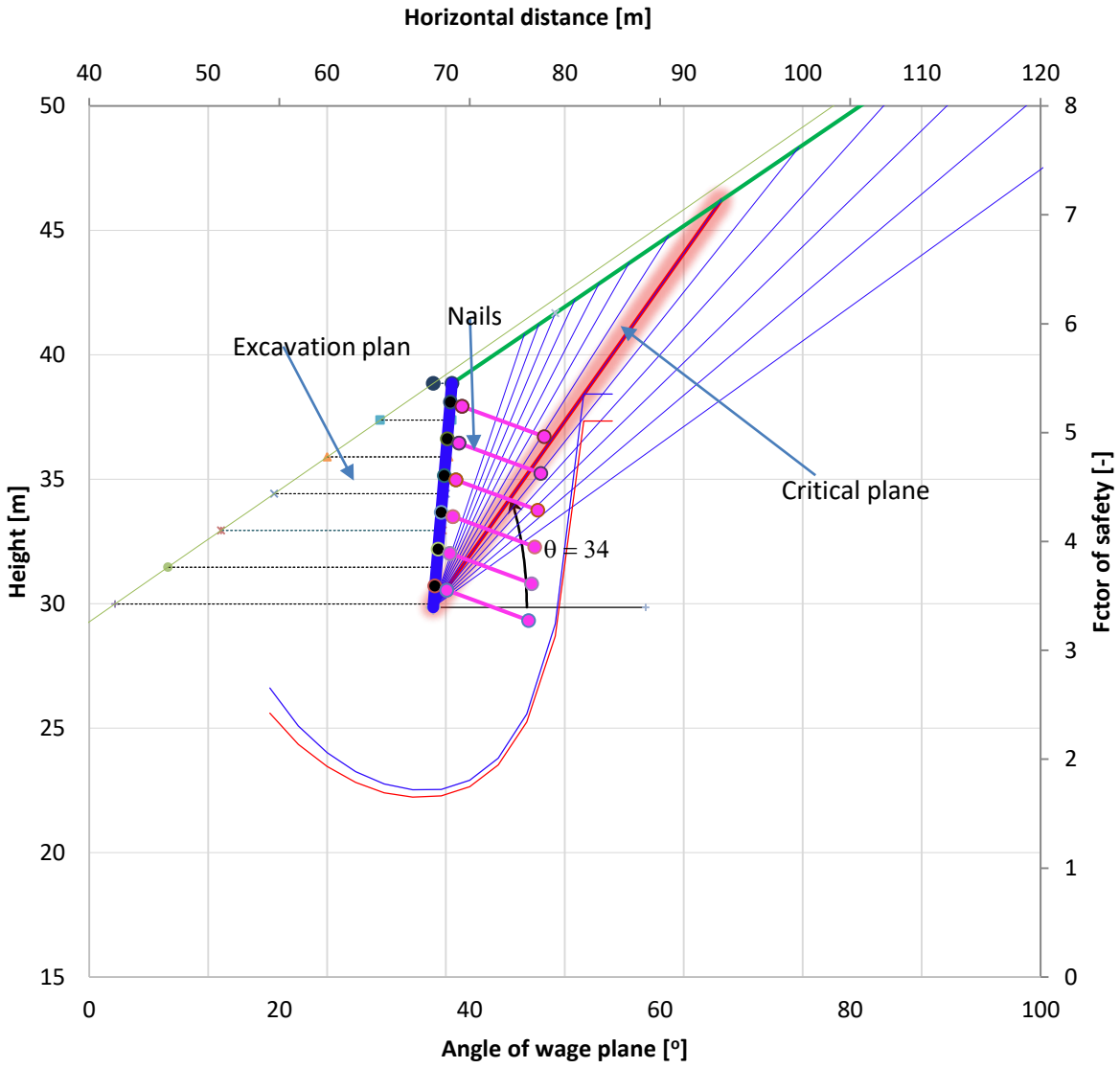

Figure D. 1: Visual presentation of the wedge analysis

Table of the different forces and calculated factors of safety for assumed wedge angle

ass	$\mathbf{L_w}$	**W**	$\mathbf{F_H}$	$\mathbf{F_V}$	$\mathbf{T_{EQ}}$	$\mathbf{F_{SGcal}}$
52.0	15.3	890.6	-33.0	-10.9	567.4	3.05
49.0	16.6	1030.3	-38.2	-12.6	533.7	2.37
46.0	18.2	1196.9	-44.3	-14.6	497.7	1.99
43.0	20.3	1399.8	-51.9	-17.1	459.1	1.78
40.0	22.8	1654.1	-61.3	-20.2	419.8	1.68
37.0	26.3	1984.2	-73.5	-24.3	384.3	1.64
34.0	31.1	2432.9	-90.1	-29.7	352.6	1.67
31.0	38.1	3082.2	-114.2	-37.7	317.2	1.74
28.0	49.3	4112.9	-152.4	-50.3	287.7	1.86
25.0	70.2	6015.4	-222.9	-73.5	257.1	2.04
22.0	122.7	10751.3	-398.3	-131.5	221.5	2.29
19.0	490.4	43822.3	-1623.6	-535.8	195.7	2.64
19	490.4	43822.3	-1623.6	-535.8	195.7	2.64

Tables of nail forces for the assumed wedge angle.

j	l_e	z_{top}	z_{bot}	$'_v$	$'_h$	$'_{average}$	T
1	2.8	1.3	4.8	63.0	23.4	43.2	52.4
2	3.3	2.8	6.3	94.5	35.0	64.8	92.0
3	4.2	4.3	7.8	126.0	46.7	86.4	158.5
4	5.2	5.8	9.3	157.5	58.4	107.9	242.8
5	6.1	7.3	10.8	189.0	70.1	129.5	345.0
6	7.1	8.8	12.3	220.5	81.7	151.1	465.2

j	l_e	z_{top}	z_{bot}	$'_v$	$'_h$	$'_{average}$	T
1	2.2	1.3	4.8	63.0	23.4	43.2	22.2
2	2.8	2.8	6.3	94.5	35.0	64.8	37.5
3	3.8	4.3	7.8	126.0	46.7	86.4	65.6

4	4.9	5.8	9.3	157.5	58.4	107.9	101.4
5	5.9	7.3	10.8	189.0	70.1	129.5	144.8
6	7.0	8.8	12.3	220.5	81.7	151.1	195.9

j	l_e	z_{top}	z_{bot}	$'_v$	$'_h$	$'_{average}$	T
1	1.7	1.3	4.8	63.0	23.4	43.2	16.6
2	2.3	2.8	6.3	94.5	35.0	64.8	30.6
3	3.4	4.3	7.8	126.0	46.7	86.4	58.6
4	4.6	5.8	9.3	157.5	58.4	107.9	95.0
5	5.7	7.3	10.8	189.0	70.1	129.5	139.8
6	6.9	8.8	12.3	220.5	81.7	151.1	193.1

j	l_e	z_{top}	z_{bot}	$'_v$	$'_h$	$'_{average}$	T
1	1.1	1.3	4.8	63.0	23.4	43.2	10.7
2	1.7	2.8	6.3	94.5	35.0	64.8	23.2
3	3.0	4.3	7.8	126.0	46.7	86.4	51.1
4	4.2	5.8	9.3	157.5	58.4	107.9	88.2
5	5.5	7.3	10.8	189.0	70.1	129.5	134.5
6	6.7	8.8	12.3	220.5	81.7	151.1	190.0

j	l_e	z_{top}	z_{bot}	$'_v$	$'_h$	$'_{average}$	T
1	0.4	1.3	4.8	63.0	23.4	43.2	4.4
2	1.1	2.8	6.3	94.5	35.0	64.8	15.3
3	2.5	4.3	7.8	126.0	46.7	86.4	43.1
4	3.9	5.8	9.3	157.5	58.4	107.9	80.9
5	5.3	7.3	10.8	189.0	70.1	129.5	128.8
6	6.6	8.8	12.3	220.5	81.7	151.1	186.7

j	l_e	z_{top}	z_{bot}	$'_v$	$'_h$	$'_{average}$	T
1	0	1.3	4.8	63.0	23.4	43.2	0.0
2	0.5	2.8	6.3	94.5	35.0	64.8	6.8

3	2.0	4.3	7.8	126.0	46.7	86.4	34.4
4	3.5	5.8	9.3	157.5	58.4	107.9	73.0
5	5.0	7.3	10.8	189.0	70.1	129.5	122.6
6	6.5	8.8	12.3	220.5	81.7	151.1	183.1

j	l_e	z_{top}	z_{bot}	$'_v$	$'_h$	$'_{average}$	T
1	0	1.3	4.8	63.0	23.4	43.2	0.0
2	0	2.8	6.3	94.5	35.0	64.8	0.0
3	1.4	4.3	7.8	126.0	46.7	86.4	24.9
4	3.1	5.8	9.3	157.5	58.4	107.9	64.4
5	4.7	7.3	10.8	189.0	70.1	129.5	115.8
6	6.4	8.8	12.3	220.5	81.7	151.1	179.3

j	l_e	z_{top}	z_{bot}	$'_v$	$'_h$	$'_{average}$	T
1	0	1.3	4.8	63.0	23.4	43.2	0.0
2	0	2.8	6.3	94.5	35.0	64.8	0.0
3	0.8	4.3	7.8	126.0	46.7	86.4	14.4
4	2.6	5.8	9.3	157.5	58.4	107.9	54.8
5	4.4	7.3	10.8	189.0	70.1	129.5	108.3
6	6.2	8.8	12.3	220.5	81.7	151.1	175.0

j	l_e	z_{top}	z_{bot}	$'_v$	$'_h$	$'_{average}$	T
1	0	1.3	4.8	63.0	23.4	43.2	0.0
2	0	2.8	6.3	94.5	35.0	64.8	0.0
3	0.2	4.3	7.8	126.0	46.7	86.4	2.8
4	2.1	5.8	9.3	157.5	58.4	107.9	44.2
5	4.1	7.3	10.8	189.0	70.1	129.5	100.0
6	6.0	8.8	12.3	220.5	81.7	151.1	170.2

j	l_e	z_{top}	z_{bot}	$'_v$	$'_h$	$'_{average}$	T
1	0	1.3	4.8	63.0	23.4	43.2	0.0
2	0	2.8	6.3	94.5	35.0	64.8	0.0

3	0	4.3	7.8	126.0	46.7	86.4	0.0
4	1.5	5.8	9.3	157.5	58.4	107.9	32.2
5	3.7	7.3	10.8	189.0	70.1	129.5	90.6
6	5.8	8.8	12.3	220.5	81.7	151.1	164.8

j	l_e	z_{top}	z_{bot}	$'_v$	$'_h$	$'_{average}$	T
1	0	1.3	4.8	63.0	23.4	43.2	0.0
2	0	2.8	6.3	94.5	35.0	64.8	0.0
3	0	4.3	7.8	126.0	46.7	86.4	0.0
4	0.9	5.8	9.3	157.5	58.4	107.9	18.5
5	3.3	7.3	10.8	189.0	70.1	129.5	79.9
6	5.6	8.8	12.3	220.5	81.7	151.1	158.6

j	l_e	z_{top}	z_{bot}	$'_v$	$'_h$	$'_{average}$	T
1	0	1.3	4.8	63.0	23.4	43.2	0.0
2	0	2.8	6.3	94.5	35.0	64.8	0.0
3	0	4.3	7.8	126.0	46.7	86.4	0.0
4	0.1	5.8	9.3	157.5	58.4	107.9	2.6
5	2.8	7.3	10.8	189.0	70.1	129.5	67.4
6	5.4	8.8	12.3	220.5	81.7	151.1	151.5

j	l_e	z_{top}	z_{bot}	$'_v$	$'_h$	$'_{average}$	T
1	0	1.3	4.8	63.0	23.4	43.2	0.0
2	0	2.8	6.3	94.5	35.0	64.8	0.0
3	0	4.3	7.8	126.0	46.7	86.4	0.0
4	0	5.8	9.3	157.5	58.4	107.9	0.0
5	2.1	7.3	10.8	189.0	70.1	129.5	52.7
6	5.1	8.8	12.3	220.5	81.7	151.1	143.0

j	l_e	z_{top}	z_{bot}	$'_v$	$'_h$	$'_{average}$	T
1	0	1.3	4.8	63.0	23.4	43.2	0.0
2	0	2.8	6.3	94.5	35.0	64.8	0.0

3	0	4.3	7.8	126.0	46.7	86.4	0.0
4	0	5.8	9.3	157.5	58.4	107.9	0.0
5	2.1	7.3	10.8	189.0	70.1	129.5	52.7
6	5.1	8.8	12.3	220.5	81.7	151.1	143.0

Appendix E: Input parameters for the embedded pile row-grouted soil nail

Embeded pile row

Properties, stifness and strength parameters		**nail#1**	**2**	**3**	**4**	**5**	**6**	**7**	**8**	**9**	**10**	**11**	**12**
Properties	**Unit**	**52/26**	**52/26**	**52/26**	**52/26**	**52/26**	**52/26**	**40/16**	**40/16**	**40/16**	**40/16**	**40/16**	**40/16**
$_{steel}$	[kN/m^3]	77	77	77	77	77	77	77	77	77	77	77	77
$_{concrete}$	[kN/m^3]	25	25	25	25	25	25	25	25	25	25	25	25
$E_{concrete}$	[kN/m^2]	3,00E+07	3,00E+07	3,00E+07	3,00E+07	3,00E+07	3,00E+07	3,00E+07	3,00E+07	3,00E+07	3,00E+07	3,00E+07	3,00E+07
E_{steel}	[kN/m^2]	2,18E+08	2,18E+08	2,18E+08	2,18E+08	2,18E+08	2,18E+08	2,18E+08	2,18E+09	2,18E+08	2,18E+08	2,18E+08	2,18E+08
Nail inside diamter	[14]	26	26	26	26	26	26	16	16	16	16	16	16
Nail outside diamater	[14]	52	52	52	52	52	52	40	40	40	40	40	40
Thickness	[14]	13	13	13	13	13	13	12	12	12	12	12	12
A	[m^2]	1,34E-03	1,34E-03	1,34E-03	1,34E-03	1,34E-03	1,34E-03	8,79E-04	8,79E-04	8,79E-04	8,79E-04	8,79E-04	8,79E-04
I	[m^4]	3,36476E-07	3,36476E-07	3,36E-07	3,36E-07	3,36E-07	3,36E-07	1,22E-07	1,224E-07	1,22447E-07	1,22447E-07	1,224E-07	1,224E-07
Moment capacity, M_p	[kN]												
Axial force capacity, N_p	[kN]												
Drill hole Diameter	[m]	0,12	0,12	0,12	0,12	0,12	0,12	0,12	0,12	0,12	0,12	0,12	0,12
$L_{spacing}$	[m]	1,5	1,5	1,5	1,5	1,5	1,5	2	2	2	2	2	2
Rayligh,	[-]												
Reyligh,	[-]												
Skin resistance													
$T_{top,max}$	[kN/m]	11,32	19,66	23,82	23,82	23,82	23,82	9,14	9,53	9,53	9,53	9,53	4,40
$T_{bot,max}$	[kN/m]	82,81	91,15	99,49	107,83	87,58	95,91	60,62	65,24	69,9	74,47	79,09	61,59
Base resistance													
F_{max}	[kN]												
Interface factors													
Axial skin stiffness factor	[-]	default	default	default	default	default	default	default	default	default	default	default	default
Lateral skin stiffness factor	[-]	default	default	default	default	default	default	default	default	default	default	default	default
Pile base stiffness factor	[-]	default	default	default	default	default	default	default	default	default	default	default	default